

1. Report No. <b>UMTRI-91-30</b>	2. Government Accession No.	3. Recipient's Catalog No.	
4. Title and Subtitle <b>Electrorheological Fluids for Aircraft Flight Control: Feasibility of a Position Servomechanism</b>		5. Report Date <b>July 1991</b>	6. Performing Organization Code
		8. Performing Organization Report No. <b>UMTRI-91-30</b>	
		7. Author(s) <b>Zheng Lou, Robert D. Ervin, Frank E. Filisko</b>	
9. Performing Organization Name and Address <b>The University of Michigan Transportation Research Institute 2901 Baxter Road, Ann Arbor, Michigan 48109</b>		10. Work Unit No. (TRAIS)	11. Contract or Grant No. <b>P.O. 1199</b>
		13. Type of Report and Period Covered <b>Final: 4/25/90-4/1/91</b>	
		12. Sponsoring Agency Name and Address <b>Dynamic Controls, Inc. 7060 Cliffwood Place Dayton, OH 45424</b>	
14. Sponsoring Agency Code		15. Supplementary Notes	
<p>16. Abstract</p> <p>In this second phase of the study, an electrorheological (ER) position control system has been designed, fabricated and assembled to test the feasibility of ER fluids in a system which is similar to flight-control servos. In a pilot-valve stage of this system, an ER bridge has been shown to be successful in producing a controlled pressure differential up to 250 psi for driving the spool of a power-stage valve. Upon closing the loop around the position of a hydraulic cylinder, the assembled system was able to control the motion of the actuator in slow-speed scenarios.</p> <p>Throughout the process of system testing, ER fluid samples were seen to be stable and consistent in performance.</p> <p>Both analysis and experiment showed that although the ER response phenomenon, itself, exhibits a bandwidth in the kilohertz range, the fixed upper bound in ER shear stress reduces the actual bandwidth of an assembled device. With a peak yield shear stress of 0.1 psi, the valve devices assembled here were computed to have a maximum possible bandwidth of 227 Hz. The basic analysis underlying a rather complete numerical simulation was formulated. Its future application in a computer code would provide for detailed examination of the nonlinear system, including interactions between the ER effect, fluid electrical impedances, fluid mechanics, and the tailoring of system control signals to account for these interactions.</p>			
17. Key Words <b>Electrorheological fluids, field-dependent fluids, position control, servo-control, valves, hydraulics, numerical simulation</b>		18. Distribution Statement	
19. Security Classif. (of this report)	20. Security Classif. (of this page)	21. No. of Pages <b>103</b>	22. Price



## ACKNOWLEDGEMENTS

The authors want to acknowledge the advice and comments from Mr. Christopher Winkler and excellent technical support and contributions from Ms. Theresa Filisko, Mr. Thomas Husen, Mr. John Koch, Mr. Michael Campbell and Mr. Greg Johnson. Gratitude is also extended to Mrs. Marlene Dyer and Mrs. Ann Grimm of the Research Information and Publications Center, UMTRI, for their great effort in searching, collecting and editing the bibliography. This work was supported by the U.S. Air Force through a contract with Dynamic Controls, Inc. The consistent encouragement and support from Dr. Gavin Jenney of Dynamic Controls, Inc. and Mr. Phil Chandler of the U.S. Air Force are greatly appreciated.



## TABLE OF CONTENTS

1. INTRODUCTION .....	1
2. ER BRIDGE.....	5
2.1. Design .....	5
2.2. Electric Circuit Activating the ER Bridge.....	7
3. ER FLUID SUPPLY .....	8
3.1. A Commercial Centrifugal Pump.....	8
3.2. A Special ER Fluid Pumping Mechanism .....	8
3.3. Diaphragm Pump.....	10
3.4. Design of the ER Fluid Tank.....	12
4. MODIFIED SERVO VALVE.....	13
4.1. General Scheme .....	13
4.2. Forces on the Spool.....	14
4.3. Diaphragm and LVDT Problems .....	15
5. ELECTRONIC CONTROL CIRCUIT.....	16
5.1. Wave Generator .....	16
5.2. Error Signal Limit .....	16
6. ER FLUID STABILITY .....	17
7. CHARACTERIZATION OF AN ER VALVE.....	18
7.1. Experimental Results.....	18
7.2. Analysis to Approximate Limitations in Bandwidth.....	21
8. BRIDGE CHARACTERIZATION .....	24
8.1. Experimental Results.....	24
8.2. Asymmetry in the ER Bridge .....	25
8.3. A Surrogate Servo Valve.....	28
9. THE FULLY-ASSEMBLED SYSTEM.....	31
10. A NUMERICAL SIMULATION.....	33
10.1. Mathematical Model .....	33
10.2. Programs.....	38
11. CONCLUSIONS .....	39
REFERENCES.....	40
APPENDIX A. PRINTS FOR THE ER BRIDGE COMPONENTS .....	41

APPENDIX B. PRINTS FOR SERVO VALVE MODIFICATION COMPONENTS.....	51
APPENDIX C. COMPUTER PROGRAM FOR A NUMERICAL SIMULATION.....	59
APPENDIX D. AN ELECTRODILATANCY TEST DEVICE.....	81
APPENDIX E. ELECTORRHEOLOGICAL FLUIDS: A BIBLIOGRAPHY.....	83

## 1. INTRODUCTION

This report presents the results of phase-two of the study entitled "The Feasibility of Using Field-Dependent Fluids in Flight Controls." This work has been sponsored by the U.S. Air Force and conducted by the University of Michigan Transportation Research Institute and the Department of Materials Science and Engineering of the College of Engineering under subcontract from Dynamic Controls, Inc. Following the results from phase-one<sup>1\*</sup>, the current effort was to test the feasibility of an electrorheological servo position control system which is illustrated in Fig. 1.1. This package is to control the position of a hydraulic cylinder by means of a two-fluid system. An ER fluid is employed in the pilot stage of a servovalve device while a conventional hydraulic fluid is supplied to the "power stage" of the valve. This hybrid design approach was prompted both by the problems of handling ER particulates in a hydraulic cylinder (with sliding seals) and by current limitations in the shear strength of ER fluids. Although the system was to demonstrate current ER capabilities for hydraulic control application, the package was not intended as a practicable application, in and of itself.

The pilot stage is an ER pressure controller. It is configured as a diamond array, or "bridge," of four individual valve elements whose flow resistance is electrorheologically-controlled. The ER bridge produces a pressure differential across the load in a manner that is analogous to the electrical Wheatstone bridge which amplifies resistance changes in the arms—generating a voltage differential across its diagonal. The ER bridge is discussed in Chapter 2.

The actuator, servo valve and ER bridge are physically connected through an integral manifold, as shown in Figure 1.2. The supply of ER fluid to the bridge device is provided through a specialized circuit of components described in Chapter 3.

The load for the ER bridge is a floating spool which comprises the power stage of a modified servo valve. A pressure differential appearing across the diagonal of the ER bridge is exerted across the spool. Movement of the spool allows flow of conventional fluid, at high pressure, to the hydraulic cylinder. Small diaphragms are employed at both ends of the spool in order to separate the two fluid systems. Ideally, such a spool element should have a critical center or slight under-lap; however, the valve employed in this package turned out to be widely underlapped, thus rendering various problems in the system performance that will be discussed. The modified valve device is discussed in Chapter 4.

Chapter 5 of this report covers the electrical circuits employed for excitation of the bridge in the push-pull fashion needed for control of differential pressure across the

---

\* The superscripts refer to the references.

diagonal. Chapter 6 reports on observation of the properties of the ER fluid samples over the course of the phase-two project.

Both an individual, parallel-plate, ER valve (discussed in Chapter 7) and the four-valve ER bridge (discussed in Chapter 8) have been experimentally characterized as stand-alone items. The complete servo control system was later experimentally characterized, as discussed in Chapter 9. A numerical simulation of the overall system was initiated during the study, but not finished due to time and budget limitations. The analytic work which provides the basis for such simulation is reported in Chapter 10. Major conclusions of the phase-two study are summarized in Chapter 11.

Electrodilatancy, as a possible alternative mechanism to drive the servo system, has been studied, although without success (Appendix D). An extensive literature search has also been performed and the resulting bibliography is included in Appendix E.



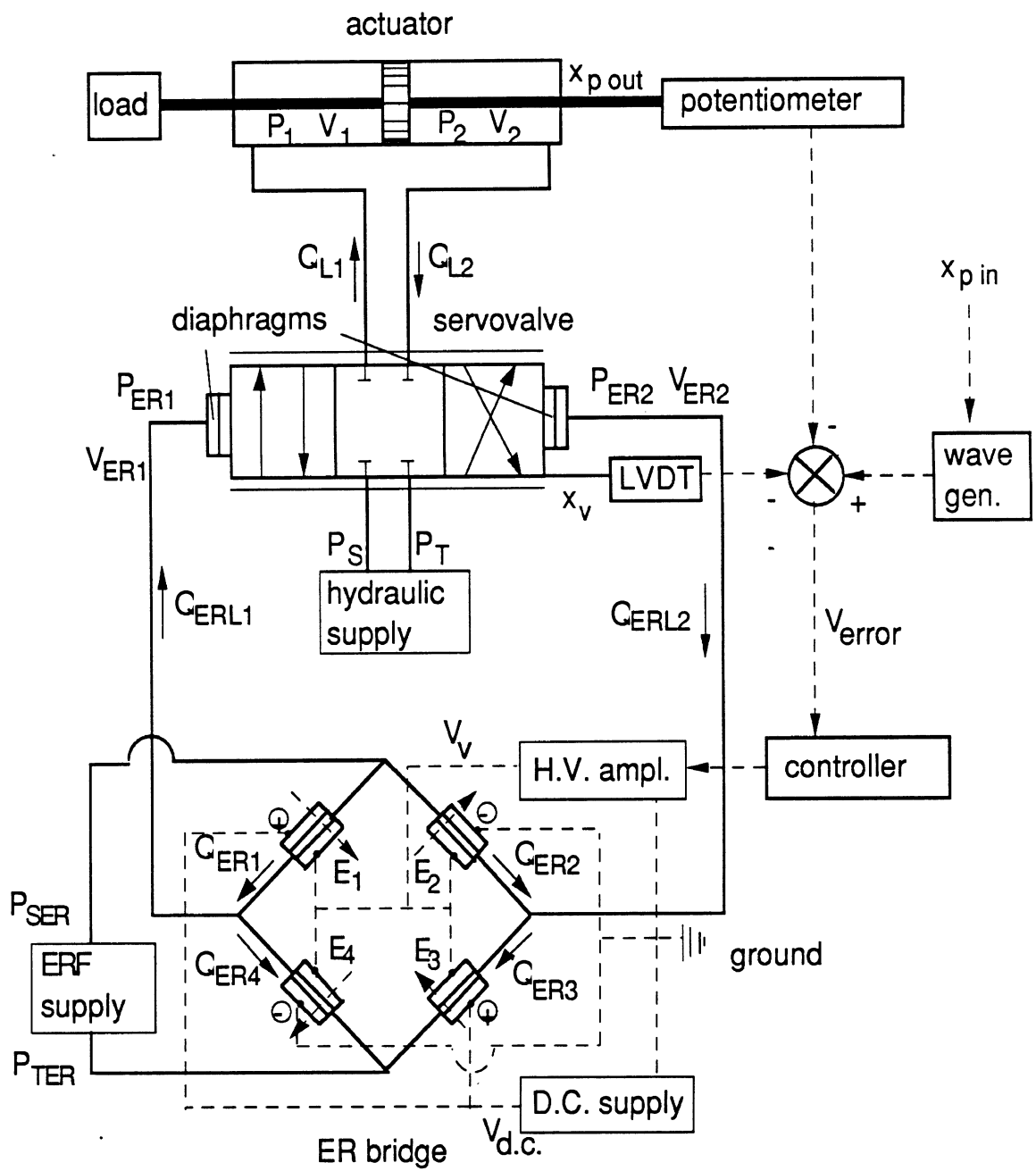


Fig. 1.1. The schematic of an electrorheological servo position control system.

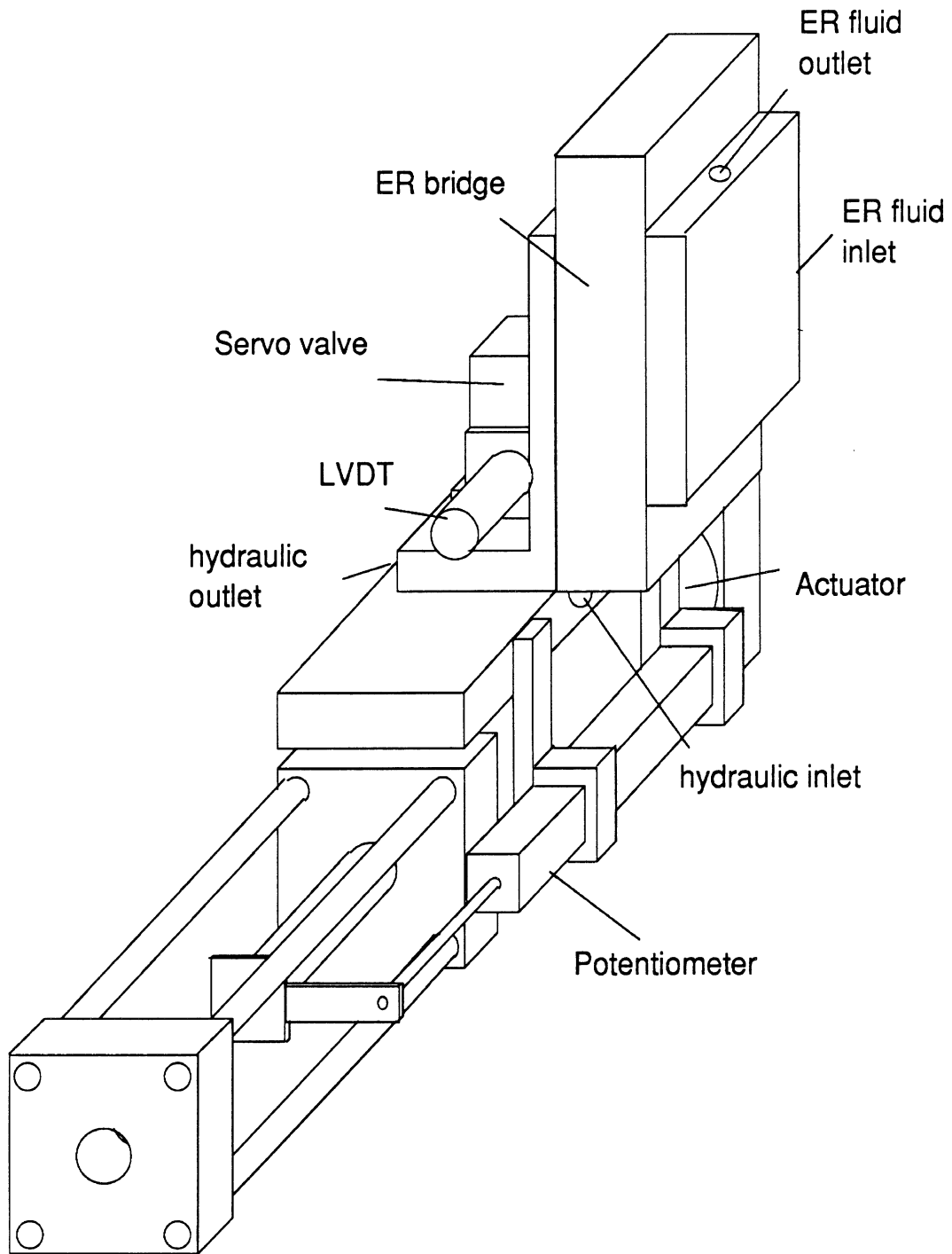


Fig. 1.2. Arrangement of components on the integrated package, including the servo valve, ER bridge, and actuator.

## 2. ER BRIDGE

### 2.1. Design

As stated in the previous chapter, an ER bridge has four identical arms or valves, each of which can be electrorheologically controlled. An analysis of the static efficiency and load pressure characteristics of such a bridge was performed in phase one of the study. For a bridge to deliver a load pressure as high as the system pressure,  $P_s$ , its flow "resistors" must be designed per the relationship,

$$\frac{L}{h} = \frac{P_s}{2\tau_{y \max}} \quad (2.1)$$

where  $L$  and  $h$  are the length and gap of each individual arm, respectively, and  $\tau_{y \max}$  is the Bingham shear stress limit for an ER fluid. If  $\tau_{y \max} = 0.1$  psi and  $L = 1$  meter, the bridge is able to deliver a maximum lock-up pressure of 200 psi, which is sufficient for driving the main stage spool of the supplied servovalve (discussed later in Section 4.2). The bridge design is driven primarily, then, by the need to accommodate the four arms, each with relatively long valve length, within a compact volume.

The ER bridge shown in Fig. 2.1 has been designed and fabricated for this purpose. The drawings for individual components of this assembly are provided in Appendix A. On each gallery plate, slotted passages are provided to comprise the four valves of the bridge. All of the plates (gallery plates, electrodes and insulators) are clamped between the top and base blocks. A problem encountered in this assembly involved some fluid leakage due to insufficient distribution of clamping forces, given the high stiffness of the the nylon insulation plates. More distributed fastening would be recommended for any future design.

The top and base blocks serve as manifolds which afford the necessary connections among the four individual ER valve sections, the ER fluid and hydraulic fluid supply ports, and the ports on the servo (spool) valve. The base block also provides two taps from which the ER pressure differential was transduced.

Design criteria for the slotted passages which formed each ER valve included the following: (1) a minimum total fluid volume so as to minimize the amount of ER fluid needed in the system; (2) a minimum base flow resistance or pressure loss; (3) a symmetric geometric layout so that the bridge response is symmetric over the full range of operation. The last two criteria are discussed in detail in Section 8.2.

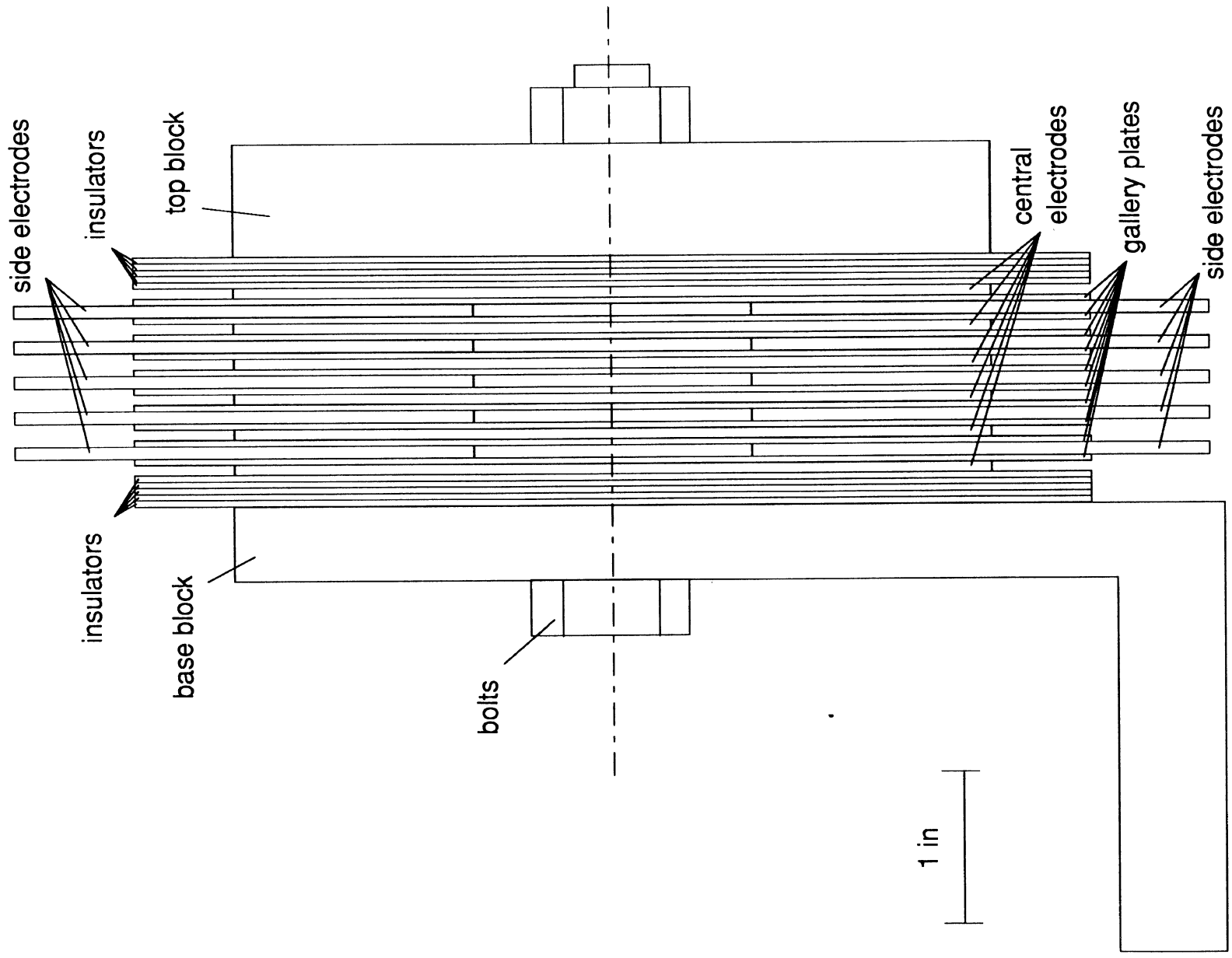


Fig. 2.1. An ER bridge.

## 2.2. Electric Circuit Activating the ER Bridge

A scheme for electrically charging four valves in the ER bridge was designed as shown in Figure 2.2. A d.c. supply with a fixed voltage of  $2V_0$  is combined with a linear high-voltage amplifier whose output is offset by a value,  $V_0$ , giving a peak-to-peak response of  $2V_0$ . When the value of the reference input signal is zero, both valve pairs (valves 1 and 3 and valves 2 and 4) are charged with a uniform voltage level of  $V_0$ . As a sinusoidal signal changes from zero to the positive peak, the potential difference for valves 1 and 3 decreases from  $V_0$  toward zero while that for valves 2 and 4 increases from  $V_0$  toward  $2V_0$ . This arrangement enables the balanced push-pull exercise of the four-arm bridge using only a single linear amplifier. Perhaps more importantly, the biased voltage retained on each valve arm provides for an elevated stiffness in the ER system response about the zero reference operating point. This feature avoids the nearly zero gain of typical ER valves around zero valve voltage.

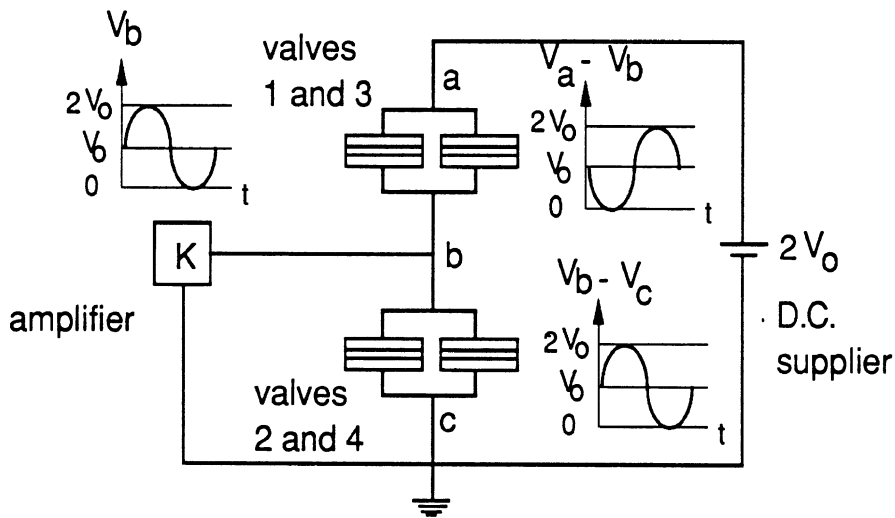


Fig. 2.2. Electric circuit for energizing the ER bridge

### **3. ER FLUID SUPPLY**

Studies were performed to find an effective way to pump ER fluids, whose solid phase poses various problems to conventional hydraulic pumps. A commercial centrifugal pump was tested and a special pumping mechanism was designed before a commercial diaphragm pump having suitable output pressure was found.

#### **3.1. A Commercial Centrifugal Pump**

As an initial trial, a pressure-booster pump (stock No. 2P280, 1 hp, 230 psi from Grainger, Inc.) was examined as a candidate for the ER fluid supply system. The pump worked satisfactorily with water and with conventional hydraulic oil as the circulated fluids. It failed, however, within two hours when a mixture of ER particulates and hydraulic oil was used. It is apparent that the ER fluid caused excessive friction along the sliding surfaces inside the pump, eventually causing overheating and failure of the thermoplastic components.

#### **3.2. A Special ER Fluid Pumping Mechanism**

In a parallel effort, a reciprocating type of pumping mechanism (Fig. 3.1) was designed. Two accumulators are used to separate the ER fluid from the hydraulic oil. This design was to avoid possible pump failure due to particulates in the ER fluid. For the system in Fig. 3.1 to work, the ER device test circuit must be a closed circuit, which makes it difficult to load ER fluids and to bleed air bubbles. If the twin accumulators are replaced with a double-diaphragm device as shown in Fig. 3.2, however, an open ER circuit is possible. Although this approach appeared to be workable, it was abandoned in this study when a commercial diaphragm pump having suitable output pressure was found.

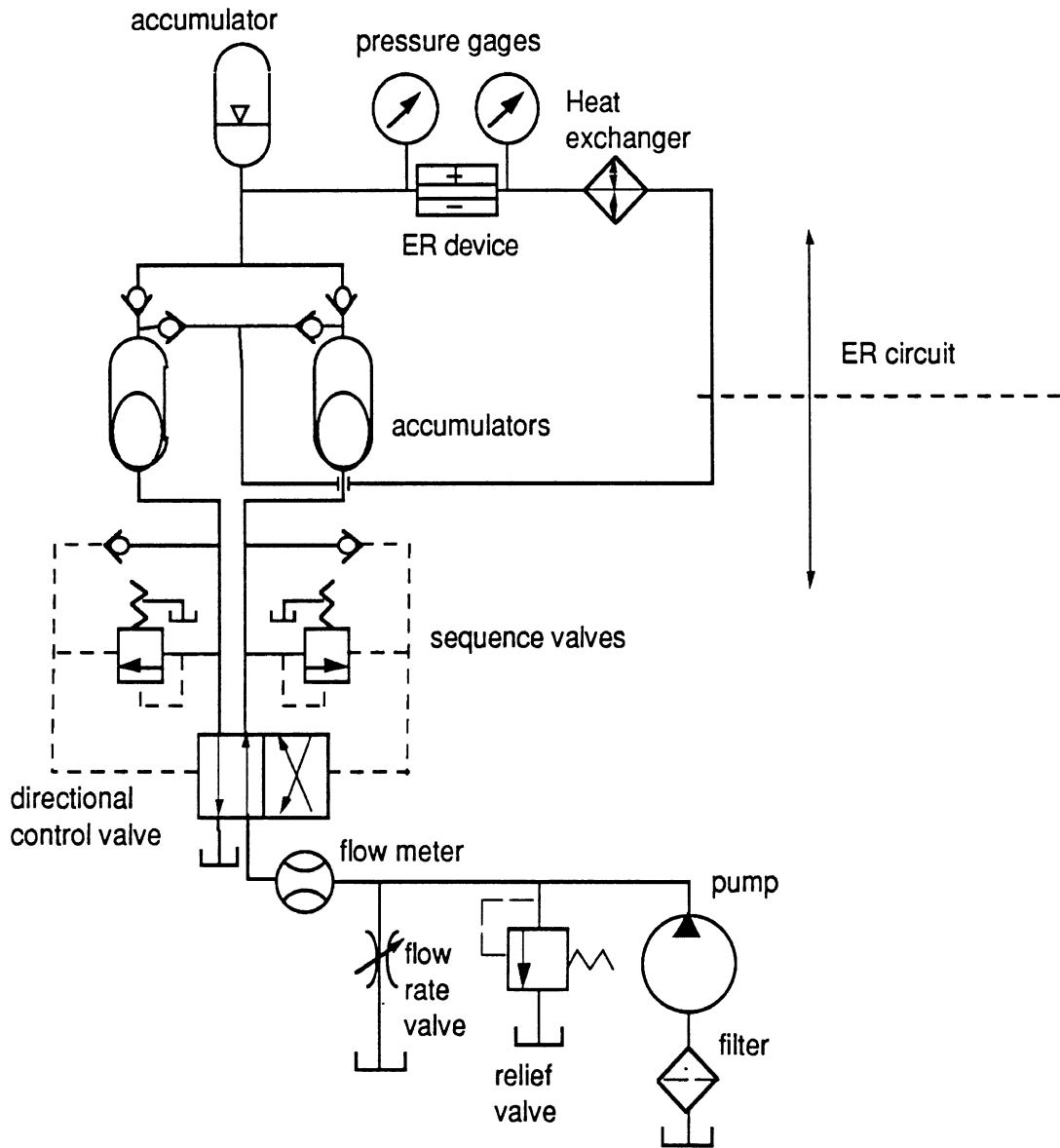


Fig. 3.1. An ER fluid pumping mechanism

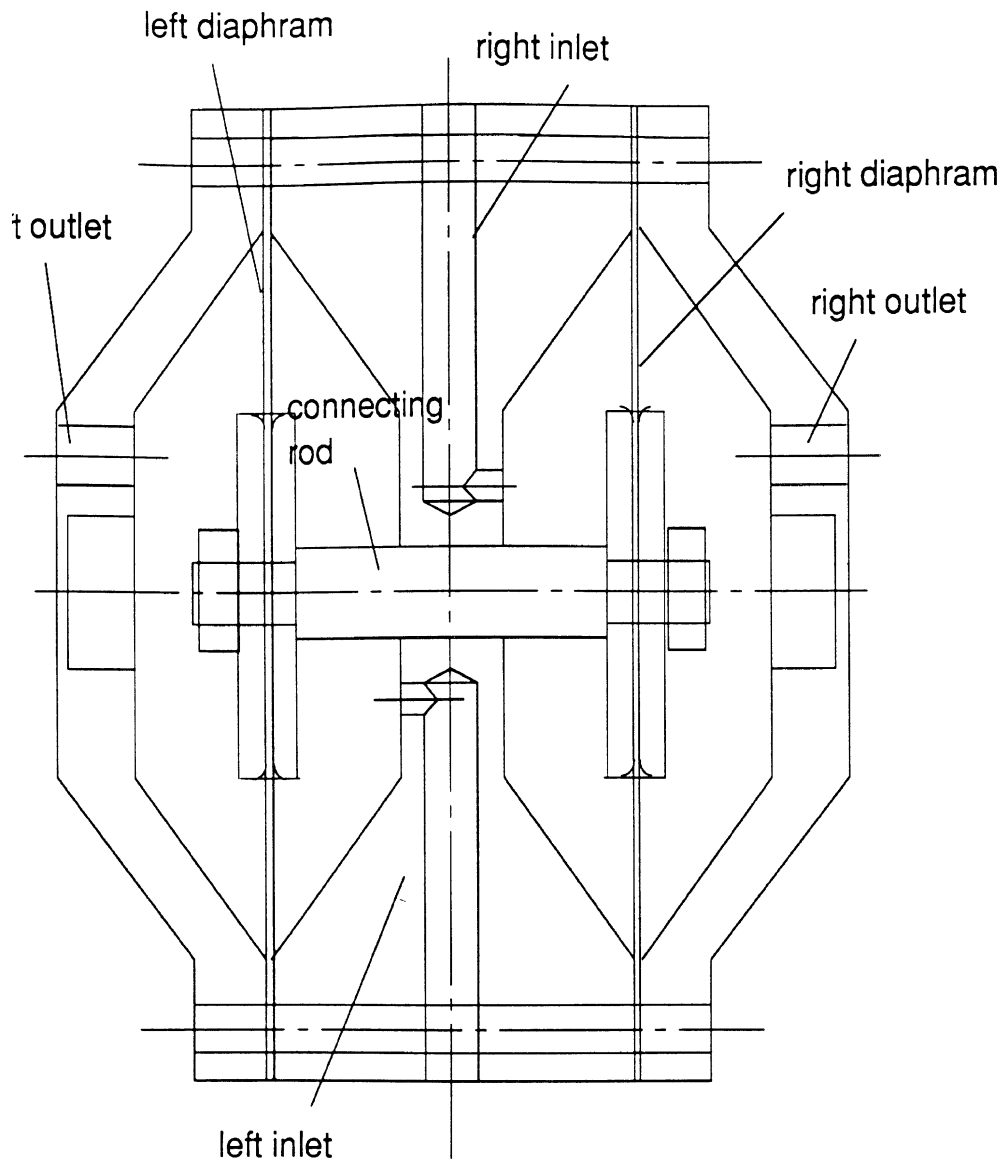


Fig. 3.2. A double-diaphragm ER fluid pumping component.

### 3. Diaphragm Pump

A commercial diaphragm pump, capable of delivering ER fluid at a flow rate of 0.8 gpm and a pressure of 225 psi or higher was obtained. It was calibrated for both kerosene-ER fluid (Fig. 3.3) and pure kerosene (Fig. 3.4). The output flow rate in gpm was measured using a graduated cylinder and a stopwatch while the flow rate control dial was varied. The pump output pressure was controlled by adjusting the downstream flow resistance. The output flow rate was found to be roughly linear to the dial value and was insensitive to the load pressure. Nevertheless, a dead zone was observed near the zero value on the flow-control dial. Some deviation in the calibrations was seen between the results obtained with pure kerosene and the higher viscosity ER fluid. Although this pump



proved to be quite reliable over the period of these experiments, it does exhibit pulsations in both output flow rate and pressure due to the reciprocating nature of its design.

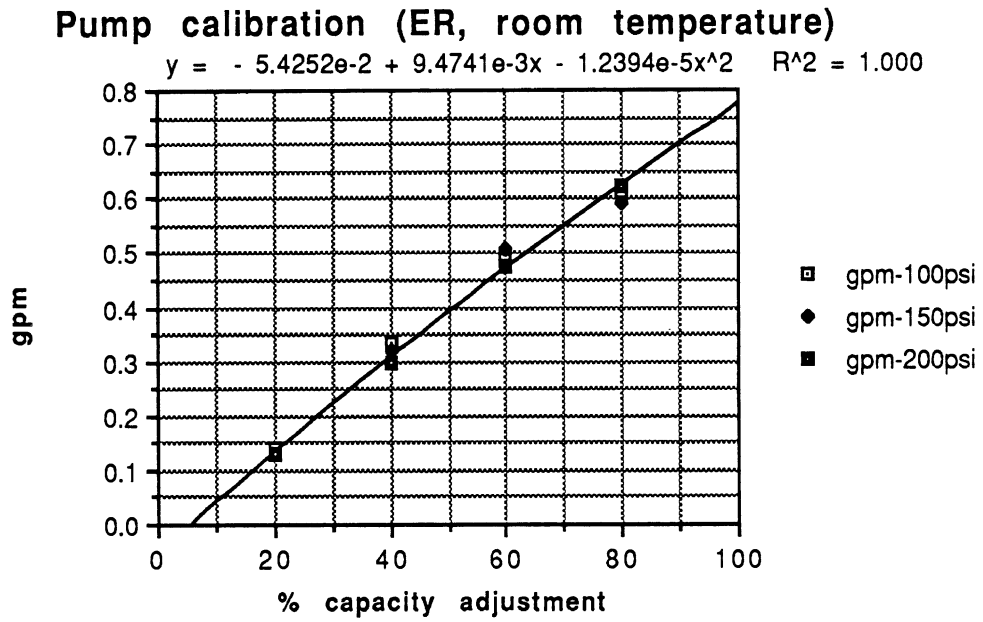


Fig. 3.3. Calibration of the diaphragm pump with an ER fluid.

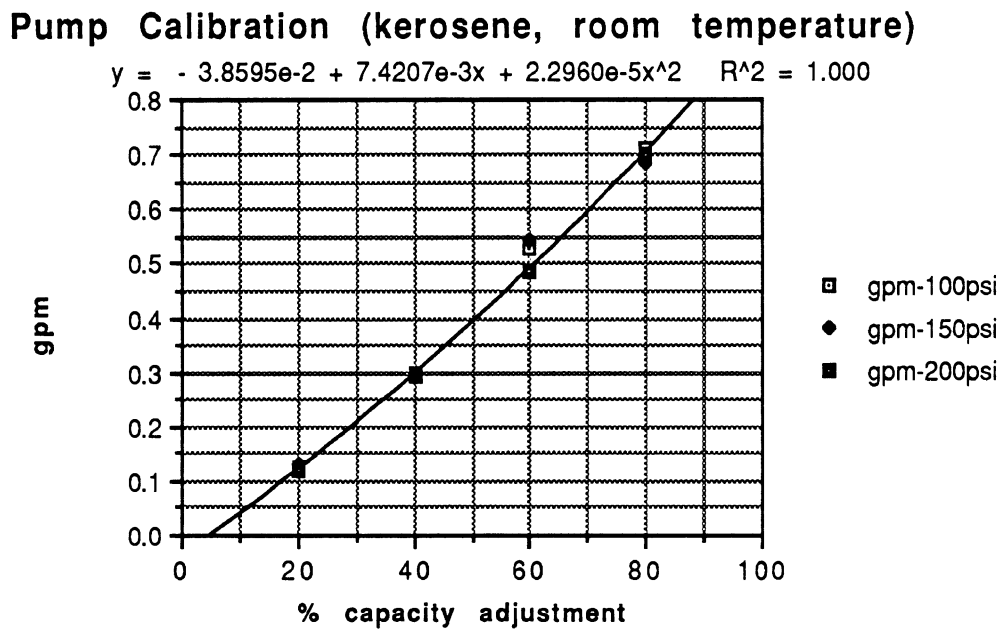


Fig. 3.4. Calibration of the diaphragm pump with kerosene.

### 3.4. Design of the ER Fluid Tank

A specialized tank or reservoir device was designed (Fig. 3.5) for storing ER fluid in the bridge-charging system. The fluid return line to this tank is immersed beneath the fluid surface to reduce or eliminate bubble generation. The tank was provided with two outlets. The pump draws relatively low or high density fluids from the upper or lower of these outlets. As a procedural convenience, it was occasionally necessary to pump the lower-density fluid into the system so as to (1) minimize the amount of ER particulate that would be lost during a partial disassembly of the apparatus, (2) to facilitate the bleeding of air bubbles, and (3) more readily flush accumulated particulate from portions of the system where insufficient flow occurs to maintain the suspension.

Alternatively, the normally high-density ER fluid is needed for a controlled operation. In these cases, the pump draws from the bottom tank port, accessing a relatively high solid content in the ER fluid which is mixed reasonably well due to flow agitation. It is nevertheless appropriate to observe that the fraction of particulate can vary substantially in a system of this type, especially during the initial period of system start-up.

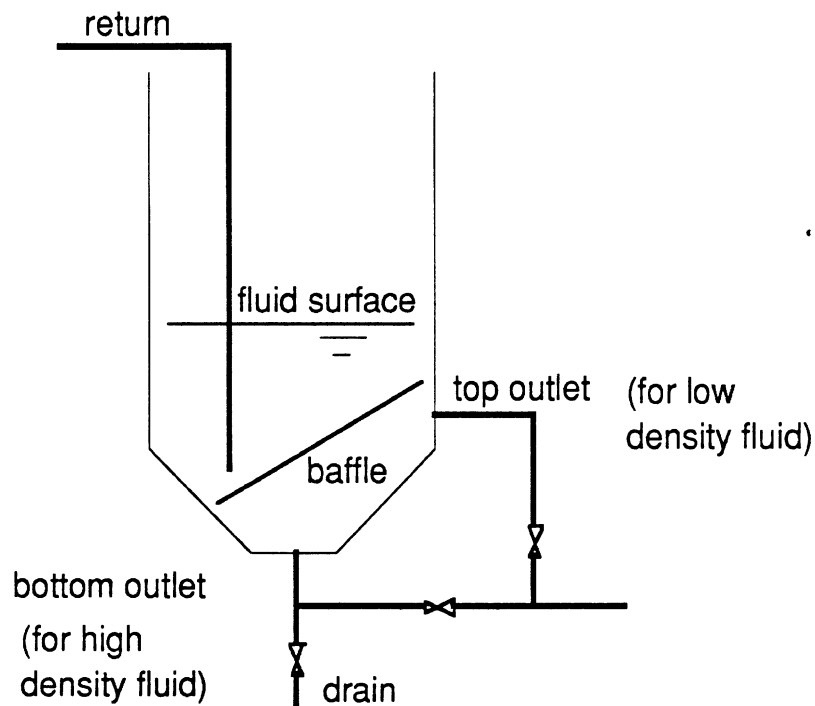


Fig. 3.5. ER fluid tank.

## 4. MODIFIED SERVO VALVE

### 4.1. General Scheme

A servo valve provided by the sponsor was modified to eliminate the electromagnetic torque motor element from the pilot stage. Fig. 4.1 illustrates the components of the valve which were provided for the hybrid operation, involving ER fluid and conventional hydraulic fluid. Drawings for the individual components of this assembly are in Appendix B. ER fluid is introduced to both ends of the spool through two ports which are in the original valve body. Diaphragms are used to prevent the ER fluid from entering the sliding clearance between the spool and sleeve. The forces from the diaphragms are transferred to the spool through two “connectors,” which slide within the cylinder sleeve. Two leak passages are drilled to channel leaking oil from the ends of the spool to the return port. Two sealing screws are used to separate the returning ports for the respective fluids. Two sealing nuts are used to seal the LVDT rod.

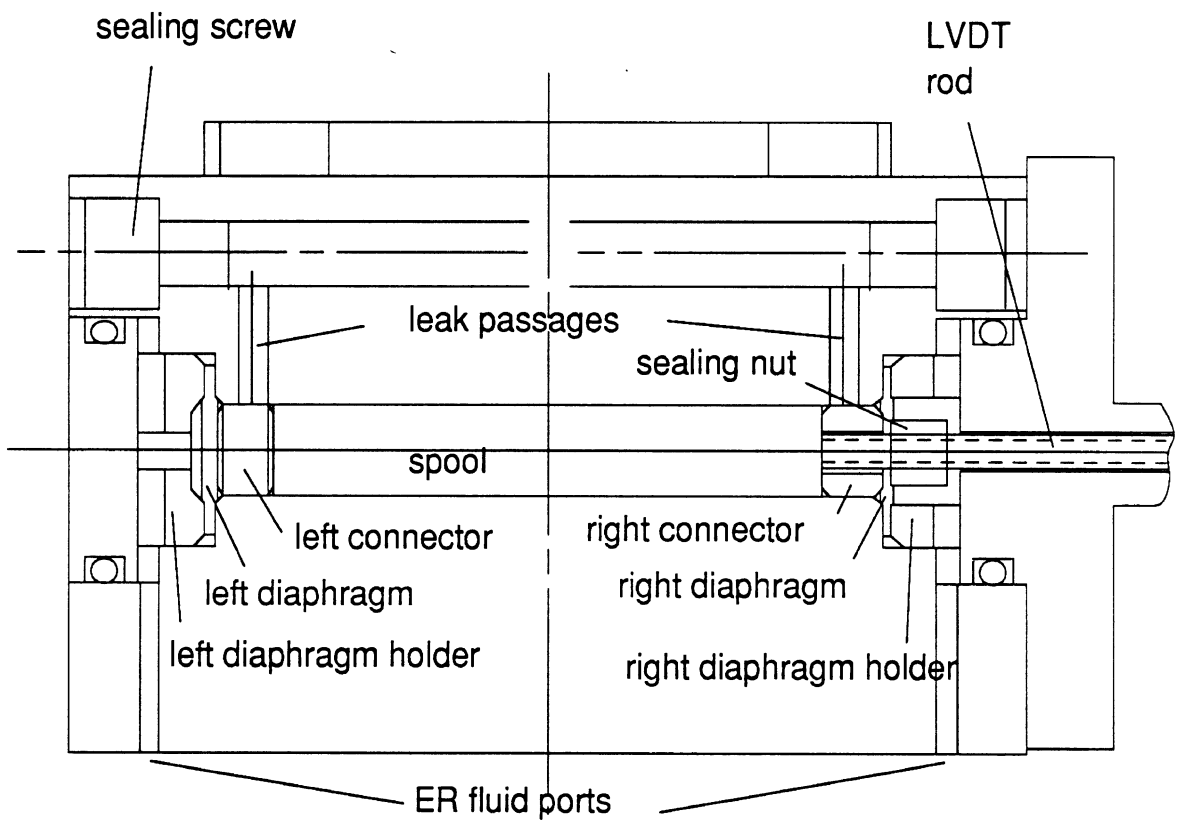


Fig. 4.1. Servo valve modifications

## 4.2. Forces on the Spool

In order to scale the level of differential pressure needed across the diagonal of the ER bridge, it was necessary to compute the peak forces required to move the power spool at the maximum mechanical frequencies of interest. This section describes this analysis.

For a four-way critical-center spool valve with a linear area gradient, no net damping length, no flow force compensation, and no reaction of the nozzle flow forces, Merritt<sup>2</sup> derived the following momentum equation

$$P_{LP}A_v = M_v \frac{d^2x_v}{dt^2} + 0.43w(P_s - P_L) x_v \quad \text{critical center} \quad (4.1)$$

where  $P_{LP}$  is the pilot valve load pressure,  $A_v$  the end area of the spool,  $M_v$  the spool mass,  $x_v$  the spool displacement,  $t$  the time,  $P_s$  the system pressure,  $P_L$  the load pressure, and  $w$  the spool wet perimeter or the area gradient. The term on the left hand side of the equation represents the driving force. On the right hand side of the equation, the first term depicts the inertia force, and the second one is the steady-state flow force. The steady-state flow force, like a spring, always tries to push the spool back to center or zero position, countering the driving force.

For an open-center servo valve, however, the steady-state flow force is twice that of a critical-center valve, and the momentum equation becomes

$$P_{LP}A_v = M_v \frac{d^2x_v}{dt^2} + 0.86w(P_s - P_L) x_v \quad \text{open center} \quad (4.2)$$

The valve used in this study happened to be an open-center valve. For example, when the actuator is locked, the entire output flow from the hydraulic pump (about 0.93 gpm) goes through the servo valve with a system pressure of about 400 psi. For an oil specific gravity of 0.9 and a discharge coefficient of 0.61, one gets

$$wU = 0.8677 \times 10^{-6} \text{ m}^2 \quad (4.3)$$

where  $U$  is the underlap. The underlap was also tested experimentally with a pressurized air line, and it was found to be slightly over (40/1000) in. If  $U = 40/1000 \text{ in} = 1.016 \text{ mm}$ , then one obtains

$$w = 0.854 \text{ mm.} \quad (4.4)$$

However, the maximum  $w$  value for the spool in question, whose diameter is 3/16", considering that the ports cover the full periphery of the spool, is 14.962 mm. Recognizing that it is difficult to measure  $w$  directly, we might only say that the real value of  $w$  is somewhere between 0.854 and 14.962 mm.

At  $P_{LP} = 250 \text{ psi}$ , the driving force is 6.9 lbf. At  $P_s = 3000 \text{ psi}$  and  $P_L = 0.0$  and with  $wx_v = wU = 0.8677 \text{ mm}^2$ , the steady-state flow force is 3.47 lbf. The inertia force from the spool mass is less than 1 lbf at 200 Hz.

This analysis shows that a 250 psi pressure differential should be sufficient to drive the spool up to 200 Hz. We should also note that, in the modified servo valve, there is also a nonlinear spring force from the diaphragms, which has not been characterized, but which acts equally on both ends of the spool.

### **4.3. Diaphragm and LVDT Problems**

When the valve was initially modified in the manner depicted in Fig. 4.1, there was an unbalanced fluid force, which tended to move the spool towards the right. It was suspected that internal hydraulic pressures at the two ends of the spool were causing an unbalanced spool force because of the asymmetry afforded by the LVDT installation through the right-side diaphragm. Also, the small hole in the right diaphragm, which was necessary to accommodate the LVDT rod, was a source of leakage. Therefore, the entire LVDT assembly was removed in the final version of the system, yielding a symmetric containment of the spool. Removal of the LVDT assembly strongly degrades the closed-loop system performance, however, such that any future system of this type should incorporate an alternative spool-displacement transducer, perhaps by strain-gaging the original leaf-type feedback spring.

## **5. ELECTRONIC CONTROL CIRCUIT**

### **5.1. Wave Generator**

A digital wave generator was used as the signal source, and its output consists of tiny step functions at a certain sampling frequency. When the load impedance seen by the following high-voltage amplifier has a relatively large capacitance, the amplifier's current output contains a large noise content at the sampling frequency. When this problem was encountered, the noise magnitude was substantially reduced by increasing the sampling frequency within the wave generator.

### **5.2. Error Signal Limit**

A large forward loop gain is required to produce suitable performance from the feedback control system. Thus, instantaneous error conditions result in extremely high output voltages even when the magnitude of the error signal is moderate. To prevent arcing from occurring within the ER valve, error signals were voltage-limited such that the maximum output from the high voltage amplifier was kept below the arcing range.

## 6. ER FLUID STABILITY

The zeolite-based ER fluid introduced in the phase-one report as "Fluid No. 2" was used throughout the position-control experiments. The fluid was prepared during summer of 1989 and was used briefly in the valve tester during the phase-one experiments<sup>1</sup>. The fluid sample was utilized throughout the testing activities of the current study, and was frequently replenished with commercially-available kerosene in order to recover from kerosene leakage in the system. Further "pollution" of this fluid sample occurred when diaphragms isolating the power spool ruptured, admitting conventional hydraulic oil into the ER fluid circuit. Even after this extent of mixing with the parent fluid sample, however, the polluted ER fluid still performed essentially as seen in the initial rheometry measurements. Perhaps this experience suggests that at least some ER fluids are rather robust in retaining their ER properties despite repeated replenishments of base liquid. Ability to tolerate contamination by conventional hydraulic oil is a fluke, of course, and would appear to have no general significance.

## 7. CHARACTERIZATION OF AN ER VALVE

### 7.1. Experimental Results

To facilitate the analysis and control of the bridge, a single ER valve has been tested and analyzed. The valve was constructed during the phase-one study but not tested because of apparatus problems. It has a length of 1 meter, a width of 1 cm and a gap of 1 mm. Figures 7.1 through 7.4 present test results using this single-chamber valve. In the figures, the pressure drop has a lower limit of 40 to 50 psi because, with the system accumulator pre-charged at this pressure, readings below this level are too noisy to be usefully measured. All the tests shown were performed under a room temperature of 69 deg. F without forced cooling of the fluid. Fluid temperature during the tests was between 80 to 90 deg. F. The reported pressure drop is the time-average value of the system pressure reading, assuming no return-line pressure loss.

The flow rate dial of the diaphragm pump was fixed at 40% (see Section 3.3) for Fig. 7.1 and 7.2 while the electric excitation frequency and the electric field strength were adjusted. Figure 7.1 shows that the pressure drop increases with the electric field strength, and that its dependence on the electric excitation frequency is rather complicated. At electric excitation frequencies beyond 60 Hz, the curves are flat, suggesting a bandwidth limit of the fluid/valve system. (The question of bandwidth limitations due to mechanical phenomena is pursued further in Section 7.2.)

Figure 7.2 depicts the electric current through the valve under the same conditions. In general, the current increases initially with both electric field strength and frequency. The frequency-related component is dominated initially by the capacitive effect, where peak current follows frequency linearly, but then shows a saturation due apparently to inherent changes in the fluid's impedance. It is interesting, but unexplained, that current begins to saturate in the same frequency region where the pressure curves become flat in Fig. 7.1. Clearly, since the current level drives the basic ER response, any increase in fluid impedance with frequency will cause the shear stress response to decline, while, conversely, capacitive effects cause increased currents which result in greater shear stresses.

The electric excitation frequency was set at 1 Hz for Fig. 7.3 and 7.4 while the flow rate and electric field strength were varied. The curve pattern in Fig. 7.3 looks similar to a typical shear stress vs. shear rate plot for a Bingham fluid. Since the pressure drop is proportional to the shear stress and the flow rate is proportional to the shear rate, one can conclude that the flow in a parallel-plate valve is similar to the flow mode in a shearing viscometer. Finally, Figure 7.4 reveals that the electric current increases with the field strength and is almost independent of the flow rate.



Q40%, no cooling, T0=69F, 2/22/91, fluid2

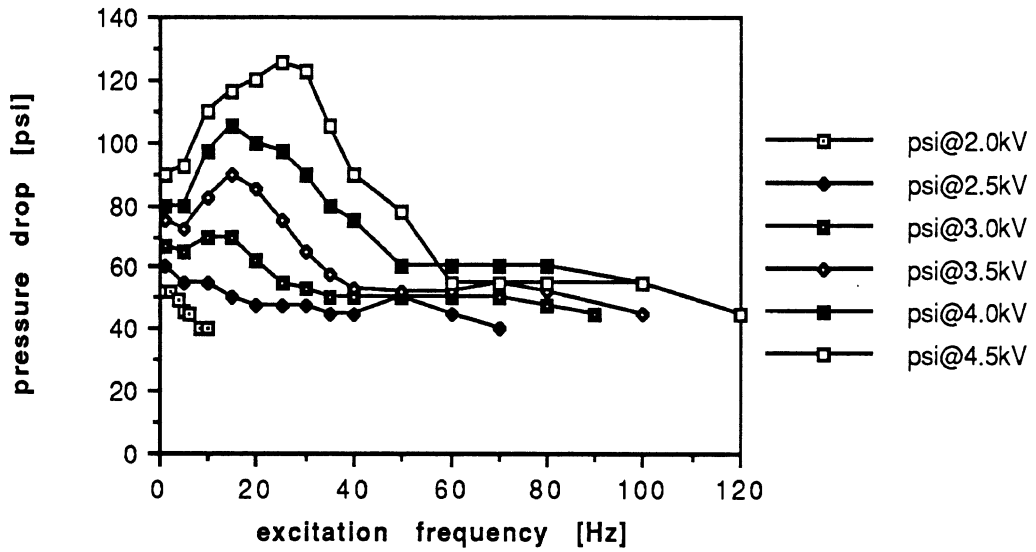


Fig. 7.1. Pressure drop through an ER valve versus electric excitation frequency at various electric field strengths.

Q40%, no cooling, T0=69F, 2/22/91, fluid2

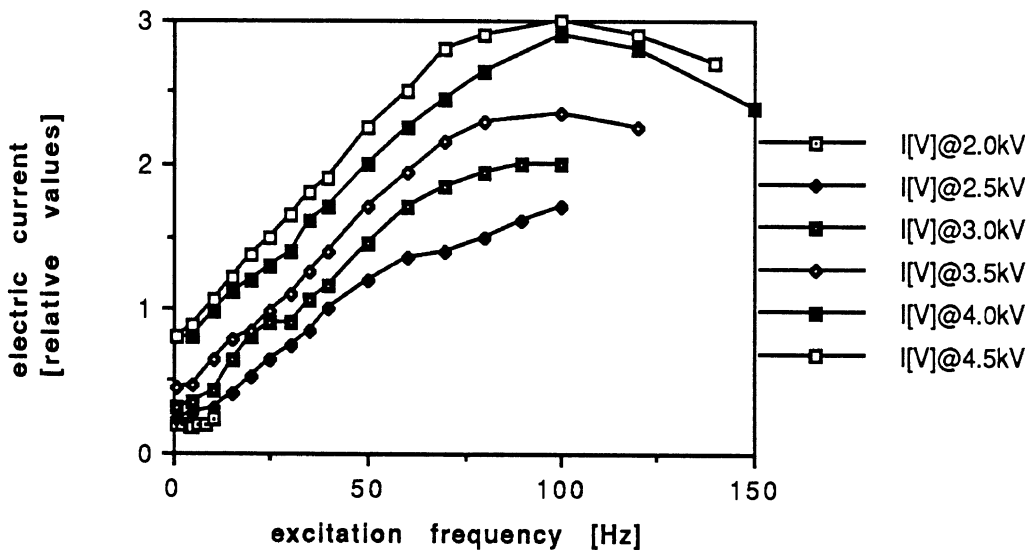


Fig. 7.2. Electric current through an ER valve versus excitation frequency at various levels of field strength.

1Hz, no cooling, T0=69F, 2/20/91, fluid2,

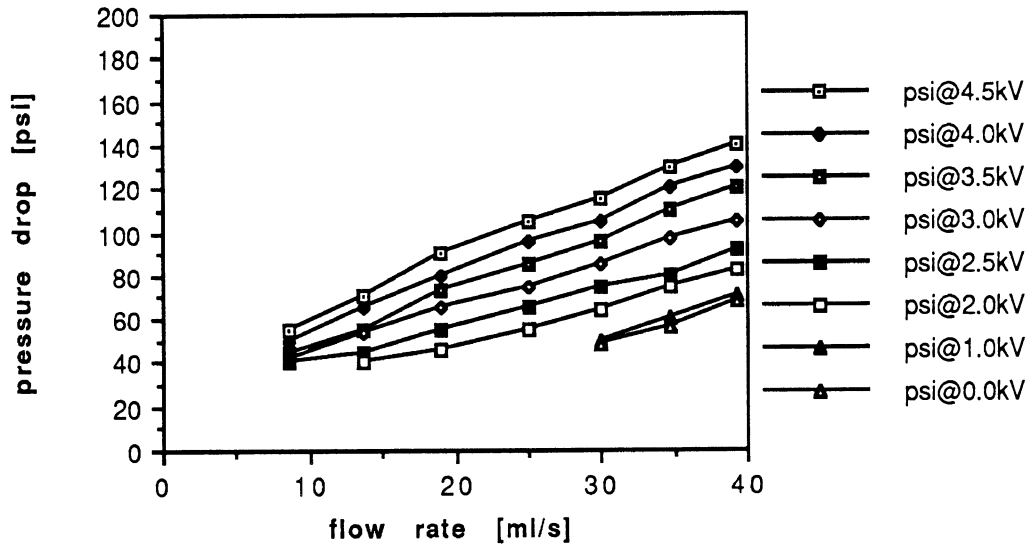


Fig. 7.3. Pressure drop through an ER valve versus flow rate at various electric field strengths.

1Hz, no cooling, T0=69F, 2/20/91, fluid2

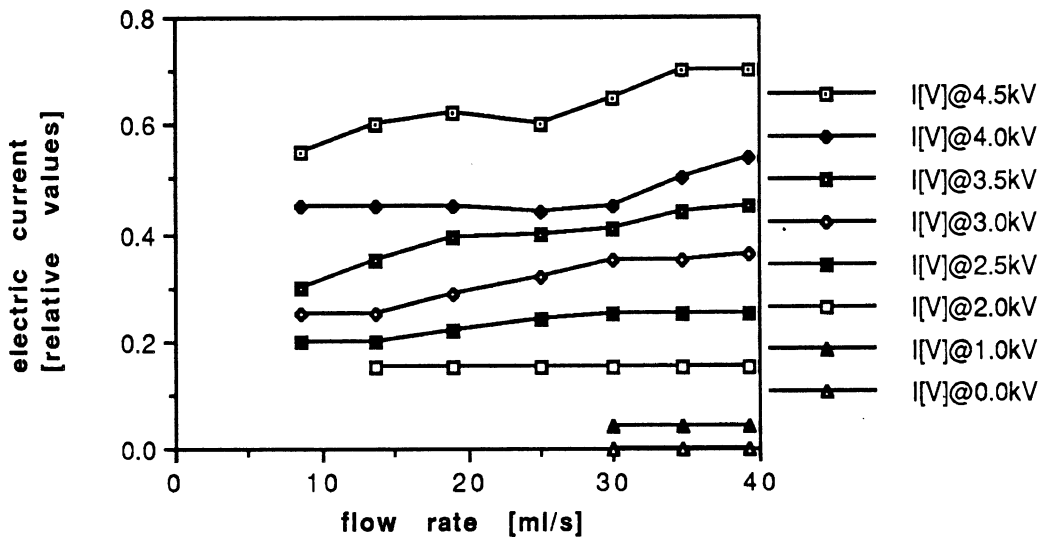


Fig. 7.4. Electric current through an ER valve versus flow rate at various electric field strengths.

## 7.2. Analysis to Approximate Limitations in Bandwidth

Although the ER fluid shear stress response to electric field exhibits a bandwidth in the kilohertz range, the fixed upper bound in shear stress reduces the actual bandwidth that can be realized with an assembled device. Some basic analysis has been performed to study the bandwidth limitations for a parallel-plate ER fluid valve.

For a parallel-plate valve with a length of  $L$ , a width of  $W$  and a fluid gap height of  $h$  (Fig. 7.5), the total fluid mass enclosed is

$$m = \rho (WhL) \quad (7.1)$$

where  $\rho$  is the fluid density. The control force on the fluid due to the electrorheologically-induced Bingham shear stress,  $\tau_y$ , can be approximated as,

$$F = 2 (WL) \tau_y \quad (7.2)$$

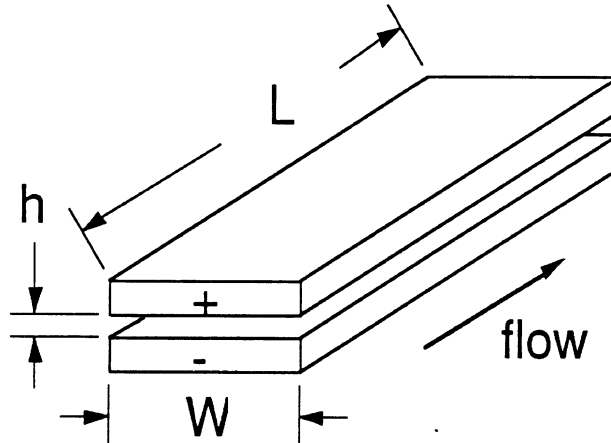


Fig. 7.5. Geometry of an ER valve

The Bingham shear stress can be changed sinusoidally with a peak stress of  $\tau_{y0}$ , thus modulating the flow through the valve section. If the frequency is  $f$  and  $u_0$  is the peak value of the mean velocity across the valve gap, the amplitude of the flow acceleration is  $2\pi f u_0$ . One can note that the most basic level of valve control requires that the amplitude of the ER-controlled force (due to shear stresses along the plate surfaces) should be equal to or greater than the peak inertia force, i.e., the mass times the amplitude of the acceleration prevailing at the desired bandwidth frequency. This inequality is expressed by

$$2 (WL) \tau_{y0} \geq \rho (WhL) 2\pi f u_0 \quad (7.3)$$

or

$$\tau_{y0} \geq \pi \rho h u_0 f \quad (7.4)$$

For fixed values of Bingham shear stress, fluid density, valve gap height and velocity amplitude, the valve can be controlled up to the frequency value,

$$f_n = \frac{\tau_{y0}}{\pi \rho h u_0} \quad (7.5)$$

which constitutes an obvious maximum bandwidth. We see that  $f_n$  is proportional to  $\tau_{y0}$  and inversely related to  $h$  and  $u_0$ . The corresponding flow rate amplitude is

$$Q_0 = hW u_0 \quad (7.6)$$

thus

$$f_n = \frac{W \tau_{y0}}{\pi \rho Q_0} \quad (7.7)$$

Figures 7.6 and 7.7 show the relationship between the bandwidth frequency and the flow rate amplitude at various values of Bingham stress limit for valves with width of 1 cm and 10 cm, respectively. A tenfold increase in  $W$ , from 1 cm to 10 cm, raises the bandwidth by a factor of 10 for a fixed flow rate amplitude, or conversely, raises the flow rate amplitude by a factor of 10 for a given bandwidth. For a valve with  $W = 10$  cm and a flow rate amplitude of 15.9 gpm, the bandwidth is 219.5 Hz. Clearly, the bandwidth will expand directly as the shear stress limits of the fluid are increased—through better formulation in the future.

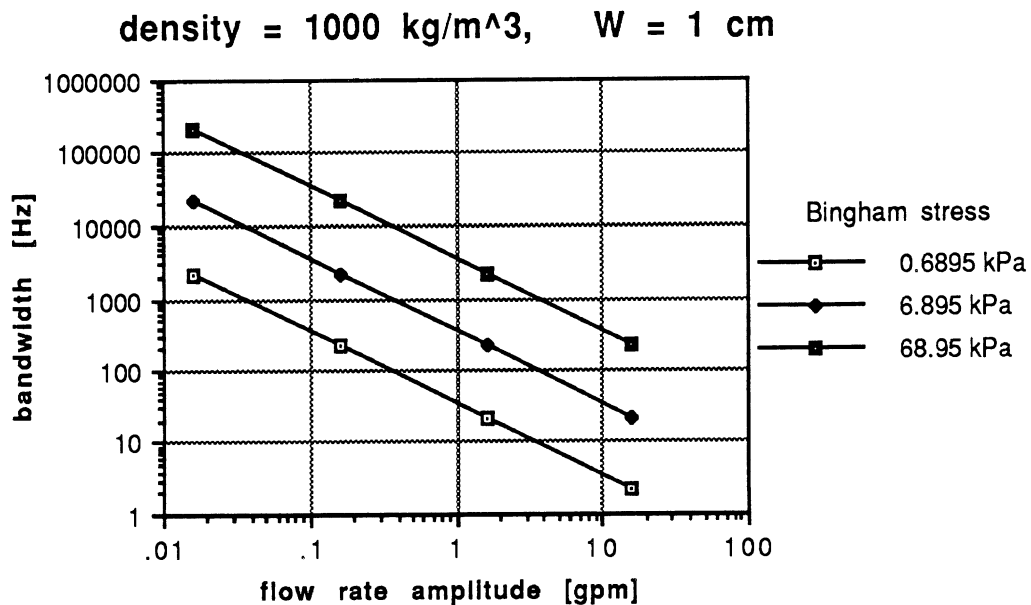


Fig. 7.6. Bandwidth and flow rate relationship for a valve with  $W = 1$  cm.

density = 1000 kg/m<sup>3</sup>, W = 10 cm

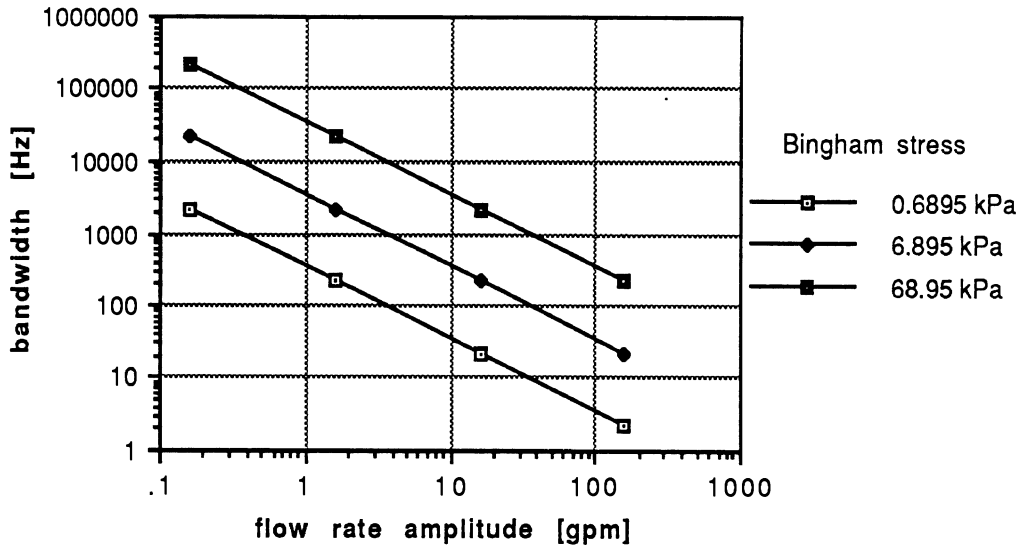


Fig. 7.7. Bandwidth and flow rate relationship for a valve with W = 10 cm.

For an example servo valve used in the ER servo position control system, the peak flow rate is

$$Q_0 = 2\pi A_{sp} x_0 f_n \quad (7.8)$$

where  $A_{sp}$  is the spool cross section area and  $x_0$  the stroke. The substitution of the above equation into Equation (7.7) results in

$$f_n = \sqrt{\frac{W\tau_{y0}}{2\pi^2\rho A_{sp}x_0}} \quad (7.9)$$

If  $W = 10$  mm,  $\tau_{y0} = 689.5$  Pa (0.1 psi),  $\rho = 1000$  kg/m<sup>3</sup>,  $A_{sp} = 17.82 \times 10^{-6}$  m<sup>2</sup>, and  $x_0 = 0.000254$  m (0.015 in), one gets  $f_n = 227$  Hz.

Finally, the bandwidth limitation considered here pertains only to the constraint imposed when inertial fluid stresses reach the ER shear stress limit. Further, this analysis provides only a crude approximation of the bandwidth-limiting phenomenon, for purposes of illustrating numerical values. To determine the bandwidth of an actual mechanical system, one must include the dynamics of the load as well as the effect of additional fluid mass in passages between the load and the valve.

## 8. BRIDGE CHARACTERIZATION

### 8.1. Experimental Results

Preliminary tests were performed on the ER bridge, itself, prior to its attachment to an active spool valve assembly. The flow passages within each arm of the bridge have gaps of 1 mm in height and a width of 1 cm. Each arm has a length of 1 meter.

Figures 8.1 and 8.2 show some of the test results. Again, fluid No. 2 was used, and the tests were performed at room temperature. The d.c. high voltage supply provided a constant voltage of 4 kV. For the test in Fig. 8.1, the flow rate dial was fixed at 90% (see the flow calibration in Section 3.3), and the amplitude of the a.c. signal was 2 kV such that the peak-to-peak amplitude of the final electric field strength on each arm was 4 kV/mm. The figures depict  $P_{\text{gage}}$  which is the ER fluid supply system pressure while  $P_{1\text{os\_pp}}$  and  $P_{2\text{os\_pp}}$  are peak-to-peak pressure readings on an oscilloscope screen, representing bridge output pressures,  $P_1$  and  $P_2$ , respectively. It is obvious from the displayed data that the behavior of the bridge is frequency dependent in a way which cannot be fully explained. If the bridge were symmetric, of course,  $P_{1\text{os\_pp}}$  and  $P_{2\text{os\_pp}}$  would be identical in their values rather than exhibiting the very different frequency responses seen in Figure 8.1.

The results shown in Fig. 8.2 were obtained when the frequency was fixed at 10 Hz and the flow rate dial at 50%. The peak-to-peak pressure readings increase with the input signal amplitude.

**Bridge-Test3-Hzs (2kVac, 4kVdc, 90%Q, fluid2, r.T)**

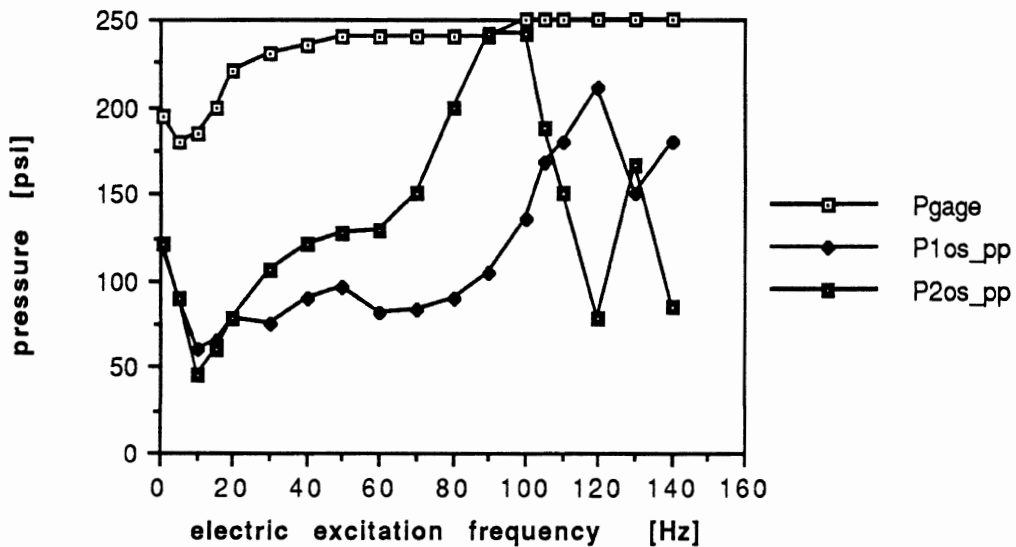


Fig. 8.1. Pressure readings versus electric excitation frequency for an ER bridge.

bridge-Test2-ACkVs (10Hz, 50%Q, fluid2, 4kVDC, 78F)

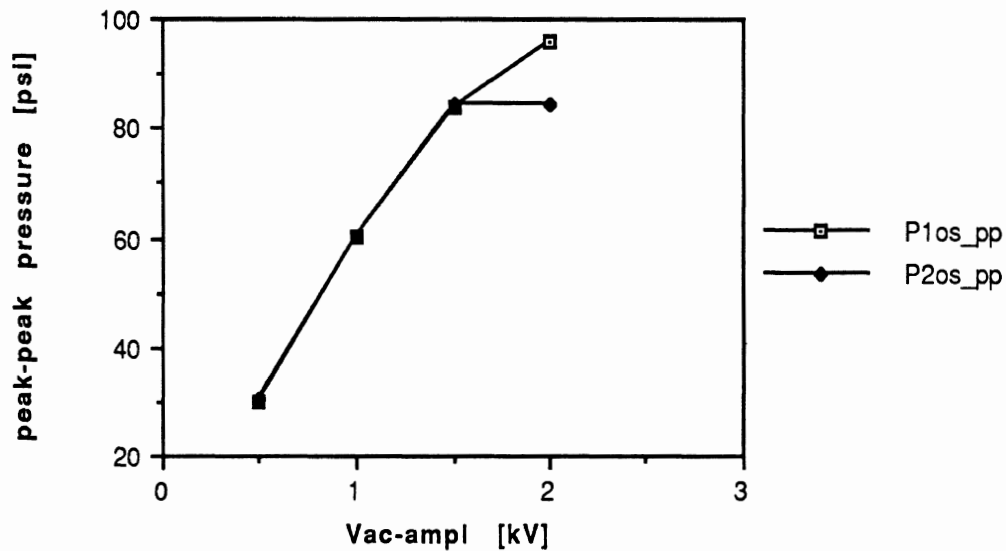


Fig. 8.2. Pressure readings versus electric field strength for an ER bridge.

## 8.2. Asymmetry in the ER Bridge

This discussion covers the mechanisms that might account for asymmetry in an ER bridge. As a reference for this discussion, Fig. 8.3 is introduced as the diagram of an ideal ER bridge, which experiences no flow resistance in any of its connecting passages. In this package, the only fluid impedances are located within the four electrorheologically-controlled resistors:  $R_1$ ,  $R_2$ ,  $R_3$ , and  $R_4$ .

A real or practical ER bridge, however, is more appropriately depicted by Fig. 8.4, where many more passive resistance elements exist within the connecting passages of the device. Even Fig. 8.4 is still somewhat simplified because resistors are shown as lumped elements instead of the distributed form which actually prevails.  $P_1$  and  $P_2$  in the figure are the actual locations of pressure sensors.

In a steady-state flow, the pressure drop or loss due to friction over a pipe of length  $L$  is

$$\Delta P_{s.s.} = 8\pi\mu Q \left( \frac{L}{A^2} \right) \quad \text{in a circular pipe} \quad (8.1)$$

where  $\mu$  is the viscosity,  $Q$  the flow rate and  $A$  the area. In a channel, however, the pressure drop is

$$\Delta P_{s.s.} = 8\pi\mu Q \left( \frac{3L}{2\pi wh^3} \right) \quad \text{in a channel} \quad (8.2)$$

where  $w$  is the channel width and  $h$  the gap. With the same flow rate and fluid viscosity, the frictional pressure loss for a steady-state flow is proportional to  $(L/A^2)$  for a circular pipe or  $(3L/2\pi wh^3)$  for a channel.

For an unsteady flow, the pressure loss due to the inertia term, for both a circular pipe and a channel, is

$$\Delta P_{inertia} = \rho \frac{dQ}{dt} \left( \frac{L}{A} \right) \quad (8.3)$$

where  $\rho$  is the density and  $t$  the time. With the same flow rate and fluid density, the inertial pressure loss is proportional to  $(L/A)$ . In an unsteady situation, the frictional loss is much more complicated and cannot be calculated using the equations for steady-state flow.

In the design of an ER bridge, it is preferable to make the connecting passages as short as possible and their cross sectional areas as large as possible, relative to those of the ER-controllable resistors, in order to reduce the pressure losses in the connecting circuit. However, passage lengths must obviously accommodate the physical arrangement and cross sectional areas will be limited by the need for compactness in the whole assembly.

Another important design criterion is to insure the symmetry of the bridge. The first step towards that goal is to design symmetric or identical controllable resistors:  $R_1$ ,  $R_2$ ,  $R_3$ , and  $R_4$ . The second step is to have symmetry in the ancillary passages. To do that, elements labelled in Figure 8.4 as  $RS_1$ ,  $RS_2$ ,  $RT_3$ , and  $RT_4$  should be identical;  $R_{14}$ ,  $R_{41}$ ,  $R_{23}$ , and  $R_{32}$  should be identical;  $R_{1L}$  and  $R_{2L}$  should be identical; and  $R_{141}$  and  $R_{232}$  should be identical. We observe that it is difficult to obtain perfect symmetry in these various connections. However, their influence on the symmetry of performance for the entire system can be reduced by cutting their absolute resistance values.

Table 8.1 shows the parametric values pertaining to the various resistor segments in the ER bridge used in this study. For those resistors that have pipes or passages whose cross section varies along their length, they are divided into sub-resistors: (a), (b), etc., and the total resistance is taken as the summation of sub-resistances. Sub-resistor  $RT(c)$ , for example, is a heat exchanger consisting of 25 small pipes in parallel. The total resistance is taken to be the equivalent of a parallel network of 25 individual resistors.  $L/A$  is the inertia resistance coefficient while  $L/A^2$  is the steady-state frictional resistance coefficient. Their normalized values, against the controllable resistor's values, are listed in the column with a superscript "\*." It is obvious that, in the actual bridge constructed for this project,  $\{R_1, R_2, R_3, \text{ and } R_4\}$  and  $\{R_{1L} \text{ and } R_{2L}\}$  are symmetric while  $\{RS_1, RS_2, RT_3, \text{ and } RT_4\}$ ,  $\{R_{14}, R_{41}, R_{23}, \text{ and } R_{32}\}$  and  $\{R_{141} \text{ and } R_{232}\}$  are not. The steady-state frictional resistances of the uncontrollable resistors is seen to be negligible—much less than 1%—compared with those of the ER-controllable elements. Thus, under steady state flow, the bridge appears virtually symmetric.

In a dynamic situation, the combined effect of  $RS$  and  $RT$  is as high as 20%, i.e. about 20% of the system pressure is lost along the pipes leading to and from the bridge. The



losses from other resistors are also relatively significant. The total asymmetry deriving from corresponding resistors,  $\{R_{14}, R_{41}, R_{23}, \text{ and } R_{32}\}$ , is 5.4%. This conclusion from analysis is consistent with our experimental observations that asymmetry is more prominent at higher frequencies, where inertial pressure losses are significant.

The above analysis of discrete resistances is valid for nominal, simplified, flow oscillation. A complete and precise analysis would take into account other factors such as the phase relation between the frictional and inertial losses, their interference, flow-developing regions, etc. Furthermore, possible asymmetry in electric circuit elements may also be important.

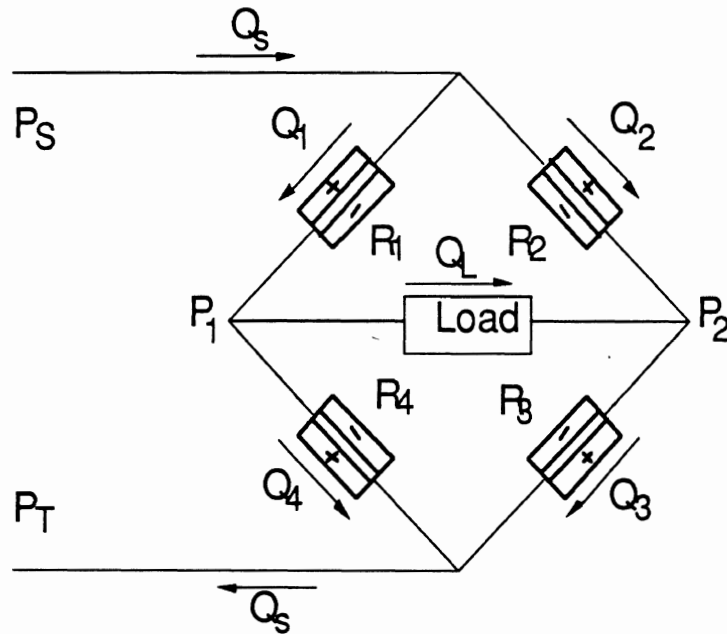


Fig. 8.3. An ideal ER bridge.

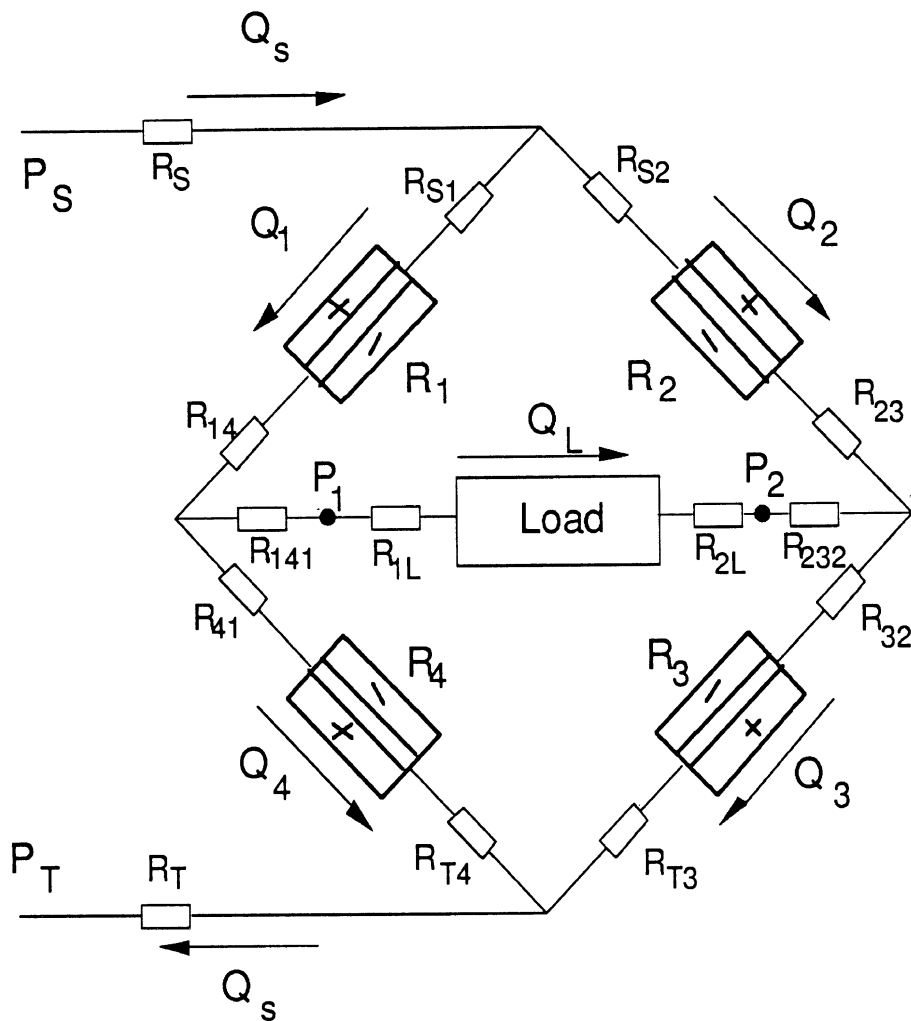


Fig. 8.4. An actual ER bridge.

### 8.3. A Surrogate Servo Valve

A surrogate servo valve (Fig. 8.5) was fabricated to evaluate the performance of the tiny spool-isolation diaphragms without risking damage to the servo valve. In particular, there was concern that introduction of ER particulates could harm the lapped finish on the spool. The surrogate valve borrowed most of the parts from the real one except for the valve body and spool. The surrogate was employed simply for testing the effect of ER fluid flow on the diaphragm. Although this test showed positive results, the introduction of high pressure hydraulic fluid to the spool-side of the diaphragms in the real valve later caused diaphragm rupture due to inadequate drain passages at the ends of the spool. This problem was corrected by improving the mechanical support for the diaphragms when their deflection exceeded a certain working range.

Table 8.1. Resistors in the ER bridge.

resistor	D	L	A	L/A	(L/A)*	L/A <sup>2</sup>	(L/A <sup>2</sup> )*
R1		40.000	0.0150	2667	1.000	795774	1.0000
R2		40.000	0.0150	2667	1.000	795774	1.0000
R3		40.000	0.0150	2667	1.000	795774	1.0000
R4		40.000	0.0150	2667	1.000	795774	1.0000
RS(a)	0.5000	13.000	0.1963	66	0.025	337	0.0004
RS(b)	0.3125	13.000	0.0767	169	0.064	2210	0.0028
RS				236	0.088	2547	0.0032
RT(a)	0.5000	12.000	0.1963	61	0.023	311	0.0004
RT(b)	0.3125	20.000	0.0767	261	0.098	3400	0.0043
RT(c)	0.2130	17.000	0.0356	478		13414	
25RT(c)				19	0.007	537	0.0007
RT				341	0.128	4248	0.0053
RS1	0.2500	1.500	0.0491	31	0.011	623	0.0008
RS2	0.2500	3.500	0.0491	71	0.027	1453	0.0018
RT4	0.2500	1.200	0.0491	24	0.009	498	0.0006
RT3	0.2500	3.000	0.0491	61	0.023	1245	0.0016
R14		0.000		0	0.000	0	0.0000
R41	0.2500	3.500	0.0491	71	0.027	1453	0.0018
R23	0.2500	3.500	0.0491	71	0.027	1453	0.0018
R32		0.000		0	0.000	0	0.0000
R141	0.2500	4.000	0.0491	81	0.031	1660	0.0021
R232	0.2500	4.500	0.0491	92	0.034	1868	0.0023
R1L(a)	0.2500	1.000	0.0491	20	0.008	415	0.0005
R1L(b)	0.1250	0.750	0.0123	61	0.023	4980	0.0063
R1L				81	0.031	5395	0.0068
R2L(a)	0.2500	1.000	0.0491	20	0.008	415	0.0005
R2L(b)	0.1250	0.750	0.0123	61	0.023	4980	0.0063
R2L				81	0.031	5395	0.0068

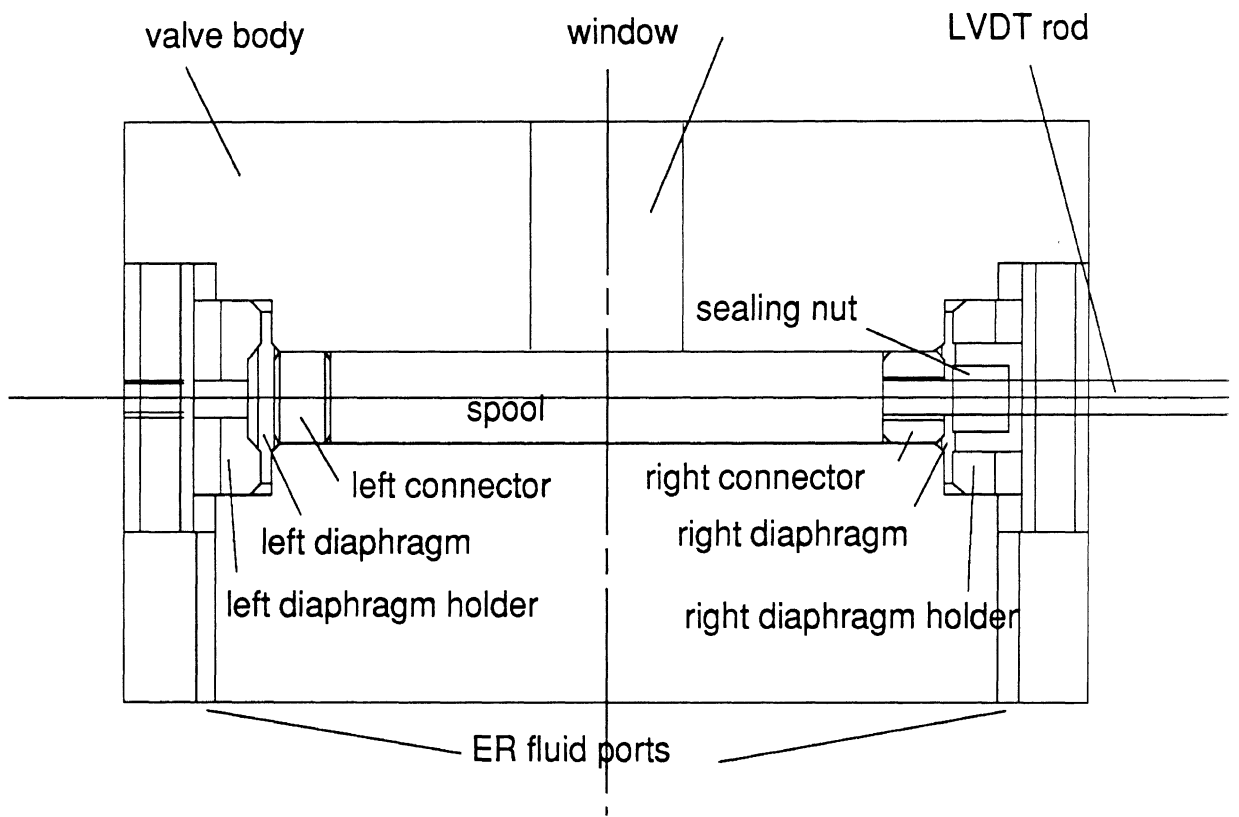


Fig. 8.5. A surrogate servo valve.

## 9. THE FULLY-ASSEMBLED SYSTEM

The full position-control servomechanism was assembled and demonstrated at the conclusion of the project. It did function in a closed-loop manner, responding to set-point position commands and achieving zero steady-state errors. Because of removal of the LVDT as a spool-position transducer, however, and the inability to develop high fluid pressures across the very under-lapped spool, system dynamic performance was minimal and was not explicitly measured.

One incident worth noting, for its experiential value, was a short circuit that appeared in the ER bridge during these tests. It was discovered that a virtual short (100 ohms resistance between adjacent valve electrodes) was derived from an inadvertent over-voltage excitation of the bridge which cause repeated and prolonged arcing between two plates within the bridge assembly. In the electronic control circuit, the error signal limit had been accidentally set at 8 kV, instead of the intended 4 kV level. The nylon insulation plate between two electrodes had become carbonized due to the arcing right at its edge, thus producing a failed, conductive section, approximately 10 mm in diameter, as seen in Fig. 9.1. This observation prompts the view that since (a) inadvertent arcing may be inevitable, sooner or later, then (b) it should be designed-for. That is, we should seek insulation materials which, if subjected to intense local heating due to nearby arcing, will fail in a manner that does not provide a low-resistance electrical path. Otherwise, an unstable condition is possible by which a temporary short causes resistance to decline, thus locally-elevating the current to thereby cause further heating, breakdown, and finally very low levels of sustained resistance.

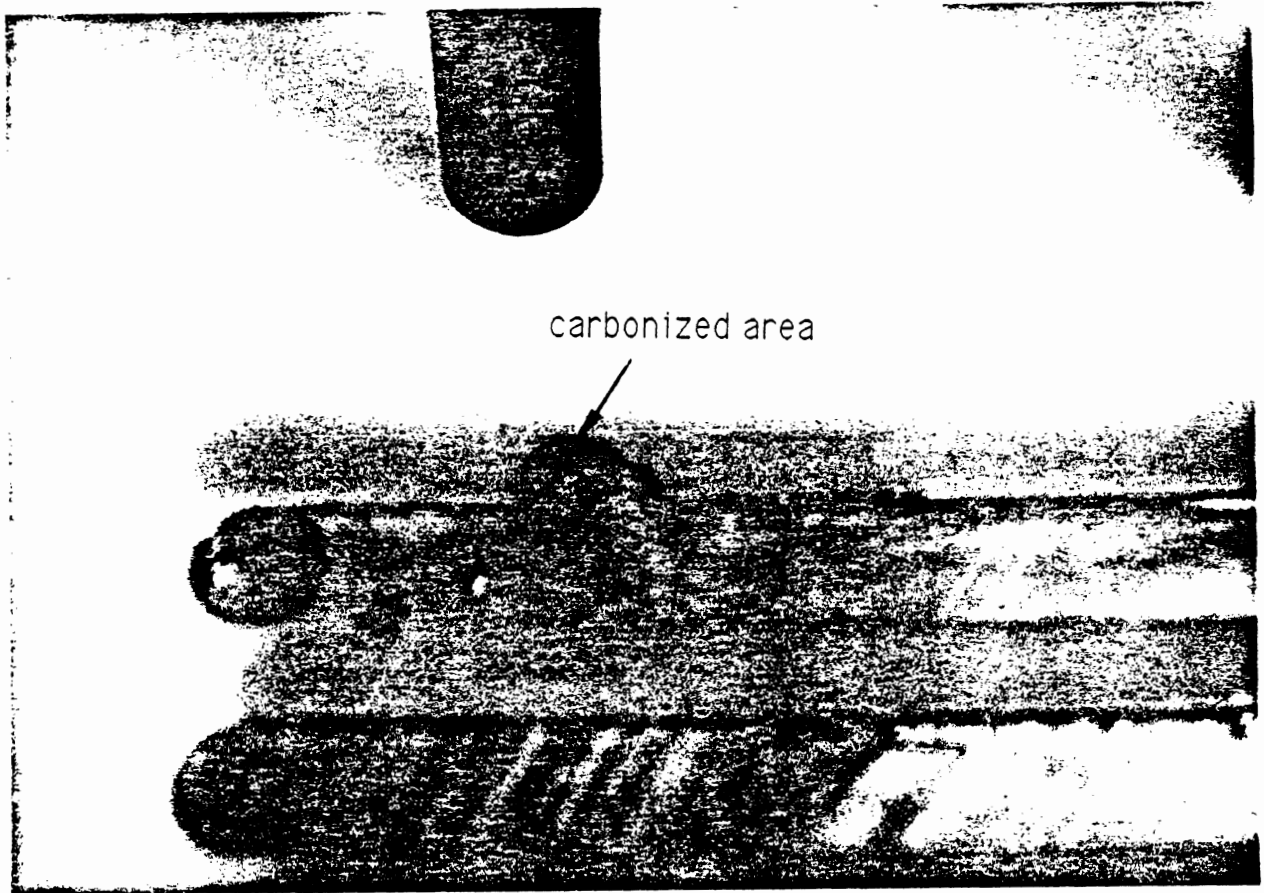


Fig. 9.1. Carbonized breakdown of a nylon plate, due to arcing.

## 10. A NUMERICAL SIMULATION

A numerical simulation of the dynamics of the entire position control system, including the description of the flow field within the ER bridge valves, was attempted but not finished due to time and budget limitations. The modelling effort is documented here as the possible point of departure for follow-on work. Since the ER stage is extremely nonlinear, it was necessary to construct a highly-generalized numerical simulation in order to approach the problems of system tuning in an orderly manner.

### 10.1. Mathematical Model

The simulation program follows the scheme outlined in Fig. 10.1. In the figure, an arrow from variable A to variable B indicates that variable B is dependent on variable A. A line of double arrows depicts an interdependency. An arrow with a solid line implies a direct calculation while one with a dotted line indicates a feedback or iteration procedure. Physical locations of most of the variables are shown in Fig. 1.1.

Each time step of the simulation starts with an input actuator or piston position signal  $x_{pin}$ , which, together with feedback signals from the spool valve and output piston positions ( $x_v$  and  $x_{pout}$ ), gives an appropriate error signal  $V_{error}$ . Through the controller and high voltage amplifier,  $V_{error}$  is translated and adjusted to  $V_v$ , a variable voltage, which, coupled with  $V_{dc}$ , the d.c. supply voltage, generates electric fields  $E_1$ ,  $E_2$ ,  $E_3$ , and  $E_4$  in four arms of the bridge

$$E_1 = E_3 = \frac{V_{dc} - V_v}{h} \quad (10.1)$$

$$E_2 = E_4 = \frac{V_v}{h} \quad (10.2)$$

In each arm, the electric field strength controls the Bingham yield shear stress of the fluid

$$\tau_{yj} = CE_j^n \quad j = 1, 2, 3, \text{ and } 4 \quad (10.3)$$

where  $C$  is some proportional constant and  $n$  an exponent, both of which are experimentally obtained.

Next, computational fluid dynamics is applied in each arm to obtain flow velocity profiles. The flow is assumed to be one-dimensional across the gap. The momentum equation is

$$\frac{\partial u}{\partial t} = \frac{1}{\rho} \frac{\Delta P}{L} + \frac{\eta}{\rho} \left( \frac{\partial \phi}{\partial y} \frac{\partial u}{\partial y} + \phi \frac{\partial^2 u}{\partial y^2} \right) \quad (10.4)$$

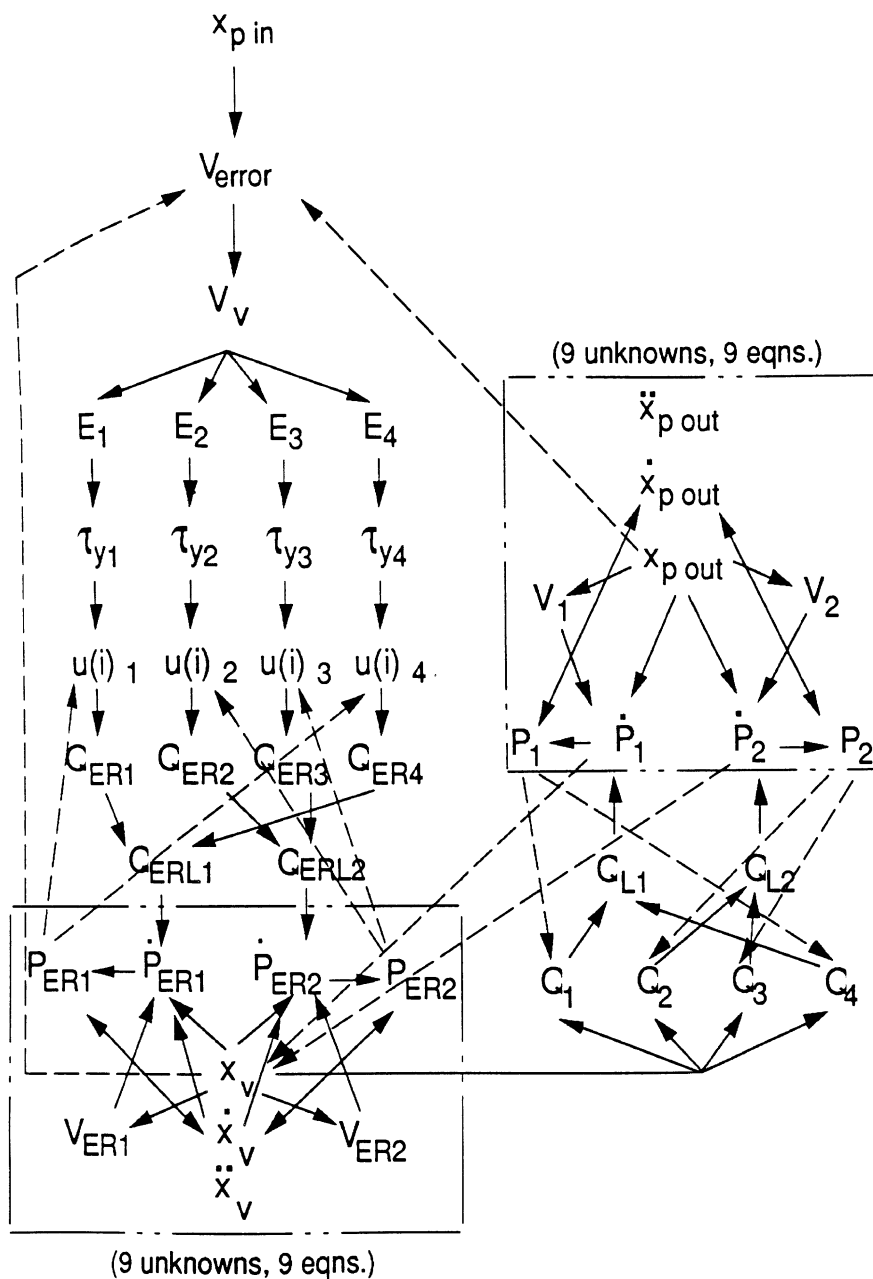


Fig. 10.1. Flow chart for a numerical simulation.

where  $u$  is the velocity,  $\eta$  the plastic viscosity,  $\rho$  the density,  $\Delta P$  the pressure drop,  $L$  the valve length,  $y$  the displacement in the gap, and  $\phi$  the viscosity function, which has the following weak form,

$$\phi = 1 + \frac{\tau_y}{\eta \frac{\partial u}{\partial y}} [1 - \exp(-n \left| \frac{\partial u}{\partial y} \right|)] \quad (10.5)$$



where n is of some finite value.

The pressure drops for arms 1, 2, 3 and 4, respectively, are

$$\Delta P_1 = P_{SER} - P_{ER1} \quad (10.6)$$

$$\Delta P_2 = P_{SER} - P_{ER2} \quad (10.7)$$

$$\Delta P_3 = P_{ER2} - P_{TER} \quad (10.8)$$

and

$$\Delta P_4 = P_{ER1} - P_{TER} \quad (10.9)$$

where  $P_{SER}$  and  $P_{TER}$  are the system and tank pressures of the ER fluid supply, respectively, while  $P_{ER1}$  and  $P_{ER2}$  are two output pressures of the ER bridge.

In each arm, the domain is discretized into individual nodes, at which velocities,  $u(i)j$  with  $i = 1, 2, \dots, imax$ , and  $j = 1, 2, 3, \text{ and } 4$ , are obtained, where  $imax$  is the number of nodes in a domain. Then, flow rates in the arms,  $Q_{ER1}$ ,  $Q_{ER2}$ ,  $Q_{ER3}$ , and  $Q_{ER4}$ , are acquired through integrating the velocities.

The bridge load flow rates are related to flow rates in the arms as

$$Q_{ERL1} = Q_{ER1} - Q_{ER4} \quad (10.10)$$

$$Q_{ERL2} = Q_{ER3} - Q_{ER2} \quad (10.11)$$

The momentum equation of the pilot main stage is

$$(P_{ER1} - P_{ER2})A_v = m_v \frac{d^2 x_v}{dt^2} + B_f \frac{dx_v}{dt} + (K_f + K_d)x_v \quad (10.12)$$

where  $A_v$  is the spool end area,  $m_v$  the spool mass,  $B_f$  the damping coefficient to transient flow force,  $K_f$  the flow force spring rate and  $K_d$  the spring constant of the diaphragms.

Further,

$$K_f = 0.43w(P_s - P_L) \text{ for a critical-centered valve}$$

$$K_f = 0.86w(P_s - P_L) \text{ for an underlapped valve}$$

$$B_f = (L_2 - L_1)C_d w \sqrt{\rho(P_s - P_L)}$$

where  $L_1$  and  $L_2$  are servo valve port distances, and they are normally equal, resulting in a zero value for  $B_f$ . The continuity gives

$$Q_{LER1} = A_v \frac{dx_v}{dt} + \frac{V_{ER1}}{\beta_{eER}} \frac{dP_{ER1}}{dt} \quad (10.13)$$

$$Q_{LER2} = A_v \frac{dx_v}{dt} - \frac{V_{ER2}}{\beta_{eER}} \frac{dP_{ER2}}{dt} \quad (10.14)$$

where  $VER_1$  and  $VER_2$  are the ER fluid volumes, between the ER bridge and the spool, on the left and right hand sides, respectively, while  $\beta_{eER}$  is the effective bulk modulus of the ER fluid which has to account for the rigidity in the structure as well as in the fluid.  $VER_1$  and  $VER_2$  are calculated using the relation,

$$VER_1 = VER_{10} + A_v x_v \quad (10.15)$$

and

$$VER_2 = VER_{20} - A_v x_v . \quad (10.16)$$

Using an implicit finite difference method, one gets

$$\frac{dP_{ER1}}{dt} = \frac{1}{2\Delta t} (3P_{ER1} - 4P_{ER1}^{p1} + P_{ER1}^{p2}) \quad (10.17)$$

$$\frac{dP_{ER2}}{dt} = \frac{1}{2\Delta t} (3P_{ER2} - 4P_{ER2}^{p1} + P_{ER2}^{p2}) \quad (10.18)$$

$$\frac{dx_v}{dt} = \frac{1}{2\Delta t} (3x_v - 4x_v^{p1} + x_v^{p2}) \quad (10.19)$$

$$\frac{d^2x_v}{dt^2} = \frac{1}{\Delta t^2} (2x_v - 5x_v^{p1} + 4x_v^{p2} - x_v^{p3}) \quad (10.20)$$

where the superscripts  $p_1$ ,  $p_2$  and  $p_3$  refers to “past time step,” “past past time step” and “past past past time step.” Among 9 equations, (10.12) to (10.20), there are 9 unknowns,  $P_{ER1}$ ,  $dP_{ER1}/dt$ ,  $P_{ER2}$ ,  $dP_{ER2}/dt$ ,  $x_v$ ,  $dx_v/dt$ ,  $dx_v^2/dt^2$ ,  $VER_1$ , and  $VER_2$ , and the system of equations can be solved analytically.

For a critical centered valve, the port flow rates are

$$Q_1 = \begin{cases} C_d w x_v \sqrt{2(P_S - P_1)/\rho} & x_v > 0 \\ 0 & x_v \leq 0 \end{cases} \quad (10.21)$$

$$Q_2 = \begin{cases} -C_d w x_v \sqrt{2(P_S - P_2)/\rho} & x_v < 0 \\ 0 & x_v \geq 0 \end{cases} \quad (10.22)$$

$$Q_3 = \begin{cases} C_d w x_v \sqrt{2(P_2 - P_T)/\rho} & x_v > 0 \\ 0 & x_v \leq 0 \end{cases} \quad (10.23)$$

$$Q_4 = \begin{cases} -C_d w x_v \sqrt{2(P_1 - P_T)/\rho} & x_v < 0 \\ 0 & x_v \geq 0 \end{cases} \quad (10.24)$$

where  $C_d$  is the discharge coefficient, and  $w$  the area gradient of each port. From continuity, one gets the load flow rates for the main stage,

$$Q_{L1} = Q_1 - Q_4 \quad (10.25)$$

and

$$Q_{L2} = Q_3 - Q_2. \quad (10.26)$$

The momentum equation for the actuator is

$$(P_1 - P_2)A_p = m_p \frac{d^2x_p}{dt^2} + B_p \frac{dx_p}{dt} + K_p x_p + F_L \quad (10.27)$$

where  $P_1$  and  $P_2$  are the actuator load pressures,  $A_p$  the piston area,  $m_p$  the piston mass,  $x_p$  the piston displacement,  $B_p$  the piston damping constant,  $K_p$  the piston spring constant and  $F_L$  other load forces.

The requirement for continuity leads to

$$Q_{L1} = A_p \frac{dx_p}{dt} + \frac{V_1}{\beta_{e1}} \frac{dP_1}{dt} + C_{im}(P_1 - P_2) + C_{em}P_1 \quad (10.28)$$

and

$$Q_{L2} = A_p \frac{dx_p}{dt} + \frac{V_2}{\beta_{e2}} \frac{dP_2}{dt} + C_{im}(P_1 - P_2) - C_{em}P_2 \quad (10.29)$$

where  $\beta_{e1}$  and  $\beta_{e2}$  are the effective hydraulic fluid bulk moduli,  $C_{in}$  the internal leakage constant,  $C_{em}$  the external leakage constant, and  $V_1$  and  $V_2$  the fluid volumes at two sides of the actuator, which can be further expressed as

$$V_1 = V_{10} + A_p x_p \quad (10.30)$$

and

$$V_2 = V_{20} - A_p x_p \quad (10.31)$$

where  $V_{10}$  and  $V_{20}$  are zero position values for  $V_1$  and  $V_2$ , respectively.

Using an implicit finite difference method, one gets

$$\frac{dP_1}{dt} = \frac{1}{2\Delta t} (3P_1 - 4P_1^{p1} + P_1^{p2}) \quad (10.32)$$

$$\frac{dP_2}{dt} = \frac{1}{2\Delta t} (3P_2 - 4P_2^{p1} + P_2^{p2}) \quad (10.33)$$

$$\frac{dx_p}{dt} = \frac{1}{2\Delta t} (3x_p - 4x_p^{p1} + x_p^{p2}) \quad (10.34)$$

and

$$\frac{d^2x_p}{dt^2} = \frac{1}{\Delta t^2} (2x_p - 5x_p^{p1} + 4x_p^{p2} - x_p^{p3}) \quad (10.35)$$

Among 9 equations, (10.27) to (10.35), there are 9 unknowns,  $P_1$ ,  $dP_1/dt$ ,  $P_2$ ,  $dP_2/dt$ ,  $x_p$ ,  $dx_p/dt$ ,  $dx_p^2/dt^2$ ,  $V_1$  and  $V_2$ , and the system of equations can be solved analytically.

## **10.2. Programs**

The programs found in Appendix C have been written for implementing the above calculation although the debugging process has not been finished due to budget and time restrictions.

## 11. CONCLUSIONS

An electrorheological (ER) servo position control system has been designed, fabricated and assembled to test the feasibility of using ER fluids in a control system which is similar to flight-control servos. In a pilot-valve stage of this system, an ER bridge has been shown to be successful in producing a controlled pressure differential up to 250 psi for driving the spool of a power-stage valve.

Upon closing the loop around the position of a hydraulic cylinder, the assembled system was able to control the motion of the actuator in slow-speed scenarios. Lack of refinement of certain details in the power-stage valve prevented the system from achieving any dynamic performance levels worth measuring.

Throughout the process of system testing, ER fluid samples were seen to be stable and consistent in performance.

Both analysis and experiment showed that although the ER response phenomenon, itself, exhibits a bandwidth in the kilohertz range, the fixed upper bound in ER shear stress reduces the actual bandwidth of an assembled device. With a peak yield shear stress of 0.1 psi, the valve devices assembled here were computed to have a maximum possible bandwidth of 227 Hz.

The basic analysis underlying a rather complete numerical simulation was formulated. Its future application in a computer code would provide for detailed examination of the nonlinear system, including interactions between the ER effect, fluid electrical impedances, fluid mechanics, and the tailoring of system control signals to account for these interactions. Incorporation of the state-of-knowledge in such a model requires assimilation of the substantial literature in ER and related areas, such as is documented in the compiled bibliography, in Appendix E.

## REFERENCES

1. Lou, Z., Ervin, R.D. & Filisko, F.E. *The Feasibility of Using Electro-Rheological Fluids in Aircraft Flight Controls: Phase 1 Report*. (UMTRI 90-10, University of Michigan Transportation Research Institute, Ann Arbor, 1990).
2. Merritt, H.E. *Hydraulic Control Systems* 1-358 (John Wiley & Sons, New York, 1967).
3. Reiner, M. *Amer. J. Mathematics* **47**, 350-362 (1945).
4. Reiner, M.A. *Lectures in Theoretical Rheology* (North Holland Publishing Company, Amsterdam, 1960).
5. White, F.M. *Viscous Fluid Flow* (McGraw-Hill, New York, 1974).
6. Gorodkin, R.G., Korobko, Ye. V., Blokh, G.M., Gleb, V.K., Sidorova, G.I., and Ragotner, M.M. *Fluid Mech. - Sov. Res.* **8**, 48-61 (1979).

**APPENDIX A. PRINTS FOR THE ER BRIDGE  
COMPONENTS**

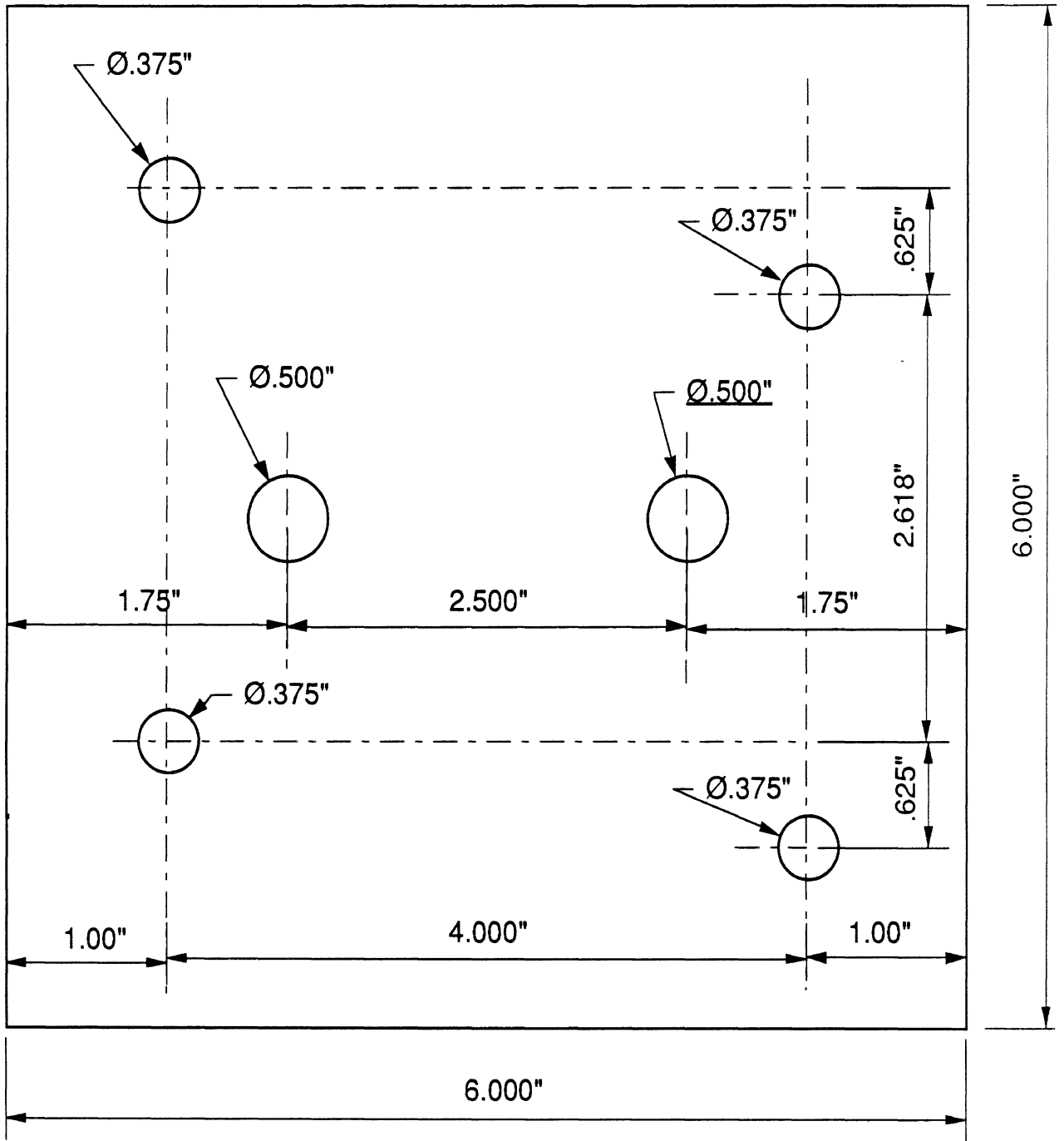
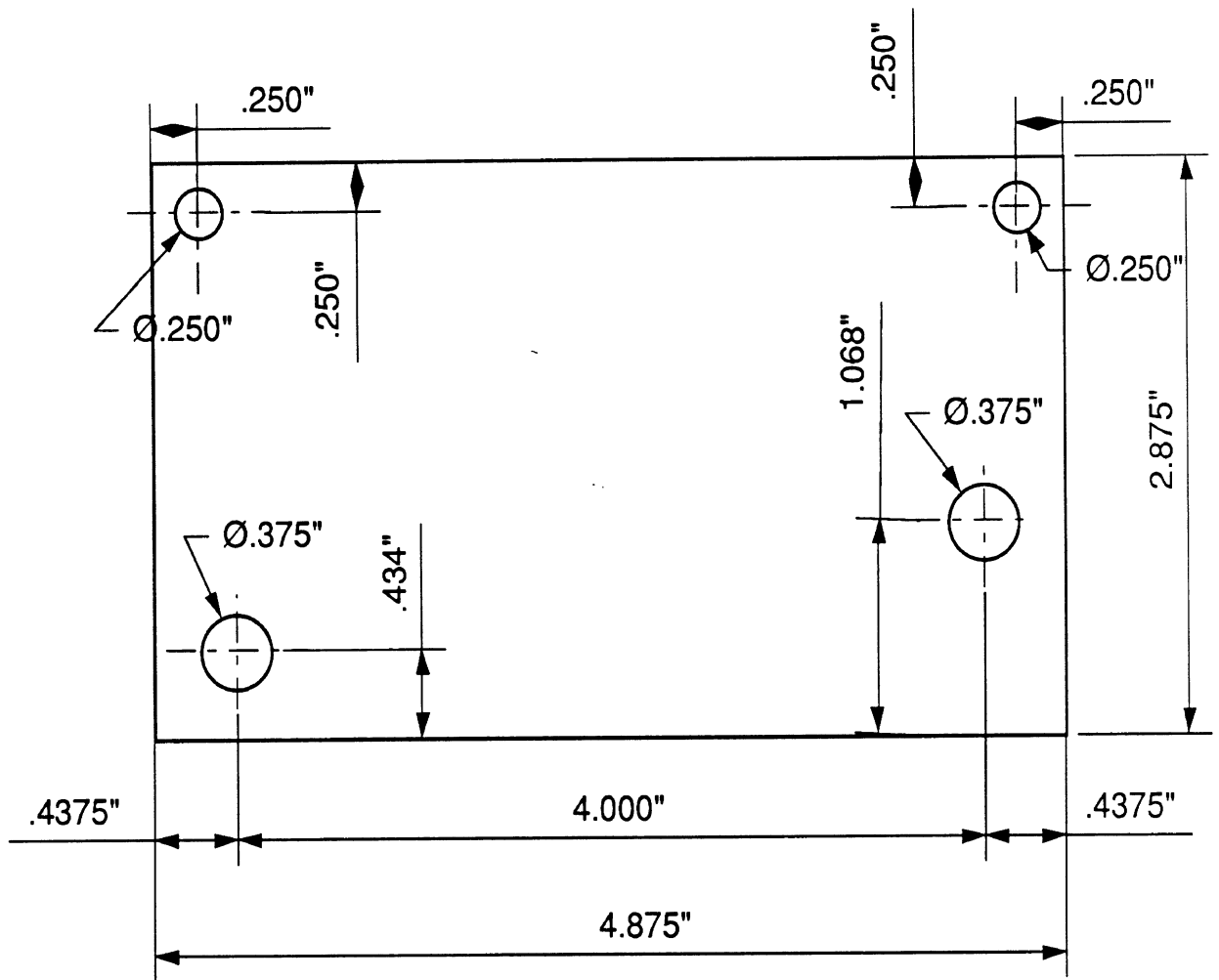


Fig. A.1. Insulator.





Material: Stainless steel  
 Thickness: 0.0781", i.e. 14 ga.

Fig. A.2. Side electrode.

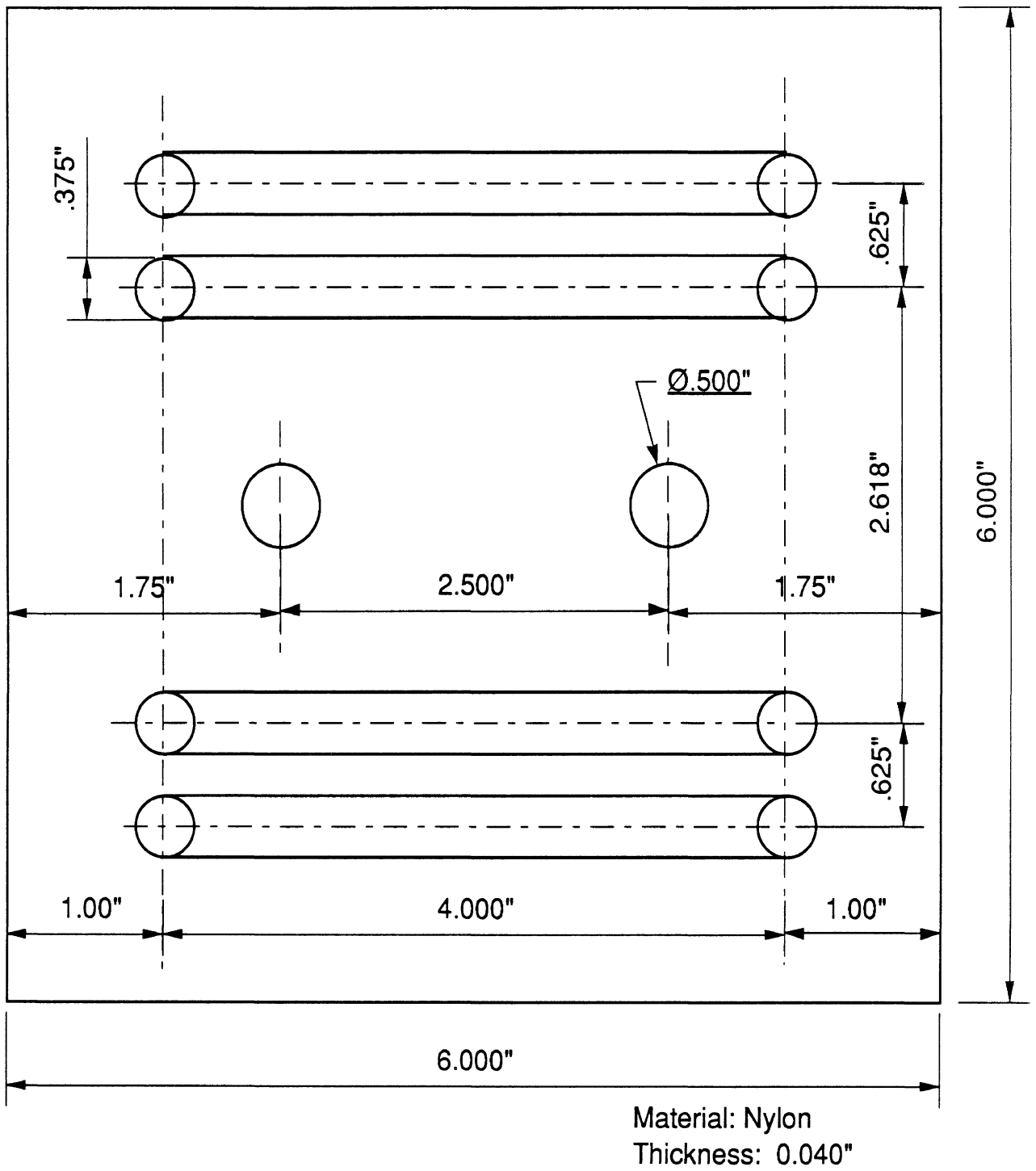
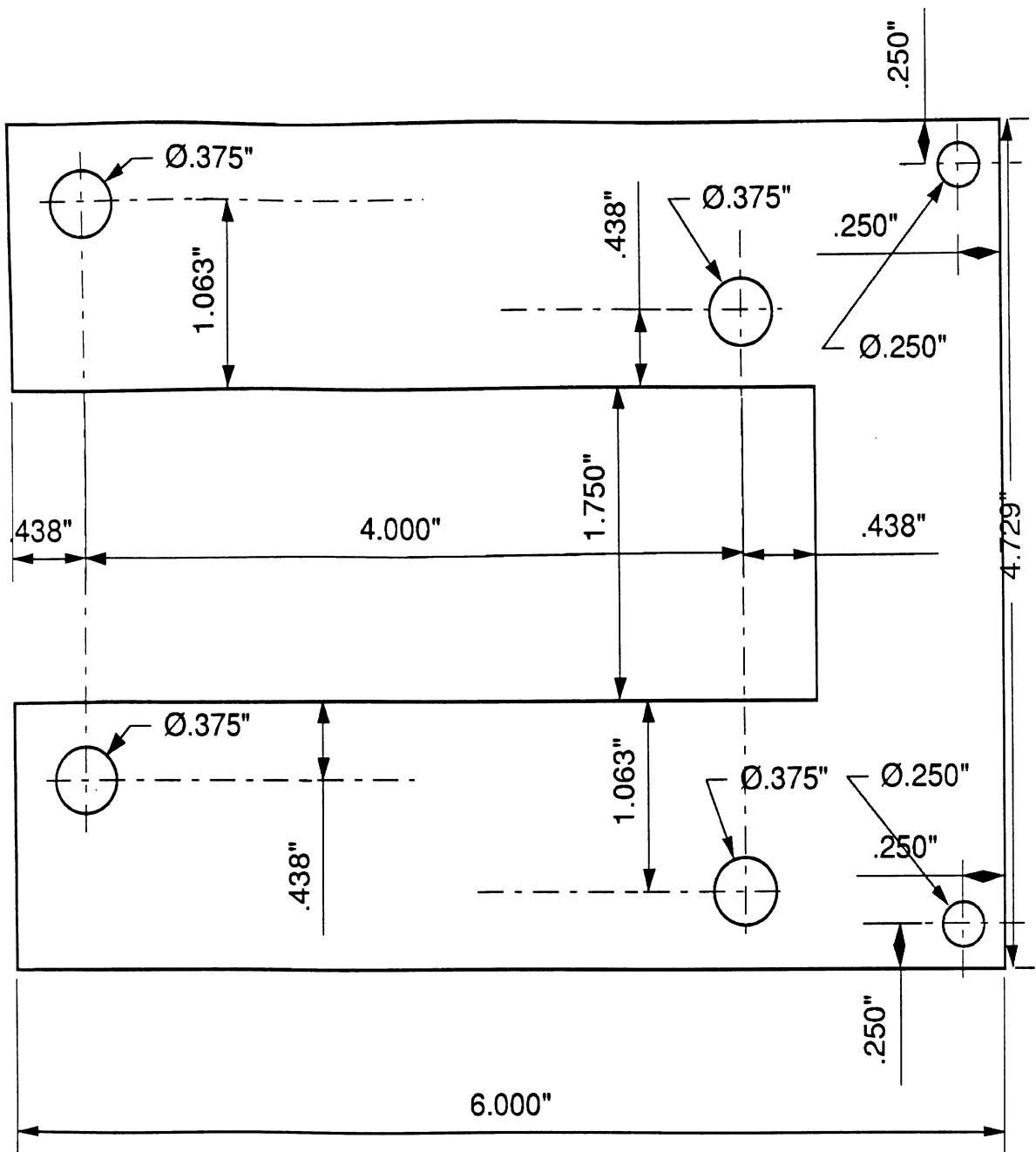
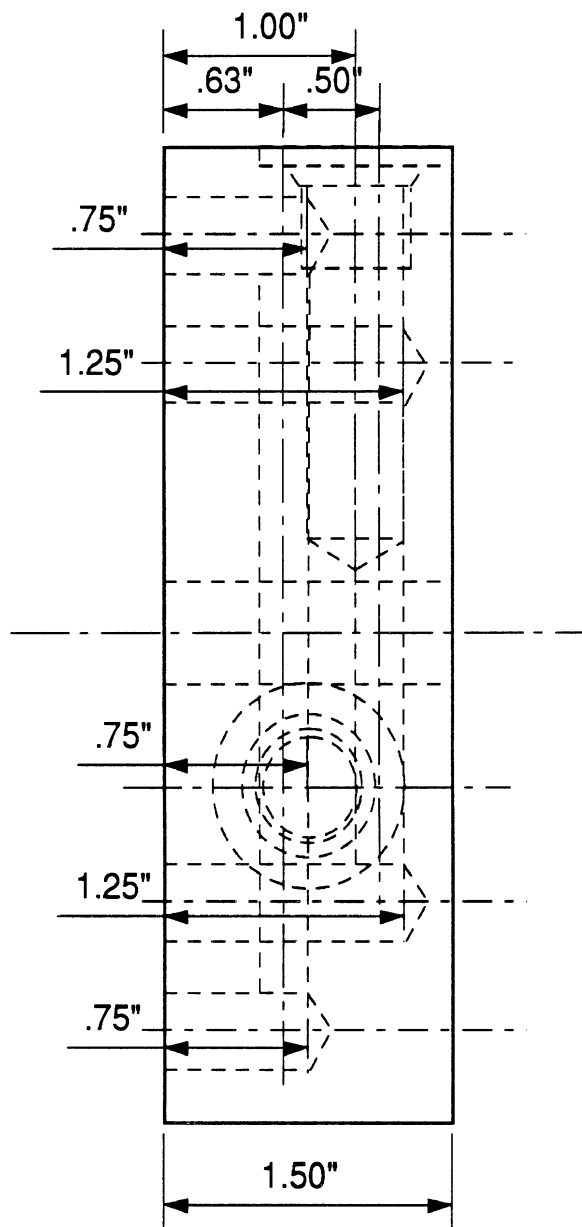


Fig. A.3. Gallery plate.



Material: Stainless steel  
 Thickness: 0.0781", i.e. 14 ga.

Fig. A.4. Central electrode.



View - A

Fig. A.5(a). Top block.

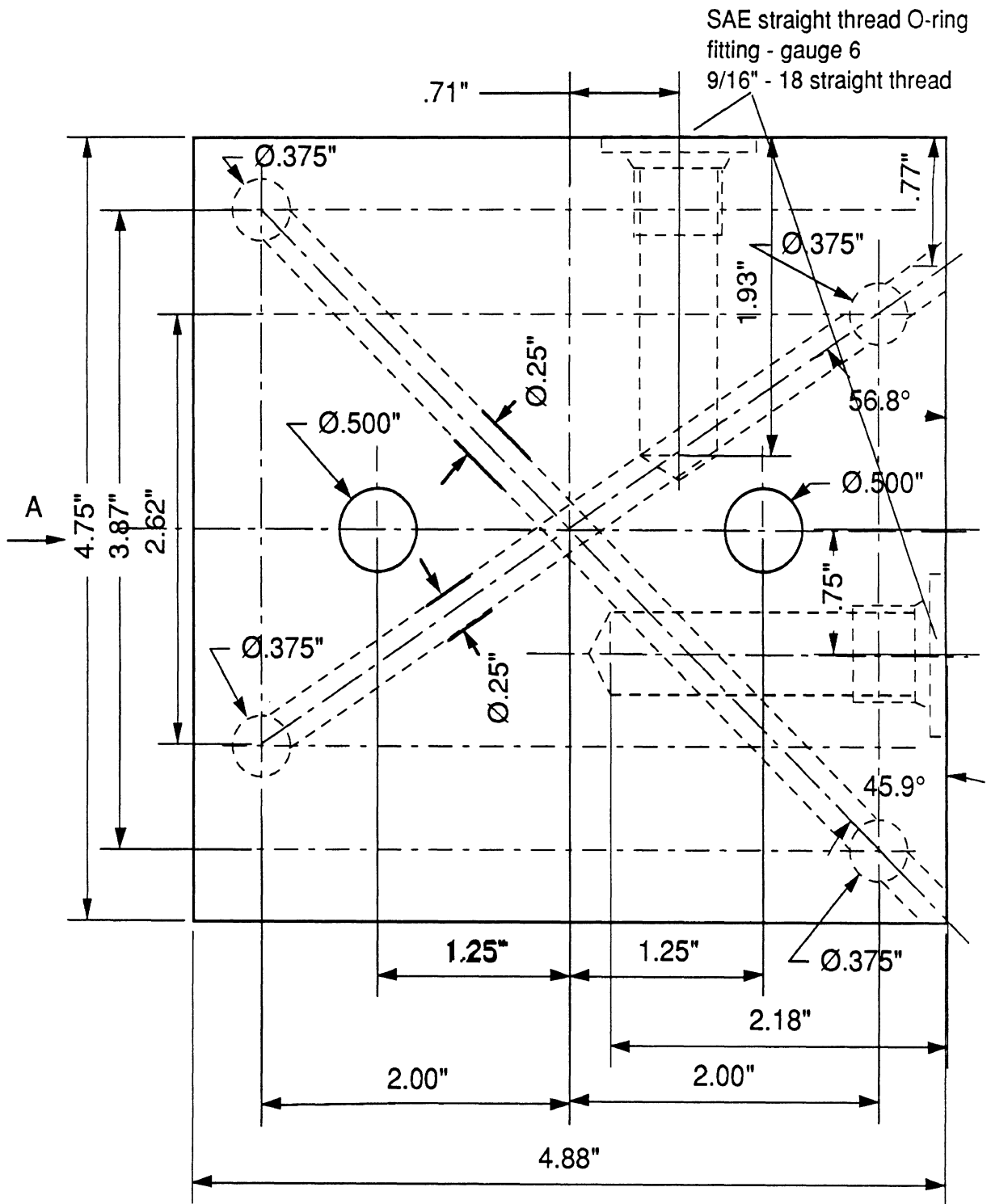


Fig. A.5(b). Top block.

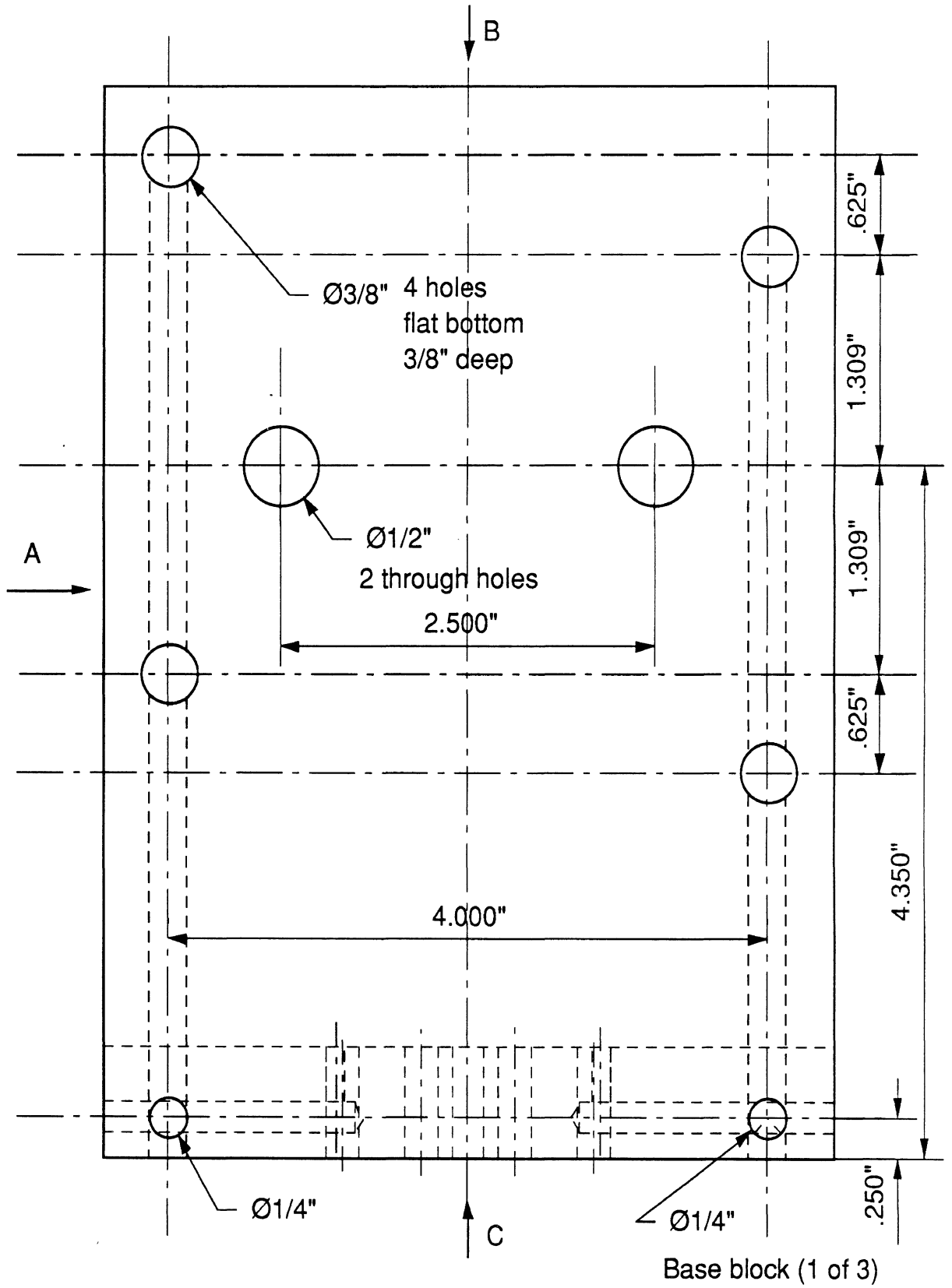


Fig. A.6(a). Base block.

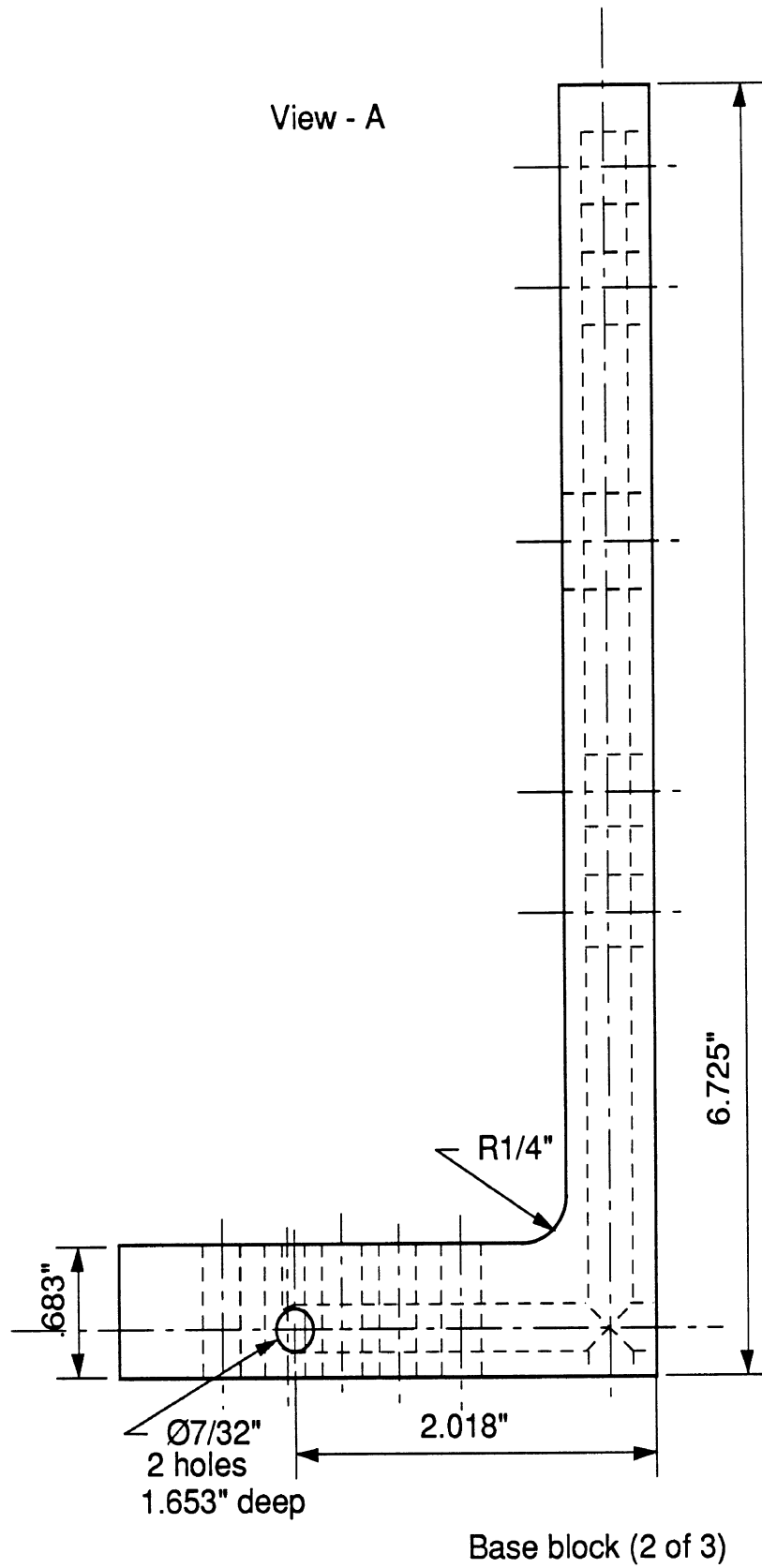


Fig. A.6(b). Base block.

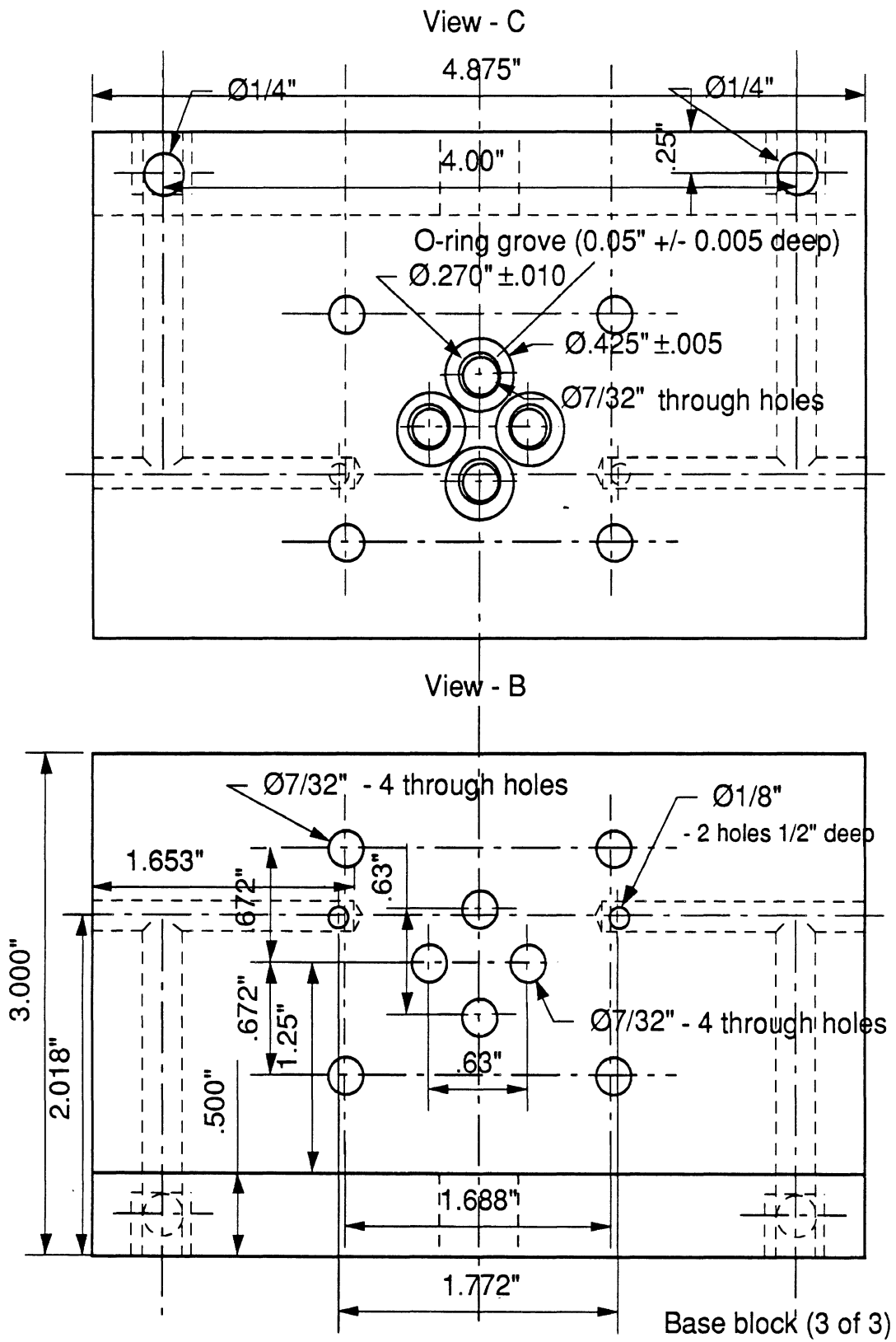


Fig. A.6(c). Base block.



**APPENDIX B. PRINTS FOR SERVO VALVE  
MODIFICATION COMPONENTS**

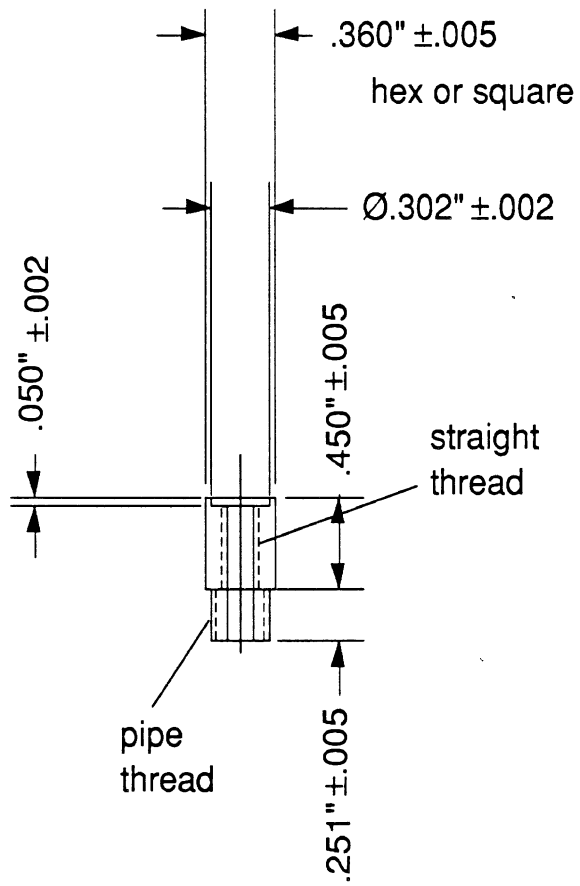
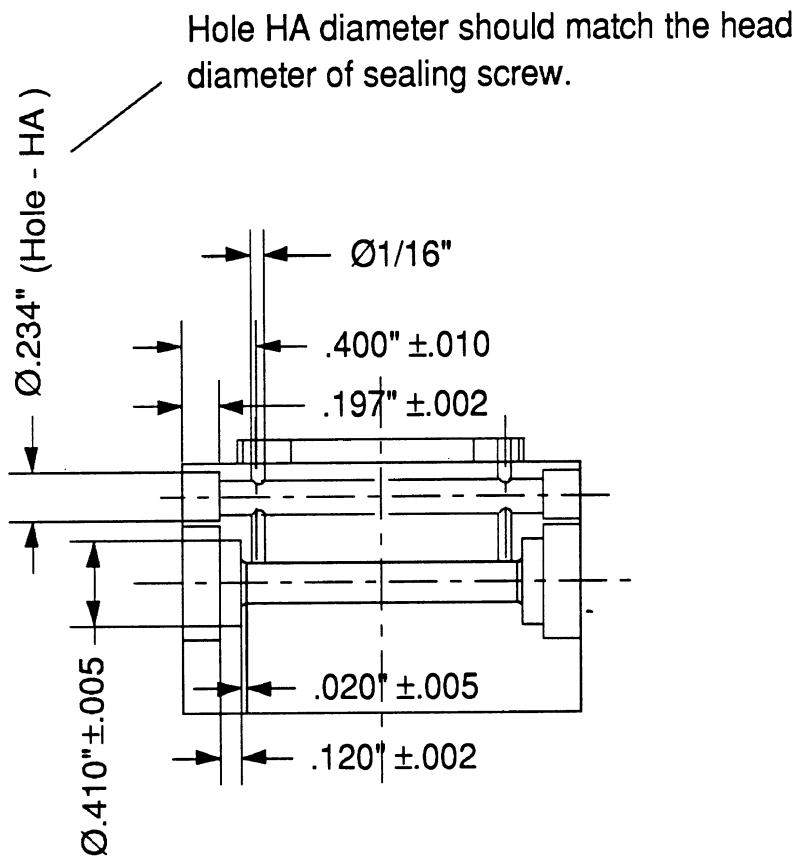


Fig. B.1. Bleeder.



Number of parts: 1

Material: the current valve body

Only those surfaces with dimension need to be machined.  
The dimensions for the surfaces on the right hand side are omitted although their machining are required.

Fig. B.2. Valve body.

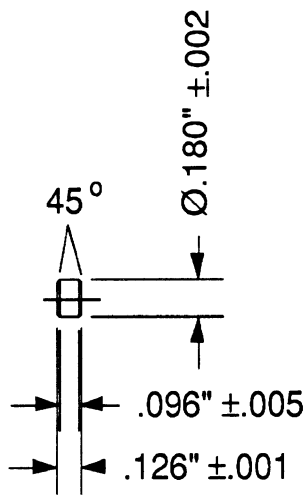


Fig. B.3. Left connector.

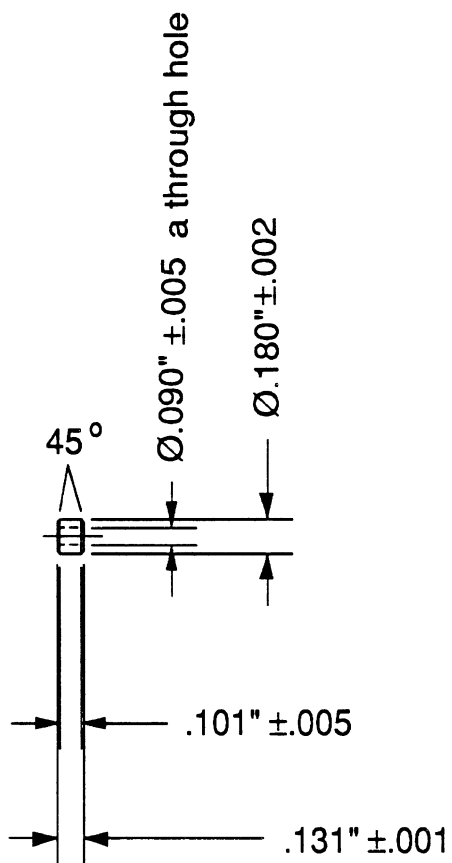


Fig. B.4. Right connector.

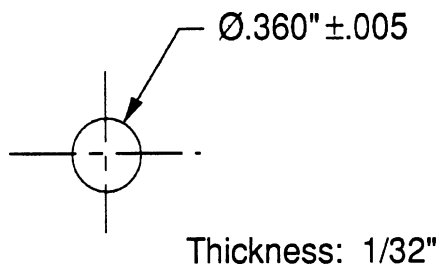


Fig. B.5. Left diaphragm

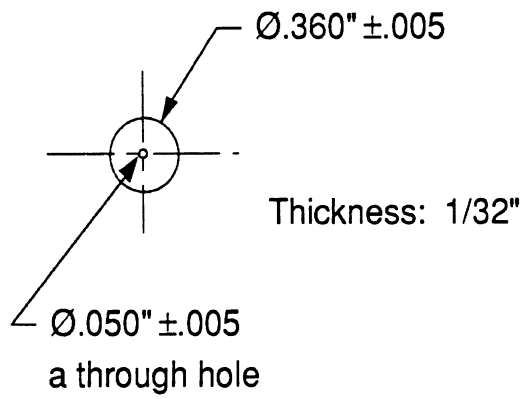


Fig. B.6. Right diaphragm.

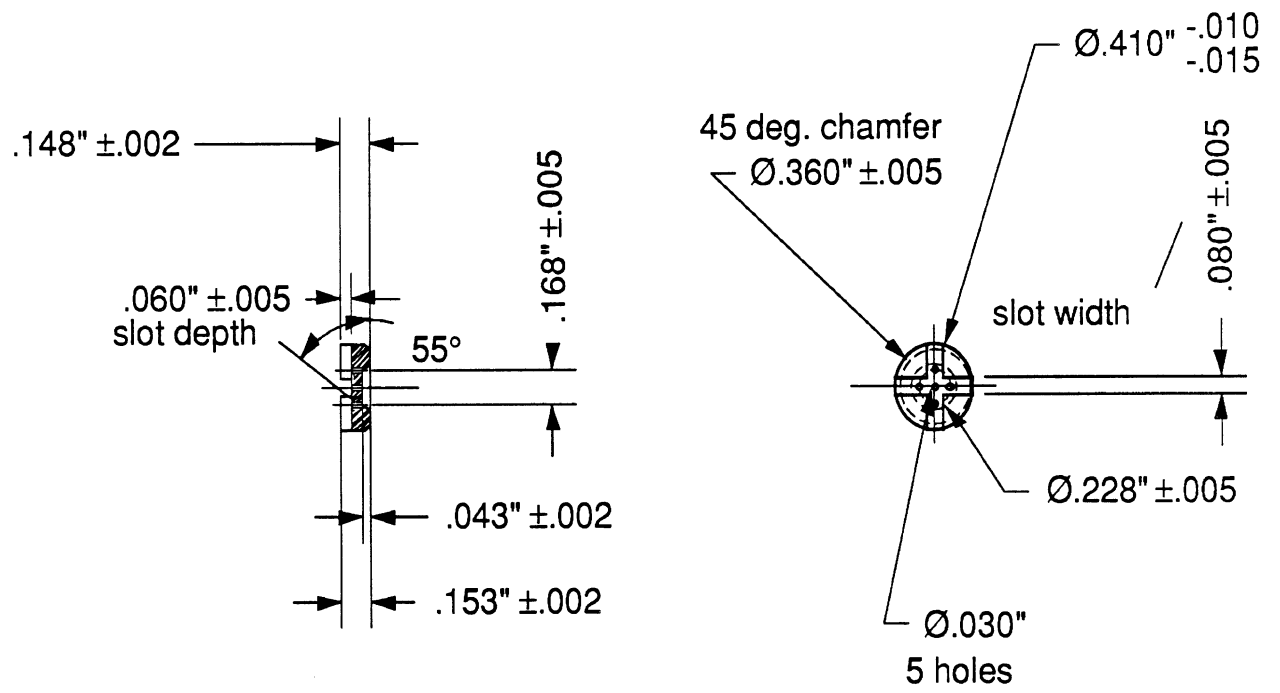


Fig. B.7. Diaphragm holders.

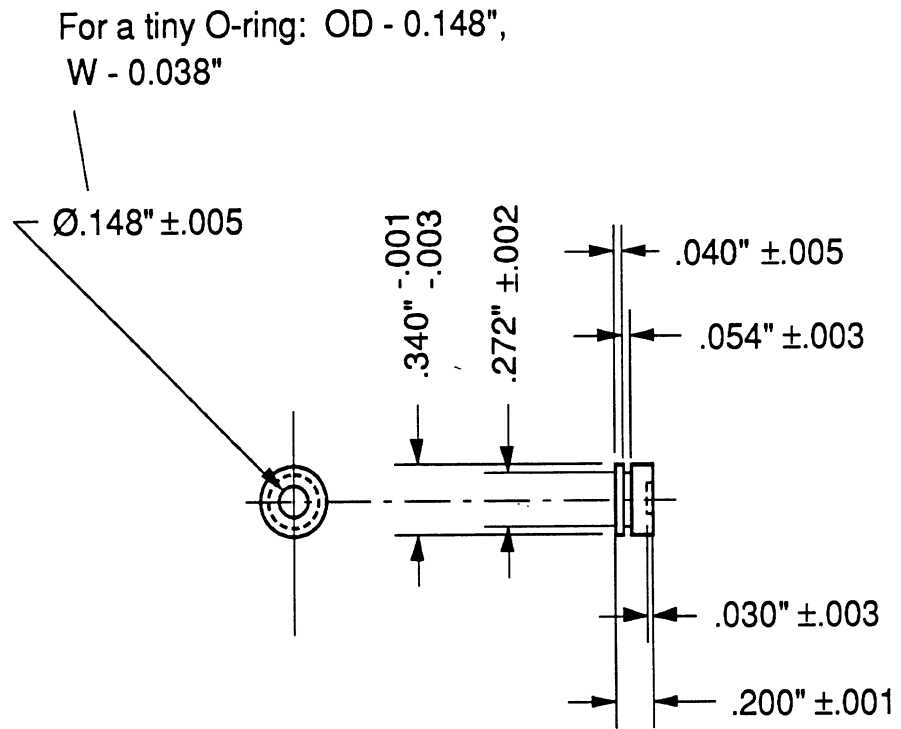
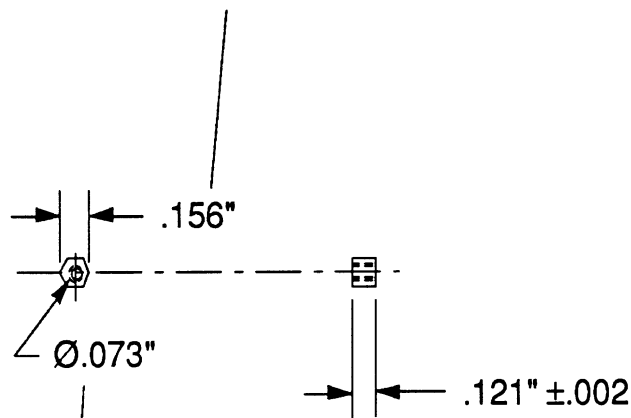


Fig. B.8. Pressure port seal.

Hex on a standard nut can be used as long as the maximum diameter of the hex is within 10% of this size.



To match the screw on the LVDT connecting rod.

Fig. B.9. Sealing nut.

To have such a size that it will fit into hole HA in valve body and have a sealing match with the hole.

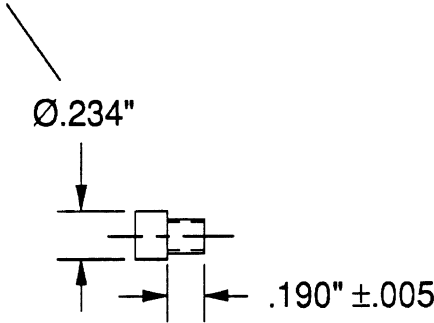


Fig. B.10. Sealing screw.

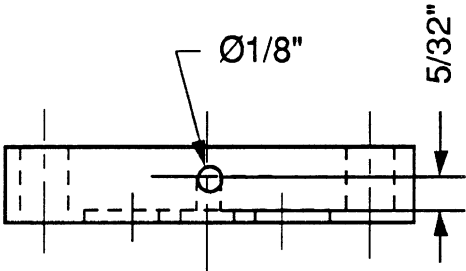
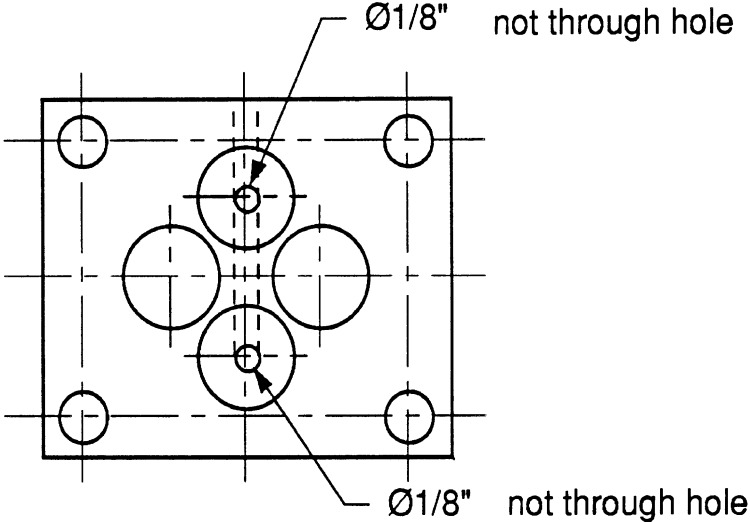


Fig. B.11. Top connector.



## APPENDIX C. COMPUTER PROGRAM FOR A NUMERICAL SIMULATION

```

C DYN.FOR
C
C TO SIMULATE THE DYNAMICS OF THE FLIGHT SYSTEM
C
C AP: PISTON AREA (INPUT)
C AV: SERVOVALVE AREA (INPUT)
C BE1,BE2: BULK MODULI FOR ACTUATOR CHAMBERS 1 AND 2
(INPUT)
C BEER1, BEER2: BULK MODULI FOR ER CHAMBERS 1 AND 2
(INPUT)
C BF: DAMPING COEFFICIENT DUE TO TRANSIENT FLOW FORCE ON
THE SERVO
C VALVE = (L2-L1)*CD*W*DSQRT(RHO(PS-PL))
C CD: THE DISCHARGE COEFFICIENT = 0.61 (INPUT)
C DT: TIME STEP SIZE (INPUT)
C E: ELECTRIC FIELD STRENGTH
C ERW: ER VALVE WIDTH (INPUT)
C ERL: ER VALVE LENGTH (INPUT)
C ERH: ER VALVE DEPTH OR THICKNESS (INPUT)
C GF0: GAIN FOR F0 [V/IN OR M] (INPUT)
C GF1: GAIN FOR F1 [V/V] (INPUT)
C GF2: GAIN FOR F2 [V/V] (INPUT)
C GF3: GAIN FOR F3 [V/V] (INPUT)
C GF8: GAIN FOR F8 [IN OR M/V] (INPUT)
C GF9: GAIN FOR F9 [V/V] (INPUT)
C GF10: GAIN FOR F10 [V/V] (INPUT)
C GF11: GAIN FOR F11 [IN OR M/V] (INPUT)
C GF12: GAIN FOR F12 [V/V] (INPUT)
C IOUT: NUMBER OF SIMULATIONS FOR EVERY OUTPUT (INPUT)
C IXPSW: WAVE FORM FOR XPS (INPUT)
C =1 IF STEP FUNCTION
C PARAMETERS:
C AXPS - AMPLITUDE
C =2 IF SLOPE FUNCTION
C PARAMETERS:
C AXPS - AMPLITUDE (OR PEAK, AFTER WHICH IT IS
FLAT)
C RTXPS - RISE TIME
C =3 IF SINCE WAVE
C PARAMETERS
C AXPS - AMPLITUDE
C FXPS - FREQUENCY
C KD: SPRING CONSTANT DUE TO THE DIAPHRAMS (INPUT)
C KF: SPRING CONSTANT DUE TO FLOW FORCE = 0.43*W(PS-PL)
C KFD=KF+KD
C L1,L2: SERVE-VALVE PORT DISTANCES (INPUT)

```

```

C MP: EFFECTIVE PISTON MASS (INPUT)
C MV: EFFECTIVE SERVOVALVE MASS (INPUT)
C P1, P2: ACTUATOR PRESSURES
C P1P=-4.0*P1P1+P1P2
C P2P=-4.0*P2P1+P2P2
C PAPAN: N IN PAPANATSASIOU METHOD (INPUT)
C PER1, PER2: PRESSURES FOR ER BRIDGE
C PER1P1, PER1P2: PER1'S AT PAST STEP AND PAST PAST
STEP
C PER2P1, PER2P2: PER2'S AT PAST STEP AND PAST PAST
STEP
C PER1P=-4.0*PER1P1+PER1P2
C PER2P=-4.0*PER2P1+PER2P2
C PERL=PER1-PER2
C PL=P1-P2
C PS: HYDRAULIC SOURCE PRESSURE (INPUT)
C PT: HYDRAULIC TANK PRESSURE (INPUT)
C PSER: ER SOURCE PRESSURE (INPUT)
C PTER: ER TANK PRESSURE (INPUT)
C QERL1, QERL2: ER LOAD FLOW RATES 1 AND 2
C Q1,Q2,Q3,Q4: FLOW RATES THROUGH DIFFERENT PORTS OF THE
SERVO-VALVE
C QL1,QL1,QL: LOAD FLOW RATES OF THE SERVO-VALVE
C RHO: OIL DENSITY (INPUT)
C RHOER: ER FLUID DENSITY (INPUT)
C THTU: RELAXATION PARAMETER FOR U ITERATION
(INPUT)
C THTXP: RELAXATION PARAMETER FOR XP ITERATION (INPUT)
C THTXV: RELAXATION PARAMETER FOR XV ITERATION (INPUT)
C TMAX: THE END OF THE SIMULATION (INPUT)
C TOUTI: INITIAL OUTPUT TIME (INPUT)
C TY: YIELD SHEAR STRESS
C TY1, TY2: TY FOR VALVES 1 &3 AND VALVES 2&4
C TYC: PROPORTIONAL CONSTANT (INPUT)
C TYN: EXPONENT (INPUT)
C U1,U2,U3,U4: FLUID VELOCITY IN ER VALVES 1, 2, 3, AND
4
C UN1,UN2,UN3,UN4: OLD FLUID VELOCITY IN ER VALVES 1,
2, 3, AND 4
C VAC: AC SIGNAL AND HIGH VOLTAGE
C VDC: DC HIGH VOLTAGE (INPUT)
C VBEER1=VER1/BEER1
C VBEER2=VER2/BEER2
C VBE1=V1/BE1
C VBE2=V2/BE2
C VER1, VER2: VOLUMES FOR ER CHAMBERS 1 AND 2 (ASSUMED
TO BE
C CONSTANT) (INPUT)
C VOFF: OFF-SET VOLTAGE IN THE WAVE GENERATOR (INPUT)
C V1, V2: VOLUMES FOR SERVOVALVE CHAMBERS 1 AND 2
(CALCULATED
C IN THE PROGRAM)
C V0: AVERAGE CONTAINED VOLUME OF EACH SERVOVALVE CHAMBER
C (INCLUDING SERVOVALVE, CONNECTING LINE OR MANIFOLD,

```

```

C      AND ACTUATOR) . (INPUT)
C  XP:  ACTUATOR DISPLACEMENT AT CURRENT TIME
C  XPS: SPECIFIED ACTUATOR DISPLACEMENT
C  XPELMT:  CONVERGENCE CRITERIOR IN XP ITERATION (INPUT)
C  XPM: OLD XP IN ITERATION
C  XPP1, XPP2:  XP'S AT PAST STEP AND PAST PAST STEP
C      XPP=-4.0*XPP1+XPP2
C      XPP2=-5.0*XPP1+4.0*XPP2-XPP3
C  XV:  SERVOVALVE DISPLACEMENT AT CURRENT TIME
C  XVELMT:  CONVERGENCE CRITERIOR IN XV ITERATION (INPUT)
C  XVM: OLD XV IN ITERATION
C  XVP1, XVP2:  XV'S AT PAST STEP AND PAST PAST STEP
C      XVP=-4.0*XVP1+XVP2
C      XVP2=-5.0*XVP1+4.0*XVP2-XVP3
C  W:  WET PERIMETER FOT THE SERVOVALVE (INPUT)
C

```

```

      IMPLICIT REAL*8 (A-H,O-Z)
      REAL*8 KD,KFD,L1,L2,MV,MP

```

```

      DIMENSION U1(101),U2(101),U3(101),U4(101)
      DIMENSION UN1(101),UN2(101),UN3(101),UN4(101)

```

```

COMMON/CERVAL/ERW,ERL,ERH,RHOER,ETA
COMMON/CNUMER/PAPAN,THTU

```

```

C  TEST
      DUMMY=0
C***** OPEN FILES

```

```

      OPEN(5,FILE='dyn.5')
      OPEN(6,FILE='dyn.6')

```

```

C***** PARAMETER INPUT

```

```

      READ(5,*) AP
      READ(5,*) AV
      READ(5,*) BE1,BE2
      READ(5,*) BEER1, BEER2
      READ(5,*) CD
      READ(5,*) DT
      READ(5,*) ERW
      READ(5,*) ERL
      READ(5,*) ERH
      READ(5,*) GF0
      READ(5,*) GF1
      READ(5,*) GF2
      READ(5,*) GF3
      READ(5,*) GF8
      READ(5,*) GF9
      READ(5,*) GF10
      READ(5,*) GF11
      READ(5,*) GF12
      READ(5,*) IOUT

```

```

READ(5,*) IXPSW
  IF (IXPSW=1) THEN
    READ(5,*) AXPS
  END IF
  IF (IXPSW=2) THEN
    READ(5,*) AXPS
    READ(5,*) RTXPS
  END IF
  IF (IXPSW=3) THEN
    READ(5,*) AXPS
    READ(5,*) FXPS
  END IF
READ(5,*) KD
READ(5,*) L1,L2
READ(5,*) MP
READ(5,*) MV
READ(5,*) PAPAN
READ(5,*) PS
READ(5,*) PT
READ(5,*) PSER
READ(5,*) PTER
READ(5,*) RHO
READ(5,*) RHOER
READ(5,*) THTU
READ(5,*) THTXP
READ(5,*) THTXV
READ(5,*) TMAX
READ(5,*) TOUTI
READ(5,*) TYC
READ(5,*) TYN
READ(5,*) VDC
READ(5,*) VER1, VER2
READ(5,*) VOFF
READ(5,*) V0
READ(5,*) XPELMT
READ(5,*) XVELMT
READ(5,*) W

```

C

C\*\*\*\*\* INITIALIZATION

C ----- ER BRIDGE

C WAVE GENERATOR

```

VAC=0.
VAC= VAC+VOFF

```

C XP FEEDBACK

```

XP=0.
VAC = VAC - XP*GF11*GF12

```

```

C  XV FEEDBACK
    XV=0.
    VAC = VAC - XV*GF8*GF9*GF10

C  NON-LINEAR AND PRE-HV AMPLIFIER
    VAC = VAC*GF2

C  HV AMPLIFIER
    VAC = VAC*GF3

C  ER FLUID LAW

C      VALVES 1 AND 3
    E=(VDC-VAC)/ERH
    CALL ERFLAW(E, TYC, TYN, TY1)
    TY3=TY1

C      VALVES 2 AND 4
    E=(VAC)/ERH
    CALL ERFLAW(E, TYC, TYN, TY2)
    TY4=TY2

C? PERHAPS NEED SOME ITERATIONS
    PER1= (PSER-PTER)/2.0
    PER1P1=PER1
    PER1P2=PER1

C? PERHAPS NEED SOME ITERATIONS
    PER2= PER1
    PER2P1=PER2
    PER2P2=PER2

C  ER VALVES (STEADY STATE SOLUTIONS)

C      VALVE 1
    CALL CFDSS (TY1, U1, PSER, PER1, QER1)

C      VALVE 2
    CALL CFDSS (TY2, U2, PSER, PER2, QER2)

C      VALVE 3
    CALL CFDSS (TY3, U3, PER2, PTER, QER3)

C      VALVE 4
    CALL CFDSS (TY4, U4, PER1, PTER, QER4)

```

```
QERL1=QER1-QER4
QERL2=QER3-QER2
```

```
DO 50 I=1, IMAX
UN1 (I) =U1 (I)
UN2 (I) =U2 (I)
UN3 (I) =U3 (I)
UN4 (I) =U4 (I)
50 CONTINUE
```

```
C ----- SERVO-VALVE
```

```
XV=0.
XVP1=XV
XVP2=XV
XVP3=XV
```

```
C ----- ACTUATOR
```

```
P1=0.0
P1P1=P1
  P1P2=P1

P2=0.
P2P1=P2
P2P2=P2
```

```
C? HOW ABOUT SOME OTHER ARBITRARY SITUATION FOR XP
```

```
XP=0.
XPP1=XP
XPP2=XP
XPP3=XP
```

```
C***** TIME DOMAIN MARCHING (BEGIN)
```

```
PER1 WRITE (6, *) 'T XPS VAC QERL
- ', 'PER2 PERL XV QL
PL ', 'XP'
```

```
T=0.0
WRITE (6, 610)
T, XPS, VAC, QERL, PER1, PER2, PERL, XV, QL, PL, XP
```

```
1 T=T+DT
```

```
DT2=DT**2
DT3=DT**3
DT4=DT**4
PI=3.14159
```

```

C***** WAVE GENERATOR

C STEP FUNCTION

      IF (IXPSW.EQ.1) THEN
          XPS=AXPS
      END IF

C SLOPE FUNCTION

      IF (IXPSW.EQ.2) THEN
          XPS=T*AXPS/RTXPS
          IF (XPS.GT.AXPS) XPS=AXPS
      END IF

C SINCE WAVE

      IF (IXPSW.EQ.3) THEN
          XPS=AXPS*DSIN(2.0*PI*FXPS*T)
      END IF

C
      VAC= XPS*GF0

C OFF-SET

      VAC= VAC+VOFF

C***** XP FEEDBACK (BEGIN)

      DO 200 ITXP=1,100

          VAC = VAC - XP*GF11*GF12

C***** XV FEEDBACK (BEGIN)

      DO 100 ITXV=1,100

          VAC = VAC - XV*GF8*GF9*GF10

C***** NON-LINEAR AND PRE-HV AMPLIFIER

          VAC = VAC*GF2

C***** HV AMPLIFIER

          VAC = VAC*GF3

C***** ER FLUID LAW

C VALVES 1 AND 3

          E=(VDC-VAC)/ERH

```

```

CALL ERFLAW(E, TYC, TYN, TY1)
TY3=TY1

C VALVES 2 AND 4

E=(VAC)/ERH
CALL ERFLAW(E, TYC, TYN, TY2)
TY4=TY2

C***** ER VALVES

C VALVE 1

CALL CFD(TY1, UN1, U1, PSER, PER1, QER1)

C VALVE 2

CALL CFD(TY2, UN2, U2, PSER, PER2, QER2)

C VALVE 3

CALL CFD(TY3, UN3, U3, PER2, PTER, QER3)

C VALVE 4

CALL CFD(TY4, UN4, U4, PER1, PTER, QER4)

C***** ER BRIDGE

QERL1=QER1-QER4
QERL2=QER3-QER2

C***** SERVO-VALVE SPOOL

AV2=AV**2

C INTERMEDIATE VARIABLES

PL=P1-P2
KF=0.43*W*(PS-PL)
BF=(L2-L1)*CD*W*DSQRT(RHO*(PS-PL))

KFD=KF+KD
VBEER1=VER1/BEER1
VBEER2=VER2/BEER2
PER1P=-4.0*PER1P1+PER1P2
PER2P=-4.0*PER2P1+PER2P2
XVP=-4.0*XVP1+XVP2
XVP2=-5.0*XVP1+4.0*XVP2-XVP3

TERM1 =

```



$$\begin{aligned}
& - \quad -12*AV*DT4*QERL2*VBEER1/(-18*AV**2*DT3*VBEER1 \\
& - \quad -18*AV**2*DT3*VBEER2 - \\
27*BF*DT2*VBEER1*VBEER2 - \\
& - \quad 18*DT3*KFD*VBEER1*VBEER2 - \\
36*DT*MV*VBEER1*VBEER2) \\
& \quad \text{TERM2} = \\
& - \quad -12*AV*DT4*QERL1*VBEER2/(-18*AV**2*DT3*VBEER1 - \\
& - \quad 18*AV**2*DT3*VBEER2 - \\
27*BF*DT2*VBEER1*VBEER2 - \\
& - \quad 18*DT3*KFD*VBEER1*VBEER2 - \\
36*DT*MV*VBEER1*VBEER2) \\
& \quad \text{TERM3} = \\
& - \quad 6*AV*DT3*PER1P*VBEER1*VBEER2/(- \\
18*AV**2*DT3*VBEER1 - \\
& - \quad 18*AV**2*DT3*VBEER2 - \\
27*BF*DT2*VBEER1*VBEER2 - \\
& - \quad 18*DT3*KFD*VBEER1*VBEER2 - \\
36*DT*MV*VBEER1*VBEER2) \\
& \quad \text{TERM4} = \\
& - \quad - 6*AV*DT3*PER2P*VBEER1*VBEER2/(- \\
18*AV**2*DT3*VBEER1 - \\
& - \quad 18*AV**2*DT3*VBEER2 - \\
27*BF*DT2*VBEER1*VBEER2 - \\
& - \quad 18*DT3*KFD*VBEER1*VBEER2 - \\
36*DT*MV*VBEER1*VBEER2) \\
& \quad \text{TERM5} = \\
& - \quad (6*AV**2*DT3*VBEER1 + 6*AV**2*DT3*VBEER2 + \\
& - \quad 9*BF*DT2*VBEER1*VBEER2)*XVP/(- \\
18*AV**2*DT3*VBEER1 - \\
& - \quad 18*AV**2*DT3*VBEER2 - \\
27*BF*DT2*VBEER1*VBEER2 - \\
& - \quad 18*DT3*KFD*VBEER1*VBEER2 - \\
36*DT*MV*VBEER1*VBEER2) \\
& \quad \text{TERM6} = \\
& - \quad 18*DT*MV*VBEER1*VBEER2*XVP2/(- \\
18*AV**2*DT3*VBEER1 - \\
& - \quad 18*AV**2*DT3*VBEER2 - \\
27*BF*DT2*VBEER1*VBEER2 - \\
& - \quad 18*DT3*KFD*VBEER1*VBEER2 - \\
36*DT*MV*VBEER1*VBEER2)
\end{aligned}$$

$$XV = \text{TERM1} + \text{TERM2} + \text{TERM3} + \text{TERM4} + \text{TERM5} + \text{TERM6}$$

$$\begin{aligned}
& \text{TERM1} = \\
& - \quad 12*AV**2*DT4*QERL2/ \\
& - \quad (-18*AV**2*DT3*VBEER1 - \\
& - \quad 18*AV**2*DT3*VBEER2 - \\
& - \quad 27*BF*DT2*VBEER1*VBEER2 - \\
& - \quad 18*DT3*KFD*VBEER1*VBEER2 - \\
& - \quad 36*DT*MV*VBEER1*VBEER2) \\
& \text{TERM2} = \\
& - \quad 6*AV**2*DT3*PER2P*VBEER2/ \\
& - \quad (-18*AV**2*DT3*VBEER1 -
\end{aligned}$$

```

-          18*AV**2*DT3*VBEER2 -
-          27*BF*DT2*VBEER1*VBEER2 -
-          18*DT3*KFD*VBEER1*VBEER2 -
-          36*DT*MV*VBEER1*VBEER2)
TERM3 =
-      - QERL1*(12*AV**2*DT4 + 18*BF*DT3*VBEER2 +
-          12*DT4*KFD*VBEER2 + 24*DT2*MV*VBEER2)/
-      (-18*AV**2*DT3*VBEER1 -
-          18*AV**2*DT3*VBEER2 -
-          27*BF*DT2*VBEER1*VBEER2 -
-          18*DT3*KFD*VBEER1*VBEER2 -
-          36*DT*MV*VBEER1*VBEER2)
TERM4 =
-      PER1P*(6*AV**2*DT3*VBEER1 +
-          9*BF*DT2*VBEER1*VBEER2 +
-          6*DT3*KFD*VBEER1*VBEER2 +
-          12*DT*MV*VBEER1*VBEER2)/
-      (-18*AV**2*DT3*VBEER1 -
-          18*AV**2*DT3*VBEER2 -
-          27*BF*DT2*VBEER1*VBEER2 -
-          18*DT3*KFD*VBEER1*VBEER2 -
-          36*DT*MV*VBEER1*VBEER2)
TERM5 =
-      (6*AV*DT3*KFD*VBEER2 + 12*AV*DT*MV*VBEER2)*XVP/
-      (-18*AV**2*DT3*VBEER1 -
-          18*AV**2*DT3*VBEER2 -
-          27*BF*DT2*VBEER1*VBEER2 -
-          18*DT3*KFD*VBEER1*VBEER2 -
-          36*DT*MV*VBEER1*VBEER2)
TERM6 =
-      - 18*AV*DT*MV*VBEER2*XVP2/
-      (-18*AV**2*DT3*VBEER1 -
-          18*AV**2*DT3*VBEER2 -
-          27*BF*DT2*VBEER1*VBEER2 -
-          18*DT3*KFD*VBEER1*VBEER2 -
-          36*DT*MV*VBEER1*VBEER2)

```

PER1 = TERM1+TERM2+TERM3+TERM4+TERM5+TERM6

```

TERM1=
-      -12*AV**2*DT4*QERL1/
-      (-18*AV**2*DT3*VBEER1 -
-          18*AV**2*DT3*VBEER2 -
-          27*BF*DT2*VBEER1*VBEER2 -
-          18*DT3*KFD*VBEER1*VBEER2 -
-          36*DT*MV*VBEER1*VBEER2)
TERM2 =
-      6*AV**2*DT3*PER1P*VBEER1/
-      (-18*AV**2*DT3*VBEER1 -
-          18*AV**2*DT3*VBEER2 -
-          27*BF*DT2*VBEER1*VBEER2 -
-          18*DT3*KFD*VBEER1*VBEER2 -
-          36*DT*MV*VBEER1*VBEER2)

```

```

TERM3 =
-   - QERL2*(-12*AV**2*DT4 - 18*BF*DT3*VBEER1 -
-       12*DT4*KFD*VBEER1 - 24*DT2*MV*VBEER1)/
-       (-18*AV**2*DT3*VBEER1 -
-       18*AV**2*DT3*VBEER2 -
-       27*BF*DT2*VBEER1*VBEER2 -
-       18*DT3*KFD*VBEER1*VBEER2 -
-       36*DT*MV*VBEER1*VBEER2)
TERM4 =
-   PER2P*(6*AV**2*DT3*VBEER2 +
-       9*BF*DT2*VBEER1*VBEER2 +
-       6*DT3*KFD*VBEER1*VBEER2 +
-       12*DT*MV*VBEER1*VBEER2)/
-       (-18*AV**2*DT3*VBEER1 -
-       18*AV**2*DT3*VBEER2 -
-       27*BF*DT2*VBEER1*VBEER2 -
-       18*DT3*KFD*VBEER1*VBEER2 -
-       36*DT*MV*VBEER1*VBEER2)
TERM5 =
-   (-6*AV*DT3*KFD*VBEER1 - 12*AV*DT*MV*VBEER1)*
-   XVP/
-   (-18*AV**2*DT3*VBEER1 -
-   18*AV**2*DT3*VBEER2 -
-   27*BF*DT2*VBEER1*VBEER2 -
-   18*DT3*KFD*VBEER1*VBEER2 -
-   36*DT*MV*VBEER1*VBEER2)
TERM6 =
-   18*AV*DT*MV*VBEER1*XVP2/
-   (-18*AV**2*DT3*VBEER1 -
-   18*AV**2*DT3*VBEER2 -
-   27*BF*DT2*VBEER1*VBEER2 -
-   18*DT3*KFD*VBEER1*VBEER2 -
-   36*DT*MV*VBEER1*VBEER2)

PER2 = TERM1+TERM2+TERM3+TERM4+TERM5+TERM6

```

C\*\*\*\*\* XV FEEDBACK (END)

```

ERROR=DABS(XV-XVM)
XV=(1.0-THTXV)*XVM+THTXV*XV
IF(ERROR.LT.XVELMT) GO TO 110
100 CONTINUE

WRITE(6,*) 'XV DOES NOT CONVERGE'

110 CONTINUE

```

C\*\*\*\*\* SERVO-VALVE LAW

```

Q1=0.
Q2=0.
Q3=0.

```

```

Q4=0.

IF (XV.GT.0.0) THEN
  Q1=CD*W*XV*SQRT(2.0*(PS-P1)/RHO)
  Q3=CD*W*XV*SQRT(2.0*(P2-PT)/RHO)
END IF

IF (XV.LT.0.0) THEN
  Q2=-CD*W*XV*SQRT(2.0*(PS-P2)/RHO)
  Q4=-CD*W*XV*SQRT(2.0*(P1-PT)/RHO)
END IF

```

C\*\*\*\*\* SERVO-VALVE BRIDGE

```

QL1=Q1-Q4
QL2=Q3-Q2
QL=QL1+QL2

```

C\*\*\*\*\* ACTUATOR

```

AP2=AP**2

```

```

V1=V0+AP*XP
V2=V0-AP*XP

```

```

VBE1=V1/BE1
VBE2=V2/BE2
P1P=-4.0*P1P1+P1P2
P2P=-4.0*P2P1+P2P2
XPP=-4.0*XPP1+XPP2
XPP2=-5.0*XPP1+4.0*XPP2-XPP3

```

```

TERM1 =
-      -((-12*AP**2*DT4 - 12*BP*CIM*DT4 -
-          8*CIM*DT**5*K - 16*CIM*DT3*MP)*QL2/
-      (-18*AP**2*DT3*VBE1 -
-          18*BP*CIM*DT3*VBE1 -
-          12*CIM*DT4*K*VBE1 -
-          24*CIM*DT2*MP*VBE1 -
-          18*AP**2*DT3*VBE2 -
-          18*BP*CIM*DT3*VBE2 -
-          12*CIM*DT4*K*VBE2 -
-          24*CIM*DT2*MP*VBE2 -
-          27*BP*DT2*VBE1*VBE2 -
-          18*DT3*K*VBE1*VBE2 - 36*DT*MP*VBE1*VBE2))

```

```

TERM2 =
-      - 18*AP*DT3*FL*VBE2/
-      (-18*AP**2*DT3*VBE1 - 18*BP*CIM*DT3*VBE1 -
-          12*CIM*DT4*K*VBE1 - 24*CIM*DT2*MP*VBE1 -
-          18*AP**2*DT3*VBE2 - 18*BP*CIM*DT3*VBE2 -
-          12*CIM*DT4*K*VBE2 - 24*CIM*DT2*MP*VBE2 -
-          27*BP*DT2*VBE1*VBE2 -
-          18*DT3*K*VBE1*VBE2 - 36*DT*MP*VBE1*VBE2)

```

```

TERM3 =
-   - QL1*(12*AP**2*DT4 + 12*BP*CIM*DT4 +
-         8*CIM*DT**5*K + 16*CIM*DT3*MP +
-         18*BP*DT3*VBE2 + 12*DT4*K*VBE2 +
-         24*DT2*MP*VBE2) /
-       (-18*AP**2*DT3*VBE1 - 18*BP*CIM*DT3*VBE1 -
-         12*CIM*DT4*K*VBE1 - 24*CIM*DT2*MP*VBE1 -
-         18*AP**2*DT3*VBE2 - 18*BP*CIM*DT3*VBE2 -
-         12*CIM*DT4*K*VBE2 - 24*CIM*DT2*MP*VBE2 -
-         27*BP*DT2*VBE1*VBE2 -
-         18*DT3*K*VBE1*VBE2 - 36*DT*MP*VBE1*VBE2)
TERM4 =
-   P2P*(6*AP**2*DT3*VBE2 + 6*BP*CIM*DT3*VBE2 +
-         4*CIM*DT4*K*VBE2 + 8*CIM*DT2*MP*VBE2) /
-       (-18*AP**2*DT3*VBE1 - 18*BP*CIM*DT3*VBE1 -
-         12*CIM*DT4*K*VBE1 - 24*CIM*DT2*MP*VBE1 -
-         18*AP**2*DT3*VBE2 - 18*BP*CIM*DT3*VBE2 -
-         12*CIM*DT4*K*VBE2 - 24*CIM*DT2*MP*VBE2 -
-         27*BP*DT2*VBE1*VBE2 -
-         18*DT3*K*VBE1*VBE2 - 36*DT*MP*VBE1*VBE2)
TERM5 =
-   P1P*(6*AP**2*DT3*VBE1 + 6*BP*CIM*DT3*VBE1 +
-         4*CIM*DT4*K*VBE1 + 8*CIM*DT2*MP*VBE1 +
-         9*BP*DT2*VBE1*VBE2 + 6*DT3*K*VBE1*VBE2 +
-         12*DT*MP*VBE1*VBE2) /
-       (-18*AP**2*DT3*VBE1 - 18*BP*CIM*DT3*VBE1 -
-         12*CIM*DT4*K*VBE1 - 24*CIM*DT2*MP*VBE1 -
-         18*AP**2*DT3*VBE2 - 18*BP*CIM*DT3*VBE2 -
-         12*CIM*DT4*K*VBE2 - 24*CIM*DT2*MP*VBE2 -
-         27*BP*DT2*VBE1*VBE2 -
-         18*DT3*K*VBE1*VBE2 - 36*DT*MP*VBE1*VBE2)
TERM6 =
-   (6*AP*DT3*K*VBE2 + 12*AP*DT*MP*VBE2)*XPP /
-       (-18*AP**2*DT3*VBE1 - 18*BP*CIM*DT3*VBE1 -
-         12*CIM*DT4*K*VBE1 - 24*CIM*DT2*MP*VBE1 -
-         18*AP**2*DT3*VBE2 - 18*BP*CIM*DT3*VBE2 -
-         12*CIM*DT4*K*VBE2 - 24*CIM*DT2*MP*VBE2 -
-         27*BP*DT2*VBE1*VBE2 -
-         18*DT3*K*VBE1*VBE2 - 36*DT*MP*VBE1*VBE2)
TERM7 =
-   -18*AP*DT*MP*VBE2*XPP2 /
-       (-18*AP**2*DT3*VBE1 - 18*BP*CIM*DT3*VBE1 -
-         12*CIM*DT4*K*VBE1 - 24*CIM*DT2*MP*VBE1 -
-         18*AP**2*DT3*VBE2 - 18*BP*CIM*DT3*VBE2 -
-         12*CIM*DT4*K*VBE2 - 24*CIM*DT2*MP*VBE2 -
-         27*BP*DT2*VBE1*VBE2 -
-         18*DT3*K*VBE1*VBE2 - 36*DT*MP*VBE1*VBE2)

P1 = TERM1+TERM2+TERM3+TERM4+TERM5+TERM6+TERM7

TERM1=
-   - ((12*AP**2*DT4 + 12*BP*CIM*DT4 +
-         8*CIM*DT**5*K + 16*CIM*DT3*MP)*QL1 /
-       (-18*AP**2*DT3*VBE1 -

```

```

-          18*BP*CIM*DT3*VBE1 -
-          12*CIM*DT4*K*VBE1 -
-          24*CIM*DT2*MP*VBE1 -
-          18*AP**2*DT3*VBE2 -
-          18*BP*CIM*DT3*VBE2 -
-          12*CIM*DT4*K*VBE2 -
-          24*CIM*DT2*MP*VBE2 -
-          27*BP*DT2*VBE1*VBE2 -
-          18*DT3*K*VBE1*VBE2 - 36*DT*MP*VBE1*VBE2))
TERM2 =
-          + 18*AP*DT3*FL*VBE1/
-          (-18*AP**2*DT3*VBE1 - 18*BP*CIM*DT3*VBE1 -
-          12*CIM*DT4*K*VBE1 - 24*CIM*DT2*MP*VBE1 -
-          18*AP**2*DT3*VBE2 - 18*BP*CIM*DT3*VBE2 -
-          12*CIM*DT4*K*VBE2 - 24*CIM*DT2*MP*VBE2 -
-          27*BP*DT2*VBE1*VBE2 -
-          18*DT3*K*VBE1*VBE2 - 36*DT*MP*VBE1*VBE2)
TERM3 =
-          - QL2*(-12*AP**2*DT4 - 12*BP*CIM*DT4 -
-          8*CIM*DT**5*K - 16*CIM*DT3*MP -
-          18*BP*DT3*VBE1 - 12*DT4*K*VBE1 -
-          24*DT2*MP*VBE1) /
-          (-18*AP**2*DT3*VBE1 - 18*BP*CIM*DT3*VBE1 -
-          12*CIM*DT4*K*VBE1 - 24*CIM*DT2*MP*VBE1 -
-          18*AP**2*DT3*VBE2 - 18*BP*CIM*DT3*VBE2 -
-          12*CIM*DT4*K*VBE2 - 24*CIM*DT2*MP*VBE2 -
-          27*BP*DT2*VBE1*VBE2 -
-          18*DT3*K*VBE1*VBE2 - 36*DT*MP*VBE1*VBE2)
TERM4 =
-          P1P*(6*AP**2*DT3*VBE1 + 6*BP*CIM*DT3*VBE1 +
-          4*CIM*DT4*K*VBE1 + 8*CIM*DT2*MP*VBE1) /
-          (-18*AP**2*DT3*VBE1 - 18*BP*CIM*DT3*VBE1 -
-          12*CIM*DT4*K*VBE1 - 24*CIM*DT2*MP*VBE1 -
-          18*AP**2*DT3*VBE2 - 18*BP*CIM*DT3*VBE2 -
-          12*CIM*DT4*K*VBE2 - 24*CIM*DT2*MP*VBE2 -
-          27*BP*DT2*VBE1*VBE2 -
-          18*DT3*K*VBE1*VBE2 - 36*DT*MP*VBE1*VBE2)
TERM5 =
-          P2P*(6*AP**2*DT3*VBE2 + 6*BP*CIM*DT3*VBE2 +
-          4*CIM*DT4*K*VBE2 + 8*CIM*DT2*MP*VBE2 +
-          9*BP*DT2*VBE1*VBE2 + 6*DT3*K*VBE1*VBE2 +
-          12*DT*MP*VBE1*VBE2) /
-          (-18*AP**2*DT3*VBE1 - 18*BP*CIM*DT3*VBE1 -
-          12*CIM*DT4*K*VBE1 - 24*CIM*DT2*MP*VBE1 -
-          18*AP**2*DT3*VBE2 - 18*BP*CIM*DT3*VBE2 -
-          12*CIM*DT4*K*VBE2 - 24*CIM*DT2*MP*VBE2 -
-          27*BP*DT2*VBE1*VBE2 -
-          18*DT3*K*VBE1*VBE2 - 36*DT*MP*VBE1*VBE2)
TERM6 =
-          (-6*AP*DT3*K*VBE1 - 12*AP*DT*MP*VBE1)*XPP/
-          (-18*AP**2*DT3*VBE1 - 18*BP*CIM*DT3*VBE1 -
-          12*CIM*DT4*K*VBE1 - 24*CIM*DT2*MP*VBE1 -
-          18*AP**2*DT3*VBE2 - 18*BP*CIM*DT3*VBE2 -
-          12*CIM*DT4*K*VBE2 - 24*CIM*DT2*MP*VBE2 -

```

```

-          27*BP*DT2*VBE1*VBE2 -
-          18*DT3*K*VBE1*VBE2 - 36*DT*MP*VBE1*VBE2)
TERM7 =
-          18*AP*DT*MP*VBE1*XPP2/
-          (-18*AP**2*DT3*VBE1 - 18*BP*CIM*DT3*VBE1 -
-          12*CIM*DT4*K*VBE1 - 24*CIM*DT2*MP*VBE1 -
-          18*AP**2*DT3*VBE2 - 18*BP*CIM*DT3*VBE2 -
-          12*CIM*DT4*K*VBE2 - 24*CIM*DT2*MP*VBE2 -
-          27*BP*DT2*VBE1*VBE2 -
-          18*DT3*K*VBE1*VBE2 - 36*DT*MP*VBE1*VBE2)

P2 = TERM1+TERM2+TERM3+TERM4+TERM5+TERM6+TERM7

TERM1 =
-          -12*AP*DT4*QL2*VBE1/
-          (-18*AP**2*DT3*VBE1 - 18*BP*CIM*DT3*VBE1 -
-          12*CIM*DT4*K*VBE1 - 24*CIM*DT2*MP*VBE1 -
-          18*AP**2*DT3*VBE2 - 18*BP*CIM*DT3*VBE2 -
-          12*CIM*DT4*K*VBE2 - 24*CIM*DT2*MP*VBE2 -
-          27*BP*DT2*VBE1*VBE2 -
-          18*DT3*K*VBE1*VBE2 - 36*DT*MP*VBE1*VBE2)
TERM2 =
-          - 12*AP*DT4*QL1*VBE2/
-          (-18*AP**2*DT3*VBE1 - 18*BP*CIM*DT3*VBE1 -
-          12*CIM*DT4*K*VBE1 - 24*CIM*DT2*MP*VBE1 -
-          18*AP**2*DT3*VBE2 - 18*BP*CIM*DT3*VBE2 -
-          12*CIM*DT4*K*VBE2 - 24*CIM*DT2*MP*VBE2 -
-          27*BP*DT2*VBE1*VBE2 -
-          18*DT3*K*VBE1*VBE2 - 36*DT*MP*VBE1*VBE2)
TERM3 =
-          6*AP*DT3*P1P*VBE1*VBE2/
-          (-18*AP**2*DT3*VBE1 - 18*BP*CIM*DT3*VBE1 -
-          12*CIM*DT4*K*VBE1 - 24*CIM*DT2*MP*VBE1 -
-          18*AP**2*DT3*VBE2 - 18*BP*CIM*DT3*VBE2 -
-          12*CIM*DT4*K*VBE2 - 24*CIM*DT2*MP*VBE2 -
-          27*BP*DT2*VBE1*VBE2 -
-          18*DT3*K*VBE1*VBE2 - 36*DT*MP*VBE1*VBE2)
TERM4 =
-          - 6*AP*DT3*P2P*VBE1*VBE2/
-          (-18*AP**2*DT3*VBE1 - 18*BP*CIM*DT3*VBE1 -
-          12*CIM*DT4*K*VBE1 - 24*CIM*DT2*MP*VBE1 -
-          18*AP**2*DT3*VBE2 - 18*BP*CIM*DT3*VBE2 -
-          12*CIM*DT4*K*VBE2 - 24*CIM*DT2*MP*VBE2 -
-          27*BP*DT2*VBE1*VBE2 -
-          18*DT3*K*VBE1*VBE2 - 36*DT*MP*VBE1*VBE2)
TERM5 =
-          FL*(12*CIM*DT4*VBE1 + 12*CIM*DT4*VBE2 +
-          18*DT3*VBE1*VBE2)/
-          (-18*AP**2*DT3*VBE1 - 18*BP*CIM*DT3*VBE1 -
-          12*CIM*DT4*K*VBE1 - 24*CIM*DT2*MP*VBE1 -
-          18*AP**2*DT3*VBE2 - 18*BP*CIM*DT3*VBE2 -
-          12*CIM*DT4*K*VBE2 - 24*CIM*DT2*MP*VBE2 -
-          27*BP*DT2*VBE1*VBE2 -
-          18*DT3*K*VBE1*VBE2 - 36*DT*MP*VBE1*VBE2)

```

```

TERM6 =
-      (6*AP**2*DT3*VBE1 + 6*BP*CIM*DT3*VBE1 +
-        6*AP**2*DT3*VBE2 + 6*BP*CIM*DT3*VBE2 +
-        9*BP*DT2*VBE1*VBE2)*XPP/
-      (-18*AP**2*DT3*VBE1 - 18*BP*CIM*DT3*VBE1 -
-        12*CIM*DT4*K*VBE1 - 24*CIM*DT2*MP*VBE1 -
-        18*AP**2*DT3*VBE2 - 18*BP*CIM*DT3*VBE2 -
-        12*CIM*DT4*K*VBE2 - 24*CIM*DT2*MP*VBE2 -
-        27*BP*DT2*VBE1*VBE2 -
-        18*DT3*K*VBE1*VBE2 - 36*DT*MP*VBE1*VBE2)

```

```

TERM7 =
-      (12*CIM*DT2*MP*VBE1 + 12*CIM*DT2*MP*VBE2 +
-        18*DT*MP*VBE1*VBE2)*XPP2/
-      (-18*AP**2*DT3*VBE1 - 18*BP*CIM*DT3*VBE1 -
-        12*CIM*DT4*K*VBE1 - 24*CIM*DT2*MP*VBE1 -
-        18*AP**2*DT3*VBE2 - 18*BP*CIM*DT3*VBE2 -
-        12*CIM*DT4*K*VBE2 - 24*CIM*DT2*MP*VBE2 -
-        27*BP*DT2*VBE1*VBE2 -
-        18*DT3*K*VBE1*VBE2 - 36*DT*MP*VBE1*VBE2)

```

```

XP = TERM1+TERM2+TERM3+TERM4+TERM5+TERM6+TERM7

```

```

C***** XP FEEDBACK (END)

```

```

      ERROR=DABS (XP-XPM)
      XV=(1.0-THTXP) *XPM+THTXP*XP
      IF (ERROR.LT.XPELMT) GO TO 110
200 CONTINUE

```

```

      WRITE (6,*) 'XP DOES NOT CONVERGE'

```

```

210 CONTINUE

```

```

C***** OUTPUT

```

```

      IF (T.GE. (TOUTI-DT/2.0)) THEN
        IF (ISIM.EQ.IOUT) THEN
          WRITE (6,610)
T, XPS, VAC, QERL, PER1, PER2, PERL, XV, QL, PL, XP
        610      FORMAT (11 (E9.3, 1X))
          ISIM=1
        ELSE
          ISIM=ISIM+1
        END IF
      ELSE
        ISIM=IOUT
      END IF

```

```

C***** UPDATE

```

```

      PER1P2=PER1P1
      PER1P1=PER1
      PER2P2=PER2P1

```



```
PER2P1=PER2
XVP3=XVP2
XVP2=XVP1
XVP1=XV
```

```
      P1P2=P1P1
P1P1=P1
      P2P2=P2P1
P2P1=P2
XPP3=XPP2
XPP2=XPP1
XPP1=XP
```

```
DO 40 I=1, IMAX
UN1 (I) =U1 (I)
UN2 (I) =U2 (I)
UN3 (I) =U3 (I)
UN4 (I) =U4 (I)
40 CONTINUE
```

```
C***** TIME DOMAIN MARCHING (END)
```

```
      IF(T.LT.TMAX) GO TO 1
```

```
      STOP
      END
```

```
C-----
      SUBROUTINE ERFLAW(E, TYC, TYN, TY)
```

```
C TO CALCULATE THE YIELD SHEAR STRESS
C FROM THE ELECTRIC FIELD STRENGTH
C
C E: ELECTRIC FIELD STRENGTH
C TY: YIELD SHEAR STRESS
C TYC: PROPORTIONAL CONSTANT
C TYN: EXPONENT
```

```
C-----
      IMPLICIT REAL*8 (A-H, O-Z)

      TY=TYC*E**TYN

      RETURN
      END
```

```
C-----
      SUBROUTINE CFD (TY, UN, U, PIN, POUT, Q)
```

```
C TO DO CFD FOR AN ER VALVE IN THE BRIDGE
C
C DPDX: PRESSURE GRADIENT
C ETA: PLASTIC VISCOSITY
```

```

C PAPAN: PAPANASTASIOU COEFFICIENT (=10.0)
C PHI: DIMENSIONLESS VISCOSITY COEFFICIENT
C PIN: PRESSURE AT THE VALVE INLET
C POUT: PRESSURE AT THE VALVE OUTLET
C RHOER: ER FLUID DENSITY
C THTU: VELOCITY RELAXATION PARAMETER
C U: VELOCITY
C UN: OLD VELOCITY
C UTEM: TEMPORARY VELOLCITY
C ERW: ER VALVE WIDTH
C ERL: ER VALVE LENGTH
C ERH: ER VALVE DEPTH OR THICKNESS
C
C
C-----
  IMPLICIT REAL*8 (A-H,O-Z)

  DIMENSION U(101),Y(101),UN(101)
  DIMENSION C1(101),C2(101),C3(101),C4(101),UTEMP(101)
  DIMENSION PHI(101)

  COMMON/CERVAL/ERW,ERL,ERH,RHOER,ETA
  COMMON/CNUMER/PAPAN,THTU

  IMAX=101
  IMXM1=IMAX-1
  IMXM2=IMAX-2
  DY=ERH/IMXM1

  A1=DT/RHOER
  A2=A1*ETA
  TDY=2.*DY
  DY2=DY**2
  OMTHT=1.0-THTU

  DPDX=(POUT-PIN)/ERL

C ----- ITERATIONS

      DO 100 IT=1,100

C CALCULATE VISCOSITY COEFFICIENTS

      DO 20 I=1,IMAX

      IF(I.EQ.1) THEN
        DUDY=- (3.*U(1)-4.*U(2)+U(3))/TDY
      ELSE
        IF(I.EQ.IMAX) THEN
          DUDY=(3.*U(IMAX)-4.*U(IMXM1)+U(IMXM2))/TDY
        ELSE
          DUDY=(U(I+1)-U(I-1))/TDY
        END IF
      END IF

```

```

END IF

      PHI (I)=1.0+TY/ (ETA*DUDY) * (1.0-DEXP (-
PAPAN*DABS (DUDY) ) )

      20 CONTINUE

C COEFFICIENTS FOR THE TRIDIAGONAL MATRIX

      DO 30 I=2,IMXM1

      DPHIDY=(PHI (I+1)-PHI (I-1) ) /TDY
      B1=A2*DPHIDY/TDY
      B2=A2*PHI (I) /DY2

      C1 (I)=- (B2+B1)
      C2 (I)=1.+2.*B2
      C3 (I)=- (B2-B1)
      C4 (I)=UN (I) -A1*DPDX

      30 CONTINUE

      UTEMP (1)=0.0
      UTEMP (IMAX)=0.0

C SOLVE THE TRI-DIAGNAL MATRIX

      CALL MATRIX (C1,C2,C3,C4,UTEMP,IMAX)
C RELAXATION AND ERROR CALCULATIONS

      DO 40 I=2,IMXM1

      ERROR=DABS (U (I) -UTEMP (I) )
      IF (ERROR.GT.ERRMAX) THEN
        ERRMAX=ERROR
      END IF
      U (I)=OMTHT*U (I) +THTU*UTEMP (I)

      40 CONTINUE

      IF (ERRMAX.GT.UELMT) GO TO 110

100 CONTINUE

      WRITE (6,*) 'OVER 100 ITERATIONS'

110 CONTINUE

C FLOW RATE INTEGRATION

      Q=0.
      DO 120 I=1,IMXM1
      Q=Q+U (I)
120 CONTINUE

```

```

      Q=Q*DY*ERW

      RETURN
      END

C-----
C
      SUBROUTINE MATRIX(CC1,CC2,CC3,BB,Y,N)

C  PURPOSE:
C  THIS IS TO SOLVE THE TRIDIAGONAL MATRIX
C
C  ARGUMENT:
C
C      C1(I),C2(I),C3(I):   COEFFECIENT MATRIX
C      CC1,CC2,CC3:       ARE USED TO INSULATE C1,C2,C3 FROM
OUTER PROGRAM
C      B(I):   LOAD VECTOR
C      BB                IS USED TO INSULATE B FROM
OUTER PROGRAMS
C      Y(I):   TARGET VECTOR
C      N:      THE SIZE OF THE MATRIX
C
C  MATRIX FORM:
C      C1(I)*Y(I-1)+C2(I)*Y(I)+C3(I)*Y(I+1) = B(I)
C      FOR I=2,N-1
C      WITH Y(1) = B(1)
C      Y(N) = B(N)
C      IT ALSO IMPLIES THAT: C2(1) = C2(N) = 1.0
C      C1(1) = C3(1) = C1(N) = C3(N)
= 0.
C-----
      IMPLICIT REAL*8(A-H,O-Z)

C
      DIMENSION C1(101),C2(101),C3(101),B(101),Y(101)
      DIMENSION CC1(101),CC2(101),CC3(101),BB(101)

C
C      INSULATION
      DO 5 I=1,N
      C1(I)=CC1(I)
      C2(I)=CC2(I)
      C3(I)=CC3(I)
      B(I)=BB(I)
5  CONTINUE

C      INITIALIZATION
      C1(1)=0.0
      C2(1)=1.0
      C3(1)=0.0
      C1(N)=0.0
      C2(N)=1.0
      C3(N)=0.0
      B(1)=Y(1)

```

```

      B(N)=Y(N)
C      SOLVE TRIDIAGNAL MATRIX
      NM1=N-1
      DO 10 I=2,NM1
      C2(I)=C2(I)*C2(I-1)-C1(I)*C3(I-1)
      C3(I)=C3(I)*C2(I-1)
      B(I)=B(I)*C2(I-1)-C1(I)*B(I-1)
C      TO AVOID ACCUMULATING VALUES
      C3(I)=C3(I)/C2(I)
      B(I)=B(I)/C2(I)
      C2(I)=1.00
10    CONTINUE
      NM2=N-2
      DO 20 I=1,NM2
      J=N-I
      Y(J)=(B(J)-C3(J)*Y(J+1))/C2(J)
20    CONTINUE

      RETURN
      END

```

```

C-----
      SUBROUTINE CFDSS(TY,U,PIN,POUT,Q)

```

```

C TO DO CFD FOR AN ER VALVE IN THE BRIDGE -- STEADY STATE
C
C DPDX:      PRESSURE GRADIENT
C ETA: PLASTIC VISCOSITY
C PAPAN: PAPANASTASIOU COEFFICIENT (=10.0)
C PHI: DIMENSIONLESS VISCOSITY COEFFICIENT
C PIN: PRESSURE AT THE VALVE INLET
C POUT:      PRESSURE AT THE VALVE OUTLET
C RHOER: ER FLUID DENSITY
C THTU: VELOCITY RELAXATION PARAMETER
C U: VELOCITY
C UTEM: TEMPORARY VELOLCITY
C ERW: ER VALVE WIDTH
C ERL: ER VALVE LENGTH
C ERH: ER VALVE DEPTH OR THICKNESS
C
C
C-----

```

```

      IMPLICIT REAL*8 (A-H,O-Z)

```

```

      DIMENSION U(101)

```

```

      COMMON/CERVAL/ERW,ERL,ERH,RHOER,ETA
      COMMON/CNUMER/PAPAN,THTU

```

```

      IMAX=101
      IMXM1=IMAX-1
      IMXM2=IMAX-2
      DY=ERH/IMXM1

```

```

A1=DT/RHOER
A2=A1*ETA
TDY=2.*DY
DY2=DY**2
OMTHT=1.0-THTU

DPDX=(POUT-PIN)/ERL

      HC=2.0*TY/(-DPDX)

C  CALCULATE VELOCITY

      UC=(H*(-DPDX)-2.*TY)**2/(8.*ETA*(-DPDX))

DO 20 I=1,IMAX

Y=(I-1.0)*DY-ERH

IF(Y.LE.(-HC/2.)) THEN
      U(I)=- (1./2.*ETA)*DPDX((ERH/2.)**2-Y**2) -
      +      TY/ETA*(ERH/2.0+Y)
      ELSE
      IF(Y.GT.(HC/2.)) THEN
      U(I)=- (1./2.*ETA)*DPDX((ERH/2.)**2-Y**2) -
      +      TY/ETA*(ERH/2.0-Y)
      ELSE
      U(I)=UC
      END IF
END IF

20 CONTINUE

C  FLOW RATE INTEGRATION

Q=0.
DO 120 I=1,IMXM1
Q=Q+U(I)
120 CONTINUE

      Q=Q*DY*ERW

      RETURN
      END

```

## APPENDIX D. AN ELECTRODILATANCY TEST DEVICE

In rheology, the term dilatancy has been used to describe either volume expansion<sup>3, 4</sup> or shear-thickening behavior<sup>5</sup>, and the former is implied in this study. According to Reiner<sup>3</sup>, “dilatancy is ‘that property of a material by which it increases in volume when it is stirred’ or, more specifically, when it is sheared.”

Gorodkin *et al.*<sup>6</sup> speculated that ER fluids may have some electrodilatanant effects: “Electrorheological suspensions, which are systems formed by finely sized particles, have special properties. When no electric field is applied, their volume is constant. When a field is applied their volume increase, but not randomly, as in Reynolds dilatancy, but of some value, that is proportional to the electric field strength. The process is reversible, and the volume returns to its initial value when the field is removed.” However, no direct evidence of electrodilatanancy has surfaced in the literature.

If the electrodilatanancy exists, it can be utilized to drive the spool of the main stage without circulating an ER fluid, which can simplify the whole system greatly.

A simple device has been designed (Fig. D.1) and fabricated to verify the existence or absence of electrodilatanancy. It consists of two connected fluid chambers of large diameters and a graduated tube of a small diameter. The speculated volume change can be detected by observing the fluid surface level in the graduated tube. No visible volume change, however, has been detected in the experiment. In the device, no attempt is made to shear the fluid, which might explain the absence of dilatancy. Dilatancy could also be fluid dependent, or the change is simply too small for the device to detect.

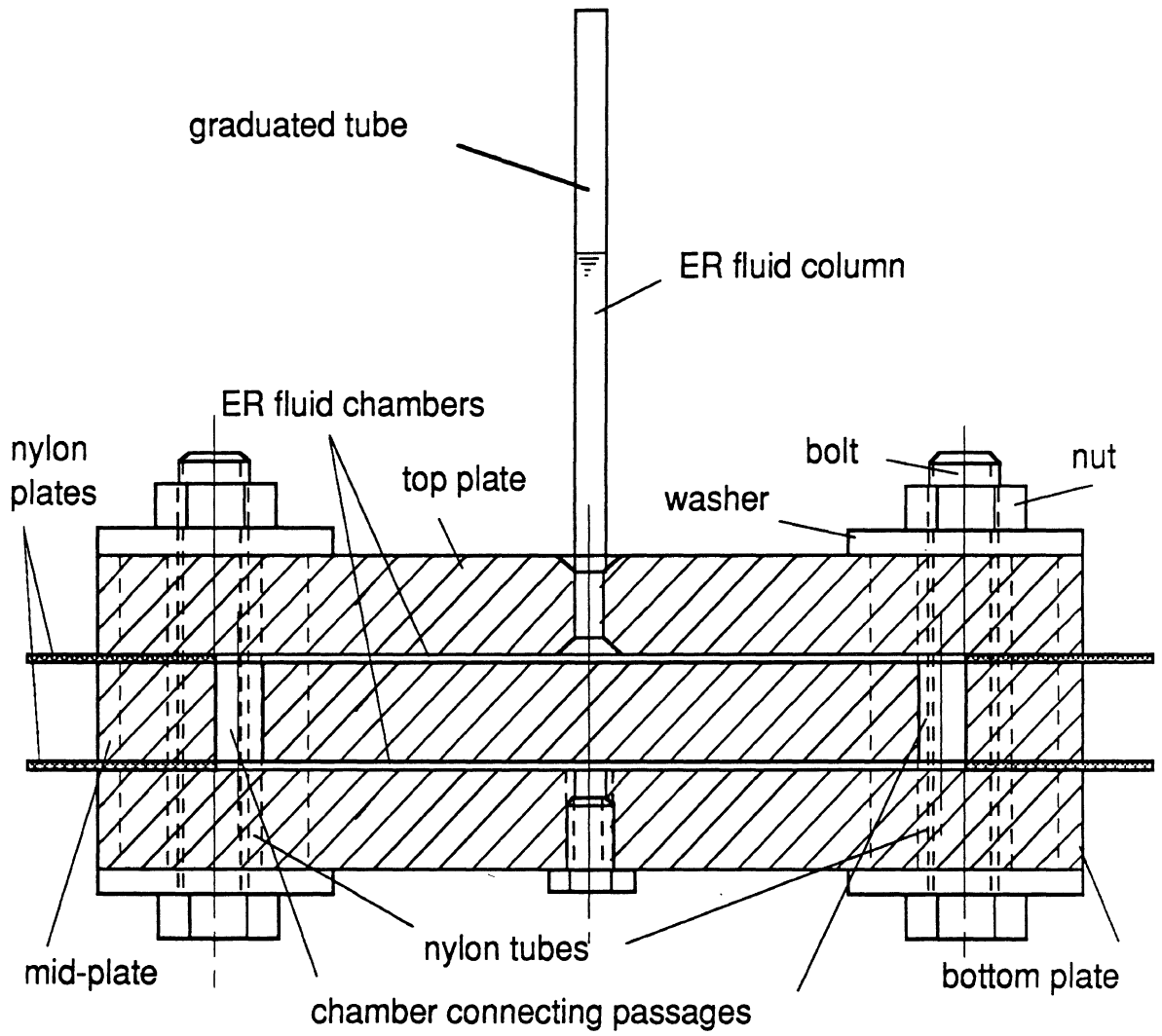


Fig. D.1. Electrodilancy test device.



## APPENDIX E. ELECTORRHEOLOGICAL FLUIDS: A BIBLIOGRAPHY

(Prepared by the Research Information and Publications Center, UMTRI)

1973. 3rd international fluid power symposium. Published by British Hydromech. Res. Assoc., Cranfield, England. 508 p. Cranfield, England, British Hydromech. Res. Assoc., 1973, 508 p. UMTRI-73-002
1985. Colloquium on electrically active fluids. [Proceedings.] Institution of Electrical Engineers, London, England. 40 p. Report No. 1985/14. UMTRI-78561
1988. Electrorheological fluids and devices. 4 p. Automotive Engineering, Vol. 96, No. 12, Dec 1988, pp. 45-48. UMTRI-57109
- Feb 1988. Electrorheological fluids. 4 p. Engineering, Feb 1988, pp. i-iv. UMTRI-77702
- Adriani, P. M.; Gast, A. P. Oct 1988. A microscopic model of electrorheology. Stanford University, Calif. 12 p. Physics of Fluids, Vol. 31, No. 10, Oct 1988, pp. 2757-2768. Sponsored by National Science Foundation, Washington, D.C.; Lord Corporation, Erie, Pa. UMTRI-78436
- Ali, S.A.; Sengupta, M. 1986. The primary electroviscous effect in aging agl sols - effect of increasing concentrations of counter ions of different valencies. Univ. Coll. Sci. Calcutta, Dept. Pure Chem., India. 9 p. J. Colloid and Interface Sci., Vol. 113, No. 1, 1986, pp. 172-187. UMTRI-86-001
- Anderson, J.L.; Koh, W. 1977. Electrokinetic parameters for capillaries of different geometries. Cornell Univ., School of Chem. Engng., Ithaca, N. Y. 10 p. J. Colloid and Interface Sci., Vol. 59, No. 1, 15 March 1977, pp. 149-158. UMTRI-77-006
- Arguelles, J.; Martin, H.R.; Pick, R. 1974. Theoretical model for steady electroviscous flow between parallel plates. Univ. Havana, Cuba/ Univ Waterloo, Ontario. 8 p. J. Mech. Eng. Sci. (GB), Vol. 16, No. 4, Aug 1974, pp. 232-239. UMTRI-74-001
- Atten, P.; Baron, R.; Goniche, M. Jan 1980. Superposition of a cylindrical Couette flow and of an electrically induced secondary flow. Centre National de la Recherche Scientifique, Bellevue, France. 4 p. Journal de Physique - Lettres, Vol. 41, No. 1, Jan 1980, pp. 1-4. UMTRI-78418
- Atten, P.; Honda, T. Feb 1982. The electroviscous effect and its explanation. I - the electrohydrodynamic origin; study under unipolar D.C. injection. Centre National de la Recherche Scientifique, Bellevue, France. 21 p. Journal of Electrostatics, Vol. 11, No. 3, Feb 1982, pp. 225-245. UMTRI-78565

- Babchin, A.J.; Piliavin, M.A.; Levich, V.G. 1976. Rheoelectric effect in a polar liquid interphase layer. Dept. of Mech., Technion, Israel Inst. of Technol., Haifa. 10 p. J. Colloid and Interface Sci, Vol. 57, No. 1, Oct 1976, pp. 1-10. UMTRI-76-002
- Bailey, W. R. 1976. Low-shear limit of secondary electroviscous effect. Princeton Univ., Dept. Chem. Engn. 15 p. J. Colloid and Interface Sci., Vol. 55, No. 3, June 1976, pp. 590-604. UMTRI-76-006
- Barnes, H. A.; Edwards, M. F.; Woodcock, L. V. 1987. Applications of computer simulations to dense suspension rheology. Unilever Research, Merseyside, England/Bradford University, West Yorkshirè, England. 18 p. Chemical Engineering Science, Vol. 42, No. 4, 1987, pp. 591-608. UMTRI-80189
- Bauwendaal, C.; Fernandez, F. 1985. Experimental study and analysis of a slit die viscometer. Raychem Corporation, Menlo Park, Calif. 7 p. Polymer Engineering and Science, Vol. 25, No. 11, Aug 1985, pp. 765-771. UMTRI-80253
- Berezov, L.V.; Ovcharenko, F.D.; Merinov, Y.A. 1982. Factors determining the rheological properties of polyvinyl chloride plastisols. 7 p. Colloid Journal of the USSR, Vol. 44, No. 1, Jan-Feb 1982, pp. 7- 13. UMTRI-82-010
- Berg, R. F.; Moldover, M. R. 1988. Viscometer for low frequency, low shear rate measurements. National Bureau of Standards, Thermophysics Division, Gaithersburg, Md. 6 p. Review of Scientific Instruments, Vol. 57, No. 8, Aug 1986, pp. 1667-1672. UMTRI-80255
- Blachford, J. 1969. Recalculation of the secondary electroviscous effect based on revised values of the zeta potential. Pulp and Paper Research Inst., Point Claire, Canada. 3 p. J. Colloid and Interface Sci., Vol. 29, No. 3, March 1969, pp. 472- 474. UMTRI-69-001
- Blachford, J.; Chan, F.S.; Goring, D.A.I. 1969. The secondary electroviscous effect including theoretical values of Huggins coefficient for charged spheres. McGill Univ., Montreal, Quebec. 17 p. Papers of the 15 Canadian High Polymer Forum (Abstracts), University of Montreal, 1969, pp. 3- 4. UMTRI-69-002
- Block, H.; Gregson, E. M.; Qin, A.; Tsangaris, G.; Walker, S. M. Sept 1983. A Couette cell with fixed stator alignment for the measurement of flow modified permittivity and electroviscosity. Liverpool University, England. 7 p. Journal of Physics Engineering, Vol. 16, No. 9, Sept 1983, pp. 896-902. Sponsored by Science and Engineering Research Council, Swindon, England. UMTRI-78417
- Block, H.; Kelly, J.P. 1985. Dielectric properties of fluids and their relation to electrorheology. Dept. of Inorg., Phys. and Ind. Chem., Liverpool Univ., England. 3 p. IEE Colloquium on Electrically Active Fluids (Digest No. 14), London, IEE, 1985, pp. 1/1- 3. UMTRI-85-004
- Block, H.; Kelly, J. P. 1988. Review article: electro-rheology. Cranfield Institute of Technology, England. 17 p. Journal of Physics D: Applied Physics, Vol. 21, 1988, pp. 1661-1677. UMTRI-80188

- Block, J.; Kelly, J. P. 6 Aug 1986. Electrorheological fluids. National Research Development Corporation, London, England. 13 p. Report No. GB 2 170 510 A. UMTRI-78901
- Bonincontro, A.; Cametti, C.; Dibiasio, A. 1982. Temperature-dependence of the secondary electroviscous effect in polystyrene lattices. Univ. Rome, Ist. Fis., Italy. 9 p. Colloids and Surfaces, Vol. 5, No. 1, 1982, pp. 55- 63. UMTRI-82-002
- Brooks, D. A. Sept 1982. Electro-rheological devices. Laser Engineering (Developments) Ltd. 3 p. Chartered Mechanical Engineering, Vol. 29, No. 9, Sept 1982, pp. 91-93. UMTRI-78415
- Brooks, D. A. Oct 1982. Electro-rheological effect adds muscle. Laser Engineering (Developments) Ltd. 2 p. Control and Instrumentation, Vol. 14, No. 10, Oct 1982, pp. 57, 59. UMTRI-78416
- Brooks, D. A. Nov 1982. Electro-rheological devices provide hydraulic/electronic interface. 3 p. Design Engineering, Nov 1982. UMTRI-78563
- Brooks, D.A. 1985. Electro-rheological fluid: basic concepts: flow behaviour and devices. 3 p. IEE Colloquium on Electrically Active Fluids (Digest No. 14), London, IEE, 1985, pp. 4/1-3. UMTRI-85-005
- Brooks, D.A.; Hjelm, C.; Marshall, L.; Aukoski, C.; Goodwin, J. 1986. Visco-elastic studies on an electro-rheological fluid. Laser Engineering, London, England. 20 p. Colloids and Surfaces, Vol. 18, No. 2-4, June 1986, pp. 293-312. UMTRI-86-003
- Bullough, W.A.; Stringer, J.D. 1973. Utilisation of the electroviscous effect in a fluid power system. Sheffield Univ., England. 16 p. 3rd International Fluid Power Symposium, Cranfield, British Hydromech. Res. Assoc., 1973, pp. F3/37-52. UMTRI-73-004
- Bullough, W.A.; Stringer, J.D. 1977. Direct flow control by electric fields. Sheffield Univ. 4 p. Hydraulic and Air Engng., Vol. 5, No. 4, Sept. 1977, pp. 11, 13, 15, 17. UMTRI-77-005
- Bullough, W. A.; Foxon, M. B. 1978. A proportionate coulomb and viscously damped isolation system. Sheffield University, England/ March Engineering Ltd., Oxfordshire, England. 10 p. Journal of Sound and Vibration, Vol. 56, No. 1, 1978, pp. 35-44. UMTRI-78414
- Bullough, W. A.; Peel, D. J. Dec 1987. [Development of electro-rheological fluids for application on mobile construction industry machinery.] Sheffield University, England. 8 p. Chinese Journal of Mechanical Engineering, Vol. 23, No. 4, Dec 1987, pp. 51-58. UMTRI-78900
- Choi, S. B.; Gandhi, M. V.; Thompson, B. S. 1989. An active vibration tuning methodology for smart flexible structures incorporating electro-rheological fluids: a proof-of-concept investigation. Michigan State University, Department of Mechanical Engineering, East Lansing. 6 p. American Control Conference. Proceedings. Vol.

1. 1989. Pp. 694-699. Sponsored by Army Research Office, Durham, N.C.; Michigan State Department of Commerce, Lansing. UMTRI-80533
- Choi, S. B.; Thompson, B. S.; Gandhi, M. V. 1989. Smart structures incorporating electro-rheological fluids for vibration-control and active-damping applications: an experimental investigation. Michigan State University, Department of Mechanical Engineering, East Lansing. 8 p. Sankar, T. S., ed. Machinery Dynamics - Applications and Vibration Control Problems - 1989 ASME Design Technical Conference. New York, ASME, 1989. Pp. 229-236. Sponsored by Army Department, Arlington, Va.; Michigan Department of Commerce, Lansing. UMTRI-80485
- Churaev, N.V. 1972. Influence of the electroviscosity effect on thermocapillary flow in wetting liquid films. Inst. Phys. Chem., Acad. Sci., Moscow. 3 p. Colloid Journal of the USSR, Vol., 34, No. 5, Sept-Oct 1972, pp. 705-707. UMTRI-72-004
- Cokelet, G.R.; Bush, R.W.; Lacelle, P.L. 1981. Electroviscous flow and electrophoretic motion during erythrocyte entry in a glass-capillary in the presence of applied electric-potential gradients. Univ. Rochester, Sch. Med. and Dent., Dept. Radiat. Biol. and Biophys. 2 p. Pflugers Archiv-European Journal of Physiology, Vol. 390, No. 1, 1981, pp. 94-95. UMTRI-81-005
- Deynega, Y. F.; Popko, K. K.; Kovganich, N. Y. 1978. Temperature dependence of the electroviscous effect and dielectric parameters of suspensions of hydrated substances in hydrocarbons. 7 p. Heat Transfer - Soviet Research, Vol. 10, No. 1, Jan-Feb 1978, pp. 50-56. UMTRI-78411
- Deynega, Y.F.; Popko, K.K.; Kovganich, N.Y. 1982. The role of bound water in the electro-rheological effect. Royal Aircraft Establishment, Farnborough, England. 10 p. Translation of Dopovidi Akademii Nauk Ukrain's'kol RSR, Seriya B, No. 9, 1975, pp. 807-810. UMTRI-82-009
- Deynega, Y.F. 1982. Some problems of the electro-rheology of dispersed systems. Royal Aircraft Establishment, Farnborough, England. 13 p. Translation of Masliny I Tekhnol. Pererab. Kauchukov Polimery I Rezinov Smesei (USSR), No. 1, 1978, pp. 29-36. UMTRI-82-008
- Duclos, T. G. 1987. An externally tunable hydraulic mount which uses electro-rheological fluid. Lord Corporation, Erie, Pa. 7 p. Report No. SAE 870963. UMTRI-74552
- Duclos, T. G. 1988. Design of devices using electrorheological fluids. Lord Corporation, Erie, Pa. 7 p. Report No. SAE 881134. UMTRI-77393
- Eige, J. J. 1963. An analysis of the fluid mechanics of electric fluids. Stanford Research Institute, Menlo Park, Calif. 6 p. Sponsored by Air Force Systems Command, Aeronautical Systems Division, Wright-Patterson AFB, Ohio. Report No. ASME 63-MD-1. UMTRI-80254

- Erdogan, M.E. 1973. Apparent viscosity of a suspension of drops in the presence of an electric field. Tech. Univ. Istanbul. 12 p. Bull. Tech. Univ. Istanbul (Turkey), Vol. 26, No. 1, 1973, pp. 11-22. UMTRI-73-003
- Fikisko, F.E. 1988. U-M scientist develops electrically sensitive fluids that work at high temperatures. [News release.] University of Michigan, College of Engineering, Ann Arbor. 5 p. p. UMTRI-76981
- Firoozian, R.; Bullough, W. A.; Peel, D. J. 1989. Time domain modelling of the response of an electro-rheological fluid in the flow mode. Sheffield University, Department of Mechanical and Process Engineering, England. 6 p. Sankar, T. S., ed. Vibration Analysis - Techniques and Applications - 1989 ASME Design Technocal Conference. New York, ASME, 1989. Pp. 45-50. Sponsored by Great Britain Ministry of Defence, London, England; Wolfson Foundation, England; Science and Engineering Research Council, Swindon, England. UMTRI-80486
- Fukuzawa, K.; Iguchi, M.; Kumeoka, Y.; Taketani, T. 1974. On the flow of an electroviscous fluid between a rotating and a stationary cylinder. [In Japanese] Mechanical Engng. Lab., Tokyo. 8 p. J. Mech. Eng. Lab. (Japan), Vol. 28, No. 4, July 1974, pp. 87-94. UMTRI-74-004
- Fukuzawa, K.; Iguchi, M.; Kumeoka, Y.; Taketani, T. 1975. Braking action of electroviscous fluid between rotating disk and stationary disk. [In Japanese] Mechanical Engng. Lab., Tokyo. 6 p. J. Mech. Eng. Lab., Vol. 29, No. 5, Sept. 1975, pp. 189-194. UMTRI-75-003
- Fukuzawa, K.; Iguchi, M.; Kumeoka, Y.; Taketani, T. 1975. Electroviscous squeeze film. [In Japanese] Mechanical Engng. Lab., Tokyo. 8 p. J. Mech. Eng. Lab. (Japan), Vol. 29, No. 4, July 1975, pp. 149-156. UMTRI-75-004
- Fukuzawa, K.; Iguchi, M.; Kumeoka, Y.; Taketani, T. 1975. Floating bed using electroviscous fluid. [In Japanese] Mechanical Engng. Lab., Tokyo. 7 p. J. Mech. Eng. Lab. (Japan), Vol. 29, No. 4, July 1975, pp. 157-163. UMTRI-75-007
- Fukuzawa, K.; Iguchi, M.; Kumeoka, Y.; Taketani, T. 1975. Squeeze film and floating bed using electroviscous fluid. [In Japanese] Mechanical Engng. Lab., Tokyo. 1 p. Trans. Jap. Soc. Mech. Eng, Vol. 41, No. 351, Nov. 1975, 1 p. UMTRI-75-008
- Gandhi, M. V.; Thompson, B. S.; Shakir, S. 1987. Electro-rheological-fluid-based articulating robotic systems. Michigan State University, Department of Mechanical Engineering, East Lansing. 10 p. Advances in Design Automation. Volume 2: Robotics, Mechanisms, and Machine Systems. New York, American Society of Mechanical Engineers, 1987. Pp. 1-10. Sponsored by Lord Corporation, Erie, Pa. UMTRI-78440
- Gandhi, M. V.; Thompson, B. S.; Choi, S. B.; Shakir, S. 1989. Electro-rheological-fluid-based articulating robotic systems. Michigan State University, Department of Mechanical Engineering, East Lansing. 9 p. Journal of Mechanisms, Transmissions, and Automation in Design, Vol. 111, No. 3, Sept 1989, pp. 328-336. UMTRI-80480

- Gandhi, M. V.; Thompson, B. S.; Choi, S. B. 1989. A new generation of innovative ultra-advanced intelligent composite materials featuring electro-rheological fluids: an experimental investigation. Michigan State University, East Lansing. 24 p. *Journal of Composite Materials*, Vol. 23, No. 12, Dec 1989, pp. 1232-1255. Sponsored by Army Research Office, Durham, N.C.; Michigan State Department of Commerce, Lansing. UMTRI-80582
- Gast, A. P.; Zukoski, C. F. 1989. Electrorheological fluids as colloidal suspension. Stanford University, Calif./ Illinois University, Urbana, Department of Chemical Engineering. 50 p. *Advances in Colloid and Interface Science*, Vol. 30, No. 3-4, Dec 1989, pp. 153-202. Sponsored by National Science Foundation, Washington, D.C.; Lord Corporation, Erie, Pa.; FMC Corporation, Santa Clara, Calif. UMTRI-80550
- Ghosh, B.N. 1976. Colloidal electrolytes - attempt to account for their electroviscous effect under different conditions. *Univ. Coll. Sci. Calcutta, Dept. Pure Chem.* 5 p. *J. Indian Chemical Society*, Vol. 53, No. 9, 1976, pp. 881-885. UMTRI-76-001
- Ghosh, B.N. 1978. Simplified derivation of an equation for electroviscous effect. *Univ. Calcutta, Coll. Sci., Dept. Chem.* 2 p. *J. Indian Chemical Society*, Vol. 55, No. 9, 1978, pp. 967- 968. UMTRI-78-002
- Ghosh, B.N. 1979. Attempt to account quantitatively for the electroviscous behavior of an association colloid. *Univ. Coll. Sci., Dept. Chem., Calcutta.* 3 p. *Journal of the Indian Chemical Society*, Vol. 56, No. 7, 1979, pp. 700-702. UMTRI-79-003
- Goldstein, G. 1990. Electrorheological fluids: applications begin to gel. 5 p. *Mechanical Engineering*, Vol. 112, No. 10, Oct 1990, pp. 48-52. UMTRI-80277
- Gonzalez-Fernandez, C.F.; Espinosa-Jiminez, M.; Gonzalez-Caballero, F. 1983. Effect of packing density of cellulose plugs on streaming potential phenomena. *Univ. Coll. of Jaen, Dep. of Physics, Jaen, Spain.* 6 p. *Colloid and Polymer Science*, Vol. 261, No. 8, Aug 1983, pp. 688-693. UMTRI-83-003
- Gonzalez-Fernandez, C.F.; Bruque, J.M.; Gonzalez-Caballero, F.; Espinosa-Jiminez, M. 1985. Electrokinetic transport of aqueous solutions of phenomenological relations. *Dept. of Phys., Granada Univ., Spain.* 4 p. *Eur. Polym. J.*, Vol. 21, No. 7, 1985, pp. 641-644. UMTRI-85-003
- Gorodkin, R.G.; Korobko, Y.V.; Blokh, G.M.; Gleb, V.K.; Sidorova, G.I.; Ragotner, M.M. 1979. Applications of the electrorheological effect in engineering practice (review of electrorheological devices). *A.V. Luikov Inst. of Heat and Mass Transfer, Belorussian Acad. of Sciences, U.S.S. R.* 14 p. *Fluid Mech. - Sov. Res.*, Vol. 8, No. 4, July-Aug. 1979, pp. 48-61. UMTRI-79-011
- Gorodkin, R. G.; Korobko, Y. V.; Blokh, G. M.; Gleb, V. K.; Sidorova, G. I.; Ragotner, M. M. 1979. Applications of the electrorheological effect in engineering practice. *Luikov Heat and Mass Transfer Institute, Minsk, USSR.* 14 p. *Dinamika Protssessov Perenosa v Reologicheski Slozhnykh Sredakh*, 1978. Pp. 147-164.

Fluid Mechanics - Soviet Research, Vol. 8, No. 4, July-Aug 1979, pp. 48-61.  
UMTRI-78568

Gur, Y.; Revina, I. 1979. Rheological electrokinetic phenomena in a single capillary. Soils and Fertilizers Lab., Faculty of Agricultural Engng, Technion, Haifa, Israel. 16 p. J. Colloid and Interface Sci., Vol. 72, No. 3, Dec. 1979, pp. 442-457. UMTRI-79-004

Headley, L.C.; Pierce, C.I.; Sawyer, W.K. 1970. Fluid flow in channels, capillaries, and porous media under the influence of an electric field. Report of investigations. Bureau of Mines, Washington, D. C. 41 p. Report No. RI-7342. UMTRI-70-003

Heywood, N. 1985. Selecting a viscometer. Warren Spring Laboratory, Stevenage, England. 5 p. Chemical Engineer, Vol. 415, June 1985, pp. 16-23. UMTRI-80256

Hinch, E.J.; Sherwood, J.D. 1983. Primary electroviscous effect in a suspension of spheres with thin double layers. Univ. of Cambridge, Dep. of Applied Mathematics and Theoretical Physics, England. 11 p. J. Fluid Mech., Vol. 132, July 1983, pp. 337-347. UMTRI-83-005

Hoburg, J.F. 1980. Inertial and equilibrium shear retardation of electrohydrodynamic instability growth. Carnegie-Mellon Univ., Dept. of Electric Engng., Pittsburgh, Pa. 5 p. Phys. Fluids, Vol. 23, No. 11, Nov. 1980, pp. 2184-2188. UMTRI-80-004

Honda, T.; Atten, P. 1975. The electroviscous effect and its explanation. Centre National de la Recherche Scientifique, Bellevue, France. 4 p. International Conference on Conduction and Breakdown in Dielectric Liquids. 5th. Proceedings. 1975. Pp. 131-134. UMTRI-78428

Honda, T.; Sasada, T. 1977. The mechanism of electroviscosity. II. Conductivity effect of dielectric liquids on electroviscosity. Tokyo Inst. of Technol., Dept. of Mech. Engng. for Production, Faculty of Engng., Tokyo, Japan. 7 p. Jpn. J. Appl. Phys., Vol. 16, No. 10, Oct. 1977, pp. 1785-1791. UMTRI-77-002

Honda, T.; Sasada, T. Oct 1977. The mechanism of electroviscosity. I. Electrohydrodynamic effect on polar liquids. Tokyo Institute of Technology, Japan. 9 p. Japanese Journal of Applied Physics, Vol. 16, No. 10, Oct 1977, pp. 1775-1783. UMTRI-78419

Honda, T.; Sasada, T. 1978. The electroviscous effect in n-hexane/acetone mixtures. Tokyo Inst. of Technol., Dept. of Mech. Engng. for Production, Faculty of Engng., Tokyo, Japan. 2 p. Jpn. J. Appl. Phys., Vol. 17, No. 11, Nov. 1978, pp. 2075-2076. UMTRI-78-004

Honda, T.; Atten, P. 1978. Electroviscous effect in poiseuille flow under electrolysis condition. Lab. d'Electrostatique, CNRS, Grenoble, France. 6 p. Proc of the Int Conf on Conduct and Breakdown in Dielectr Liq, 6th, Mont-Saint-Aignan, Fr, Jul 24-28 1978, published by Ed Front, Dreux, Fr, 1978, pp. 315-320. UMTRI-78-001

- Honda, T.; Sasada, T.; Kurosawa, K. 1978. The electroviscous effect in the MBBA liquid crystal. Tokyo Inst. of Technol., Dept. of Mech. Engng. for Production, Faculty of Engng., Tokyo, Japan. 6 p. Jpn. J. Appl. Phys., Vol. 17, No. 9, Sept. 1978, pp. 1525-1530. UMTRI-78-003
- Honda, T.; Kurosawa, K.; Sasada, T. 1979. Electroviscous effect in liquid crystals. Tokyo Inst. of Technol., Dept. of Mech. Engng. for Production, Faculty of Engng., Tokyo, Japan. 2 p. Jpn. J. Appl. Phys., Vol. 18, No. 5, May 1979, pp. 1015-1016. UMTRI-79-007
- Honda, T.; Sasada, T. 1979. The electroviscous effect of water. Tokyo Inst. of Technol., Dept. of Mech. Engng. for Production, Tokyo, Japan. 2 p. Jpn. J. Appl. Phys., Vol. 18, No. 3, March 1979, pp. 675-676. UMTRI-79-009
- Honda, T.; Sasada, T.; Sakamoto, T. June 1979. Electroviscous effect in non-polar liquids. Tokyo Institute of Technology, Japan. 7 p. Japanese Journal of Applied Physics, Vol. 18, No. 6, June 1979, pp. 1031-1037. UMTRI-78421
- Honda, T.; Sasada, T. Aug 1979. Electroviscous effect in chloroform. Tokyo Institute of Technology, Japan. 2 p. Japanese Journal of Applied Physics, Vol. 18, No. 8, Aug 1979, pp. 1663-1664. UMTRI-78420
- Honda, T.; Sasada, T. Aug 1979. Electroviscous effect in liquids of low permittivity. Tokyo Institute of Technology, Japan. 2 p. Japanese Journal of Applied Physics, Vol. 18, No. 8, Aug 1979, pp. 1605-1606. UMTRI-78422
- Honda, T.; Kurosawa, K.; Sasada, T. Nov 1979. Transient pressure-drop fluctuations in electroviscous effect. Tokyo Institute of Technology, Japan. 5 p. Japanese Journal of Applied Physics, Vol. 18, No. 11, Nov 1979, pp. 2059-2063. UMTRI-78423
- Honda, T.; Kurosawa, K.; Sasada, T. Aug 1980. A.C. characteristics of the electroviscous effect. Tokyo Institute of Technology, Japan. 4 p. Japanese Journal of Applied Physics, Vol. 19, No. 8, Aug 1980, pp. 1463-1466. UMTRI-78424
- Honda, T.; Sasada, T.; Kurosawa, K. 1981. Electroviscous effect in dielectric liquids. Htgr. and Fusion Technol. Dev. Office, Toshiba Corp., MITA, Tokyo. 5 p. 7th International Conference on Conduction and Breakdown in Dielectric Liquids, Proceedings. New York, IEEE, 1981, pp. 361-365. UMTRI-81-003
- Jordan, T. C.; Wong, W.; Shaw, M. T. 1988. A rheo-optical and materials approach to electrorheology. Connecticut University, Storrs. 7 p. UMTRI-78437
- Kenaley, G. L.; Cutkosky, M. R. 1989. Electrorheological fluid-based robotic fingers with tactile sensing. Integrated Systems, Inc., Santa Clara, Calif./ Stanford University, Palo Alto, Department of Mechanical Engineering, Calif. 5 p. Robotics and Automation, Vol. 1, May 1989, pp. 132-136. UMTRI-80481
- Kirichok, I.F. 1980. Heat release associated with the electroelastic modes of piezoelectric ceramic disks. Inst. of Mech., Acad. of Sci., Kiev, USSR. 5 p. Sov. Appl. Mech., Vol. 16, No. 10, Oct. 1980, pp. 902-905. UMTRI-80-005



- Klass, D. L.; Martinek, T. W. 1967. Electroviscous fluids. I. Rheological properties. Institute of Gas Technology, Chicago, Ill./ Tee-Pak, Inc., Danville, Ill. 8 p. Journal of Applied Physics, Vol. 38, No. 1, Jan 1967, pp. 67-74. UMTRI-79972
- Klass, D. L.; Martinek, T. W. 1967. Electroviscous fluids. II. Electrical properties. Institute of Gas Technology, Chicago, Ill./ Tee-Pak, Inc., Danville, Ill. 6 p. Journal of Applied Physics, Vol. 38, No. 1, Jan 1967, pp. 75-80. UMTRI-79973
- Klingenberg, D. J.; van Swol, F.; Zukoski, C. F. 1989. Dynamic simulation of electrorheological suspensions. Illinois University, Urbana, Department of Chemical Engineering. 8 p. Journal of Chemical Physics, Vol. 91, No. 12, 15 Dec 1989, pp. 7888-7895. Sponsored by Fannie and John Hertz Foundation, Livermore, Calif.; National Science Foundation, Washington, D.C. UMTRI-80478
- Klingenberg, D. J.; van Swol, F.; Zukoski, C. F. 1989. Dynamic simulation of electrorheological suspensions. Illinois University, Urbana, Department of Chemical Engineering. 2 p. Polymeric Materials: Science and Engineering. Proceedings. Vol. 61. American Chemical Society, 1989. Pp. 154-155. UMTRI-80538
- Korobko, Y.V.; Bukovich, I.V.; Chobot, M.A.; Artemenkov, A.N.; Kornienko, A.A. 1987. Ultrasonic propagation peculiarities in electrorheological suspensions. Vestsi Akad. Nauk BSSR. 5 p. Vestsi Akad. Nauk BSSR Ser. Fiz. Energ. Nauk no. 2, 1987, 105-109. Sponsored by V. UMTRI-87-001
- Korobko, Y. V.; Bukovich, I. V.; Chobot, M. A.; Artemenkov, A. N.; Kornienko, A. A. 1987. [Ultrasonic propagation peculiarities in electrorheological suspensions.] Luikov Heat and Mass Transfer Institute, Minsk, USSR. 5 p. Vestsi Akad. Nauk BSSR Ser. Fiz. Energ. Nauk no. 2, 1987, pp. 105-109. UMTRI-80553
- Kovganich, N.Y.; Deynega, Y.F.; Popko, K.K. 1978. Electro-rheological and dielectric studies of hydrocarbon suspensions of clayish minerals. [In Russian] Acad. Sci. UKSSR, Inst. Colloid and Water Chem., Kiev. 4 p. Ukrainskii Khimicheskii Zhurnal, Vol. 44, No. 2, 1978, pp. 209-212. UMTRI-78-007
- Kovganich, N. Y.; Deinega, Y. F.; Popko, K. K. 1980. Electrorheological and dielectric investigations [sic] of hydrocarbon suspensions of clayey minerals. Institute of Colloidal Chemistry and Chemistry of Water, U.S.S.R. 3 p. Soviet Progress in Chemistry, Vol. 44, 1978, pp. 96-98. UMTRI-80187
- Krieger, I.M. 1972. Rheology of monodisperse lattices. Case Western Reserve Univ., Cleveland. 26 p. Adv. Colloid and Interface Sci., Vol. 3, No. 2, June 1972, pp. 111-136. UMTRI-72-002
- Krieger, I.M.; Eguiluz, M. 1976. Second electroviscous effect in polymer lattices. Case Western Reserve Univ., Dept. of Chem. and Macromolecular Sci., Cleveland, Ohio. 17 p. Trans. Soc. Rheol., Vol. 20. No. 1, Jan-March 1976, pp. 29-45. UMTRI-76-007

- Lang, J.H.; Hoburg, J.F.; Melcher, J.R. 1976. Field induced mixing across a diaphragm. Dept. of Electrical Engng., MIT, Cambridge, MA. 2 p. Phys. Fluids, Vol. 19, No. 6, June 1976, pp. 917-918. UMTRI-76-005
- Lemaitre, J.; Chaboche, J.L.; Munakata, Y. 1974. Method of metal characterization for creep and slow cycle fatigue prediction in structures. Example of UDIMET 700. ONERA, Chatillon, France. 11 p. 1973 Symposium on Mechanical Behavior of Materials, Kyoto, Soc. Materials Sci, 1974, pp. 239-249. UMTRI-74-003
- Levine, S.; Marriott, J.R.; Robinson, K. 1975. Theory of electrokinetic flow in a narrow parallel-plate channel. Univ. Manchester, England. 11 p. J. Chem. Soc. Faraday Trans. II (GB), Vol. 71, Pt. 1, 1975, pp. 1-11. UMTRI-75-009
- Likhterov, S. D.; Shor, G. I.; Lapin, V. P.; Fufaev, A. A. 1980. Electroviscous effect in oils with additives. All-Union Scientific-Research Institute for Petroleum Processing, U.S.S.R. 3 p. Chemistry and Technology of Fuels and Oils, Vol. 16, No. 1, Sept 1980, pp. 58-60. UMTRI-80568
- Lingard, S.; Bullough, W. A.; Shek, W. M. 1989. Tribological performance of an electro-rheological fluid. Hong Kong University/ Sheffield University, England. 7 p. Journal of Physics D: Applied Physics, Vol. 22, No. 11, 14 Nov 1989, pp. 1639-1645. UMTRI-80487
- Lumry, R.; Hon-Sang Yue, R. 1965. Dielectric dispersion of protien solutions containing small zwitterions. Minnesota University, Minneapolis Lab for Biophysical Chemistry. 2 p. J. Physical Chemistry, Vol. 69, No. 4, Apr 1965, pp. 1162-1174. UMTRI-65-001
- Lykov, A. V.; Shul'man, Z. P.; Gorodkin, R. G.; Matsepuro, A. D. 1970. Mechanical behavior of electroviscous nonaqueous disperse systems in shear flow in a transverse electric field. Academy of Sciences of the Belorussian SSR, Minsk, Russia. 6 p. Journal of Engineering Physics, Vol. 18, No. 6, June 1970, pp. 669-674. UMTRI-80537
- McDonogh, R.W.; Hunter, R.J. 1983. Primary electroviscous effect. Univ. of Sydney, Sch. of Chemistry, Australia. 11 p. J. Rheol., Vol. 27, No. 3, June 1983, pp. 189-199. UMTRI-83-001
- Menjivar, J.A.; Rha, C. 1983. A theory on the electroviscous effect - a method for the estimation of the viscosity of dispersions of charged spherical colloidal particles. MIT, Dept. Nutr. and Food Sci., Biomat. Sci. and Engn. Lab, Cambridge, MA. 4 p. J. Chem. Phys., Vol. 79, No. 2, 15 July 1983, pp. 953-956. UMTRI-83-006
- Miller, W.G. 1983. Electro-rheology, the basis of novel activators. [In German] 2 p. Funk-Tech. (Germany), Vol. 38, No. 6, June 1983, pp. 249-250. UMTRI-83-002
- Mooney, M. 1931. Explicit formulas for slip and fluidity. United States Rubber Company, General Laboratories, Passaic, N.J. 7 p. Journal of Rheology, Vol. 2, No. 2, April 1931, pp. 210-216. UMTRI-80067

- Ohtsuki, T. 1981. Dynamical properties of strongly interacting Brownian particles. I. Dynamic shear viscosity. Dept. of Appl. Phys., Faculty of Engng., Univ. of Tokyo, Japan. 18 p. *Physica A (Netherlands)*, Vol. 108A, No. 2-3, Sept. 1981, pp. 441-458. UMTRI-81-002
- Petrie, E.M. 1976. Effect of surfactant on the viscosity of Portland cement-water dispersions. Carnegie-Mellon Univ., Pittsburgh, PA. 8 p. *Industrial and Engineering Chemistry, Product Research and Development*, Vol. 15, No. 4, Dec 1976, pp. 242-249. UMTRI-76-004
- Phillips, R. W.; Auslander, D. M. 1974. The electroplastic flow modulator. Sandia Laboratories, Livermore, Calif./ California University, Berkeley. 9 p. *Flow: Its Measurements and Control in Science and Industry*, Vol. 1, No. 3, 1974, pp. 1243-1251. UMTRI-78412
- Polak, P.; Burton, P.T. 1971. Improving suspension damping. 5 p. *J. Automot. Eng.*, Vol. 2, No. 2, Feb 1971, pp. 13-17. UMTRI-71-001
- Rakhmatulin, K.A.; Abutaliev, F.B.; Sultanbekov, R.I. 1977. Equalizing the hydromechanics of compressible fluids taking the electroviscosity effect into consideration. [In Russian] *Izv. Akad. Nauk USSR*. 5 p. *Izv. Akad. Nauk UZSSR Ser. Tekh. Nauk*, No. 4, 1977, pp. 58-62. UMTRI-77-007
- Robinson, R.D.; Chalifoux, H.D.; Parrot, T.L. 1968. High frequency piezoelectric motor pump for internal energy conversion. United Aircraft Corp., Farmington, Ct. 228 p. 1968 NEREM Record 234, New York, IEEE, 1968, 234 p. UMTRI-68-002
- Robinson, R.D.; Chalifoux, H.D.; Parrot, T.L.; Peters, J.C. 1968. High frequency piezoelectric motor pump for implanted energy conversion. United Aircraft Corp., Farmington, Ct. 1 p. *Proceedings of the Annual Conference on Engineering in Medicine and Biology*, Vol. 10, New York, IEEE, 1968, 1 p. UMTRI-68-003
- Saitoh, S.; Sakai, T.; Kusama, H. 1972. Fluidic electro-fluid converter by use of electro-viscous fluid. Tokyo Institute of Science, Japan. 9 p. UMTRI-80482
- Saitoh, S.; Sakai, T.; Kusama, H. March 1976. Experimental investigation on electrically operated fluidic amplifiers by use of electro-viscous fluid. 10 p. *Japan Society of Mechanical Engineers. Transactions*, Vol. 42, No. 355, March 1976, pp. 837-846. UMTRI-78566
- Saitoh, S.; Sakai, T.; Kusama, H. 1977. An experimental investigation on a liquid fluidic frequency demodulating circuit. *Sci. Univ. of Tokyo, Japan*. 8 p. *Bull. JSME (Japan)*, Vol. 20, No. 149, Nov. 1977, pp. 1461-1468. UMTRI-77-001
- Sasada, T.; Kishi, T.; Kamijo, K. 1974. On the electroviscous effect in colloidal liquids. Tokyo Inst. of Technol., Japan. 4 p. *Jpn. Congr. on Mater. Res., 17th Annual Proceedings*. Kyoto, Jpn. Soc. Mater. Sci., 1974, pp. 228-231. UMTRI-74-002
- Sasada, T.; Makijo, K.; Kishi, T. 1974. On the electroviscous effect in single phase liquids. Tokyo Inst. of Technol., Japan. 4 p. *Jpn. Congr. on Mater. Res., 17th*

- Annual Proceedings. Kyoto, Jpn. Soc. Mater. Sci., 1974, pp. 224-227. UMTRI-74-005
- Sasada, T.; Kishi, T.; Kamijo, K. 1975. Electroviscous effect in liquids with dispersed polymer or solid particles. [In Japanese] 7 p. Trans. Jap. Soc. Mech. Eng., Vol. 41, No. 342, Feb 1975, pp. 568-574. UMTRI-75-005
- Sasada, T.; Makijo, K.; Kishi, T. 1975. Electroviscous effect in single phase liquids. [In Japanese] Tokyo Inst. of Technol./ Japanese Nat. Aerospace Lab./ National Aerospace Lab./ Japan Fuji Photo Film Co, Ltd. 1 p. Trans. J.S.M.E., 41, March 1975, p. 343. UMTRI-75-006
- Schlosser, W.M.J. 1975. Classification of hydraulic transmissions as infinitely variable power transmissions devices. [In German] 11 p. Conf. on Hydraulic Transmissions, Dusseldorf, VDI-Verlag, 1975, pp. 15-25. UMTRI-75-002
- Schulman, Z. P.; Korobko, Y. V.; Matsepuro, A. D.; Khusid, B. M. 1978. Influence of the electroviscous effect on heat transfer in the channel between coaxial cylinders. 8 p. Heat Transfer - Soviet Research, Vol. 10, No. 1, Jan-Feb 1978, pp. 66-73. UMTRI-78410
- Schulman, Z. P.; Khusid, B. M.; Khizhinskii, B. P.; Korobko, E. V. Feb 1987. Characteristics of an electrorheological damper in a vibration insulator. Luikov Heat and Mass Transfer Institute, Minsk, USSR. 5 p. Journal of Engineering Physics, Vol. 52, No. 2, Feb 1987, pp. 175-179. UMTRI-78441
- Schurz, J. 1979. Electroviscous effects and their application to the control of product quality. [In German] 1 p. Papier, Vol. 33, No. 10, 1979, p. 469. UMTRI-79-002
- Scott, D.; Yamaguchi, J. Nov 1983. Solidifying fluid transforms clutches and flow valves. 6 p. Automotive Engineering, Vol. 91, No. 11, Nov 1983, pp. 61-66. UMTRI-78569
- Scott, D.; Yamaguchi, J. Nov 1985. ER fluid devices near commercial stage. 5 p. Automotive Engineering, Vol. 93, No. 11, Nov 1985, pp. 75-79. UMTRI-78570
- Sengupta, M.; Ali, S.A. 1973. Primary electroviscous effect some numerical estimates from Booths theory. Univ. Coll. Sci., Dept. Chem., Calcutta. 3 p. J. Indian Chemical Society, Vol. 50, No. 12, 1973, pp. P764-766. UMTRI-73-001
- Sherwood, J.D. 1980. Primary electroviscous effect in a suspension of spheres. Dept. Appl. Math and Theoret. Phys., Cambridge, England. 21 p. J. Fluid Mech., Vol. 101, No. 3, 1980, pp. 609-629. UMTRI-80-003
- Sherwood, J.D. 1981. Primary electroviscous effect in a suspension of rods. Unilever Ltd., Port Sunlight Lab, Cheshire, England. 20 p. J. Fluid Mech., Vol. 111, 1981, pp. 347-366. UMTRI-81-004
- Shima, A.; Tsujino, T.; Nanjo, H. 1985. The behavior of bubbles in electroviscous fluids. Tohoku University, Sendai, Japan. 16 p. Tohoku Daigaku, Series B, Vol. 50, No. 374, 1985, pp. 43-58. UMTRI-78408

- Shor, G.I.; Lapin, V.P.; Shkolnikov, V.M.; Likhterov, S.D. 1976. Electroviscous effects in lubricating oils. All-Union Sci. Res. Inst. Oil Refining. 8 p. Proc. JSLE-ASLE International Lubrication Conf., Tokyo, Amsterdam, Elsevier, 1976, pp. 623-630. UMTRI-76-008
- Shor, G. I.; Lapin, V. P.; Likhterov, S. D.; Shkolnikov, V. M. 1976. Electroviscous effects in lubricating oils. All-Union Scientific-Research Institute for Petroleum Processing, U.S.S.R. 5 p. Chemistry and Technology of Fuels and Oils, Vol. 11, No. 5-6, May-June 1976, pp. 469-473. UMTRI-80569
- Shoureshi, R.; Graf, P.L.; Houston, T.L. 1986. Adaptive hydraulic engine mounts. Purdue University, West Lafayette, School of Mechanical Engineering, Ind. 11 p. Report No. SAE 860549. UMTRI-77932
- Shulman, Z.P.; Matsepuro, A.D. 1973. Influence of nonisothermicity on the electro-rheological and electrophysical properties of suspensions. [In Russian] 5 p. Vestsi Akad. Nauk BSSR Ser. Fiz. Energ. Nauk, No. 4, 1973, pp. 125-129. UMTRI-73-005
- Shulman, Z. P.; Korobko, E. V. 1976. [Intensification of convective heat transfer of weakly conducting suspensions with the aid of electric fields.] 5 p. Elektronaya Obrabotka Materialov, Vol. 72, No. 6, 1976, pp. 71-75. UMTRI-78409
- Shulman, Z. P.; Korobko, E. V. May 1978. Convective heat transfer of dielectric suspensions in coaxial cylindrical channels. Luikov Heat and Mass Transfer Institute, Minsk, USSR. 6 p. International Journal of Heat and Mass Transfer, Vol. 21, No. 5, May 1978, pp. 543-548. UMTRI-78413
- Shulman, Z.P.; Matsepuro, A.D.; Khusid, B.M. 1982. Structure formation in electro-rheological suspensions in an electric field. I. Qualitative considerations. Royal Aircraft Establishment, Farnborough, England. 9 p. Translation of Vestsi Akademii Nauk Belaruskai SSR (USSR), No. 3, 1977, pp. 116-121. UMTRI-82-007
- Shulman, Z.P.; Khusid, B.M.; Matsepuro, A.D. 1982. Structure formation of electro-rheological suspensions in an electric field. II. Quantitative evaluations. Royal Aircraft Establishment, Farnborough, England. 11 p. Trans. of Vestsi Akademii Nauk Belaruskai SSR (USSR), No. 3, 1977, pp. 122-127. UMTRI-82-006
- Shulman, Z.P.; Matsepuro, A.D. 1985. Nature of charge carriers in electrorheological suspensions. Royal Aircraft Establishment, Farnborough, England. 7 p. Translation of Teplo Massoperenos: Teor. Prakt Prilozh (USSR), 1983, pp. 19-21. UMTRI-85-008
- Shulman, Z. P.; Korobko, E. V.; Yanovskii, Y. G. 1989. The mechanism of the viscoelastic behaviour of electrorheological suspensions. Luikov Heat and Mass Transfer Institute, Minsk, U.S.S.R. 16 p. Journal of Non-Newtonian Fluid Mechanics, Vol. 33, No. 2, Oct 1989, pp. 181-196. UMTRI-80483
- Sproston, J. L.; Stevens, N. G.; Page, I. M. 1987. An investigation of torque transmission using electrically stressed dielectric fluids. Liverpool University,

- Department of Mechanical Engineering, England. 6 p. Electrostatics '83. Proceedings. 1987. Pp. 53-58. UMTRI-79530
- Stangroom, J. E. 3 Aug 1982. Hydraulic servo valve. Great Britain Ministry of Defence, London, England. 5 p. Report No. Patent 4,342,334. UMTRI-78904
- Stangroom, J. E. 1984. Electro-rheological fluids. ER Fluid Developments, Ltd. 3 p. Automotive Engineer, Vol. 9, No. 2, April/May 1984, p. 12, 14, 16. UMTRI-78564
- Stangroom, J. E. April 1984. Giving micro-electronics some working muscle. Sheffield University, England. 3 p. Automation and Control, Vol. 14, No. 3, April 1984, pp. 15-17. UMTRI-78562
- Stangroom, J. E. 24 April 1984. Viscous shear clutch. Great Britain Ministry of Defence, London, England. 9 p. Report No. Patent 4,444,298. UMTRI-78903
- Stangroom, J.E. 1985. The electro-osmotic theory of electro-rheological fluids. 2 p. IEE Colloquium on Electrically Active Fluids (Digest No. 14), London, IEE, 1985, pp. 5/1-2. UMTRI-85-007
- Stangroom, J. E. 15 Jan 1985. Electro-rheological transducer. National Research Development Corporation, London, England. 7 p. Report No. Patent 4,493,615. UMTRI-78902
- Stangroom, J. E.; Eckersley, J. S. Feb 1985. Pipework snubbers based on electro-rheological fluids. E. R. Fluid Developments Ltd., Sheffield, England/ Woodhead, Jonas, and Sons, Ossett, England. 6 p. Pipework Design and Operation Conference. London, Institution of Mechanical Engineers, Feb 1985. Pp. 279-284. Report No. C29/85. UMTRI-78427
- Stanway, R.; Sproston, J. L.; Stevens, N. G. 1985. Non-linear identification of an electro-rheological vibration damper. Liverpool University, Department of Mechanical Engineering, England. 6 p. International Federation on Automatic Control Symposium on Identification and System Parameter Estimation. 7th. Proceedings. 1985. Pp. 195-200. Sponsored by Ford Motor Company, Essex, England. UMTRI-78426
- Stanway, R.; Stevens, N.G.; Mottershead, J.E. 1985. Non-linear models of EV fluids in vibration. 3 p. IEE Colloquium on Electrically Active Fluids (Digest No. 14), London, IEE, 1985, pp. 6/1-3. UMTRI-85-010
- Stanway, R.; Sproston, J. L.; Stevens, N. G. Dec 1987. Non-linear modelling of an electro-rheological vibration damper. Liverpool University, Department of Mechanical Engineering, England. 18 p. Journal of Electrostatics, Vol. 20, No. 2, Dec 1987, pp. 167-184. Sponsored by Ford Motor Company, Ltd., Essex, England. UMTRI-78438
- Stanway, R.; Sproston, J.; Firoozian, R. March 1989. Identification of the damping law of an electro-rheological fluid: a sequential filtering approach. Liverpool University, Department of Mechanical Engineering, England. 6 p. Journal of Dynamic Systems,

Measurement and Control, Vol. 111, No. 1, March 1989, pp. 91-96. UMTRI-78022

- Stevens, N. G.; Sproston, J. L.; Stanway, R. 1984. Experimental evaluation of a simple electroviscous damper. Liverpool University, Department of Mechanical Engineering, England. 9 p. Journal of Electrostatics, Vol. 15, 1984, pp. 275-283. UMTRI-79975
- Stevens, N.G.; Sproston, J.L.; Stanway, R. 1987. On the mechanical properties of electro-rheological fluids. University of Liverpool, Department of Mechanical Engineering, England. 3 p. UMTRI-87-002
- Stevens, N. G.; Sproston, J. L.; Stanway, R. June 1988. An experimental study of electro-rheological torque transmission. Liverpool University, Department of Mechanical Engineering, England. 7 p. Journal of Mechanism, Transmissions, and Automation in Design, Vol. 110, No. 2, June 1988, pp. 182-188. Sponsored by Ford Motor Company, Dearborn, Mich. UMTRI-78439
- Stone-Masiu, J.; Watillar, A. 1968. Electroviscous effects in dispersions of monodisperse polystyrene lattices. Free Univ. Brussels, Belgium. 16 p. J. Colloid and Interface Sci., Vol. 28, No. 2, Oct. 1968, pp. 187-202. UMTRI-68-001
- Stone-Masiu, J.; Watillar, A. 1970. Note on the electroviscous effects in polystyrene lattices. Free Univ. Brussels, Belgium. 3 p. J. Colloid and Interface Sci., Vol. 34, No. 2, Oct 1970, pp. 327-329. UMTRI-70-001
- Strandrud, H. T. 1966. Electric-field valves inside cylinder control vibrator. 5 p. Hydraulics and Pneumatics, Sept 1966, pp. 139-143. UMTRI-79976
- Stukel, J.J.; Soo, S.L. 1969. Turbulent flow of a suspension into a channel. Univ. Illinois, Urbana. 2 p. Powder Technol., Vol. 2, No. 5, June 1969, pp. 278-289. UMTRI-69-004
- Sugimoto, N. 1977. Winslow effect in ionic exchange resin dispersion. Res. Inst. of Ind. Safety, Minist. of Labour of Tokyo, Japan. 8 p. Bull. JSME (Japan), Vol. 20, No. 149, Nov. 1977, pp. 1476-1483. UMTRI-77-004
- Sugimoto, N. 1985. The application of Winslow's effect to the new actuators. Japan Ministry of Labor, Tokyo. 6 p. Japan Society of Lubrication Engineers Journal, Vol. 30, No. 12, 1985, pp. 859-864. UMTRI-78567
- Sundukov, A. N.; Ivanov, P. A. 1972. EVIS-69S electroviscosimeter for studying the viscous properties of non-Newtonian fluids. 2 p. Instruments and Experimental Techniques, Vol. 15, No. 3, Part 2, May-June 1972, pp. 968-969. UMTRI-78425
- Suyazov, V. M. 1973. Magnetohydrodynamics of a microstructural medium. The rheoelectric effect. 6 p. Magnetohydrodynamics, Vol. 9, No. 4, Oct-Dec 1973, pp. 486-491. UMTRI-80536
- Tadros, T.F. (Ed.) 1986. Suspensions: papers from the international suspension symposium. Imperial Chemical Industries Ltd., Plant Protection Div., Bracknell,

Engl. 304 p. Colloids and Surfaces, Vol. 18, No. 2-4, June 1986, pp. 135-483.  
UMTRI-86-002

Tao, R.; Woestman, J. T.; Jaggi, N. K. 1989. Electric field induced solidification. Northeastern University, Boston, Mass. 3 p. Applied Physics Letters, Vol. 55, No. 18, 30 Oct 1989, pp. 1844-1846. UMTRI-80479

Tregubov, N.N.; Fomicheva, E.V. 1974. Comparative evaluation of liquefying enzymes with the aid of an automatic electroviscosimeter. [In Russian] Izv. Vuz. Pishch. Tekhnol., USSR. 3 p. Izv. Vuz. Pishch. Tekhnol. (USSR), No. 1, 1974, pp. 154-156. UMTRI-74-007

Uejima, H. 1972. Dielectric mechanism and rheological properties of electro- fluids. Waseda Univ., Tokyo. 8 p. Jap. J. Appl. Phys., Vol. 11, No. 3, March 1972, pp. 319- 326. UMTRI-72-001

Ushijima, T.; Takano, K.; Kojima, H. 1988. High performance hydraulic mount for improving vehicle noise and vibration. Bridgestone Corporation, Tokyo, Japan. 11 p. Report No. SAE 880073. UMTRI-77930

Ushijima, T.; Takano, K.; Noguchi, T. 1988. Rheological characteristics of ER fluids and their application to anti-vibration devices with control mechanism for automobiles. Bridgestone Corporation, Japan. 11 p. Report No. SAE 881787. UMTRI-77619

Van de Ven, T.G.M. 1984. Electro-viscoelastic properties of dilute suspensions. Dept. of Chem., McGill Univ., Montreal. 16 p. J. Chem. Soc. Faraday Trans. I (GB), Vol. 80, Pt. 10, Oct 1984, pp. 2677-2692. UMTRI-84-001

Verkholantsev, V.V. 1969. Conversion of highly carboxylated lattices into solutions or dispersions of polyelectrolytes. Lensovet Technol. Inst., Leningrad. 4 p. Colloid Journal of the USSR, Vol. 31, No. 4, July-Aug 1969, pp. 385-388. UMTRI-69-005

Wang, Y.L. 1970. Electroviscous effects of concentrated polystyrene latexes. Dow Chemical Co., Midland, Mich. 9 p. J. Colloid and Interface Sci., Vol. 32, No. 4, April 1970, pp. 633-641. UMTRI-70-002

Watterson, I.G.; White, L.R. 1981. Primary electroviscous effect in suspensions of charged spherical-particles. Australian Natl. Univ., Res. Sch. Phys. Sci., Inst. Adv. Studies, Dept. Appl. Math, Canberra. 14 p. J. Chem. Society Faraday Trans. II, Vol. 77, P.7, 1981, pp. 1115-1128. UMTRI-81-001

Whittle, M. Aug 1989. Modelling two-phase fluids. Manchester University, England. 4 p. Physics World, Vol. 2, Aug 1989, pp. 39-42. Sponsored by Eletro-Rheological Research Syndicate; Micanite and Insulators Company, Ltd. UMTRI-79291

Wong, W.; Shaw, M. T. 1989. The role of water in electrorheological fluids. Connecticut University, Storrs. 6 p. UMTRI-80484



- Wysocki, J.J.; Adams, J.; Haas, W. 1969. Electroviscosity of a cholesteric liquid-crystal mixture. Xerox Corp., Rochester, N. Y. 2 p. J. Appl. Phys., Vol. 40, No. 9, Aug 1969, pp. 3865-3866. UMTRI-69-003
- Yoshimura, A.; Prud'homme, R. K. 1988. Wall slip corrections for Couette and parallel disk viscometers. Princeton University, N.J. 15 p. Journal of Rheology, Vol. 32, No. 1, 1988, pp. 53-67. UMTRI-79974

